DISSERTATION

A FRAMEWORK FOR THE ANALYSIS OF COASTAL INFRASTRUCTURE VULNERABILITY UNDER GLOBAL SEA LEVEL RISE

Submitted by

Patrick S. O'Brien

Department of Civil and Environmental Engineering

In partial fulfillment of the requirements

For the Degree of Doctor of Philosophy

Colorado State University

Fort Collins, Colorado

Fall 2017

Doctoral Committee:

Advisor: Pierre Y. Julien

Chester C. Watson
Robert Ettema
Sara L. Rathburn

ABSTRACT

A FRAMEWORK FOR THE ANALYSIS OF COASTAL INFRASTRUCTURE VUNERABILTY UNDER GLOBAL SEA LEVEL RISE

The assumption of hydrologic stationarity has formed the basis of coastal design to date. At the beginning of the 21st century, the impact of climate variability and future climate change on coastal water levels has become apparent through long term tide gauge records, and anecdotal evidence of increased nuisance tidal flooding in coastal areas. Recorded impacts of global sea rise on coastal water levels have been documented over the past 100 to 150 years, and future water levels will continue to change at increasing, unknown rates, resulting in the need to consider the impacts of these changes on past coastal design assumptions. New coastal infrastructure plans, and designs should recognize the paradigm shift in assumptions from hydrologic stationarity to non-stationarity in coastal water levels. As we transition into the new paradigm, there is a significant knowledge gap which must address built coastal infrastructure vulnerability based on the realization that the underlying design assumptions may be invalid.

A framework for the evaluation of existing coastal infrastructure is proposed to effectively assess vulnerability. The framework, called the Climate Preparedness and Resilience Register (CPRR) provides the technical basis for assessing existing and future performance. The CPRR framework consists of four major elements: (1) datum adjustment, (2) coastal water levels, (3) scenario projections and (4) performance thresholds. The CPRR framework defines methodologies which: (1) adjust for non-stationarity in coastal water levels and correctly make projections under multiple scenarios; (2) account for past and future tidal to geodetic datum adjustments; and (3) evaluate past and future design performance by applying performance

models to determine the performance thresholds. The framework results are reproducible and applicable to a wide range of coastal infrastructure types in diverse geographic areas.

The framework was applied in two case studies of coastal infrastructure on the east and west coasts of the United States. The east coast case study on the Stamford Hurricane Barrier (SHB) at Stamford CT, investigated the navigation gate closures of the SHB project. The framework was successfully applied using two performance models based on function and reliability to determine the future time frame at which relative sea level rise (RSLR) would cause Navigation Gate closures to occur once per week on average or 52 per year. The closure time analysis also showed the impact of closing the gate earlier to manage internal drainage to the Harbor area behind the Stamford Hurricane Barrier. These analyses were made for three future sea level change (SLC) scenarios.

The west coast case study evaluated four infrastructure elements at the San Francisco Waterfront, one building and three transportation elements. The CPRR framework applied two performance models based on elevation and reliability to assess the vulnerability to flooding under four SLC scenarios. An elevation-based performance model determined a time horizon for flood impacts for king tides, 10 and 100-year annual exceedance events. The reliability-based performance model provided a refinement of results obtained in the elevation-based model due to the addition of uncertainty to the four infrastructure elements.

The CPRR framework and associated methodologies were successfully applied to assess the vulnerability of two coastal infrastructure types and functions in geographically diverse areas on the east and west coasts of the United States.

ACKNOWLEDGEMENTS

I would like to acknowledge and thank my family, committee and my advisor, Dr. Pierre Julien who guided me through my classwork and research with great skill, patience and a lot of encouragement when it was most needed. As I complete this work, I lose a great adviser and gain a lifelong friend and colleague. Special recognition goes to two people who supported me and never gave up on me, even at times when I thought I wouldn't complete this work; Kate White and Tim Pangburn. Both stepped up with support and sponsorship at a time when I needed it the most. I will be forever grateful to Kate, for bringing me into the USACE Climate program and guiding me into my research topic.

Lastly, I want to acknowledge my twin brother, Michael. Mike was a climate expert in his own right, and taught me many things. He was with me 100% when I made a somewhat risky and controversial decision to leave my job and home in Portland, OR and start my PhD in 2008. He passed away last year as I was nearing completion of my research and one of our last conversations was about finishing this work.

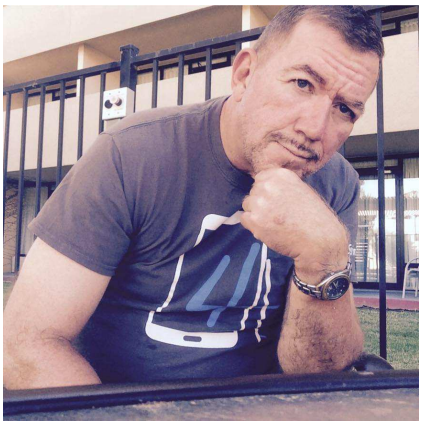

Mike O'Brien 1958-2016

Patrick O'Brien

TABLE OF CONTENTS

LIST OF TABLES

LIST OF FIGURES

LIST OF ABBREVIATIONS

AEP	Annual Exceedance Probability
CCFVI	Coastal City Flooding Vulnerability Index
CDF	Cumulative Distribution Function
cfs	Cubic feet per second
CM	Common Methodology
CPRR	Climate Preparedness and Resilience Register
CVI	Coastal Vulnerability Index
DIVA	Dynamic and Interactive Vulnerability Assessment
DTL	Mean Diurnal Tide Level
ENSO	EL Nino Southern Oscillation
EO	Executive Order
EV	Expanded Vulnerability
FCSDR	Flood and coastal storm damage reduction
FEMA	Federal Emergency Management Agency
ft.	Feet
GEV	Generalized Extreme Value Distribution
GPD	Generalized Pareto Distribution
GSLR	Global Sea Level Rise
HP	Horsepower
IAV	Interannual Variability
IVA	Initial Vulnerability Assess
IPCC	Intergovernmental Panel on Climate Change
MHHW	Mean Higher High Water
MHW	Mean High Water
MLLW	Mean Lower Low Water

MSL	Mean Sea Level
MSL29	Sea Level Datum of 1929
MTL	Mean Tide Level
MMSLA	Mean Monthly Seal Level Anomalies
NAVD88	North American Vertical Datum of 1988
NGVD29	National Geodetic Vertical Datum of 1929
NGC	Navigation Gate Closures
NOAA	National Oceanic and Atmospheric Administration
NORMSDIST	Microsoft Excel function
NRC	National Research Council
NTDE	National Tidal Datum Epoch
NWLON	National Water Level Observation Network
PAR	Pressure and Release
PDF	Probability Density Function
RH	Risk Hazard
RSLC	Relative Sea Level Change
RSLR	Relative Sea Level Rise
SS	Storm Surge
S	Swash
SHB	Stamford Hurricane Barrier
STND	Station Datum
SWL	Still Water Level
TWL	Total Water Level
USACE	United States Army Corps of Engineers
VA	Vulnerability Assessment
VLM	Vertical land movement

LIST OF SYMBOLS

β	Reliability index
$\bar{\eta}$	Mean water level in the presence of waves
η'	Low frequency water level fluctuations due to waves
η_A	Astronomic tide
η_{NTR}	Non-tidal residual
ξ	Shape parameter, GEV distribution
σ	Scale parameter, GEV distribution
σ	Standard deviation, Normal distribution
μ	Location parameter, GEV distribution
μ	Mean, Normal distribution
Γ	Factor of safety
A	Tidal amplification factor
b	Constant, acceleration factor in non-linear future sea level rise trajectories
E	Eustatic sea level rise
G	Failure function
G	Performance function
GC	Stamford Harbor water level at which gate is closed
GO	Stamford Harbor water level at which gate is opened
M	RSLC (meters), published rate from tide gauge data or linear trend
p1	Linear regression coefficient, RSLC rate
p2	Linear regression coefficient
P	Precipitation
P_f	Probability of failure
Q	Discharge
R	Resistance

R	Reliability
S	Load
SH	Peak Stamford Harbor water level
t	Time
T_f,	Return period in years
y_t	Detrending adjustment factor

1.0: INTRODUCTION

At the beginning of the 21st century, as the impacts and understanding of climate variability and future climate change on coastal water levels became apparent, assumptions of hydrologic stationarity which formed the basis of coastal designs over the last 100 to 150 years are now understood to be invalid. Recorded impacts of sea level change on coastal water levels from tide gauge records have been documented over the past 100 to 150 years, and future water levels will continue to change at unknown rates, resulting in the need to reconsider past coastal design assumptions. Figure 1 shows failure of a sea wall in Pacifica, CA in 2015. The seawall was constructed in 1984.

Figure 1 - Seawall failure, Pacifica, CA, winter 2015-2016. Photo by Patrick O'Brien

1.1 Coastal Infrastructure Design Assumptions in the 20th Century

Systems for management of water throughout the developed world have been designed and operated under the assumption of stationarity. Stationarity, the idea that natural systems fluctuate within an unchanging envelope of variability, is a foundational concept that permeates training and practice in water-resource engineering (Milly 2007)

The old paradigm was that engineers designed coastal infrastructure using a fixed average return period under assumptions of stationarity. Engineers treated uncertainty about the future by increasing design capacity by using factors of safety. Practice in the late 20th century using probabilistic methods applied for designing coastal structures generally assumed that extreme events are stationary. Figure 2 shows the impact of sea level rise on return periods based on that record for a coastal infrastructure design level.

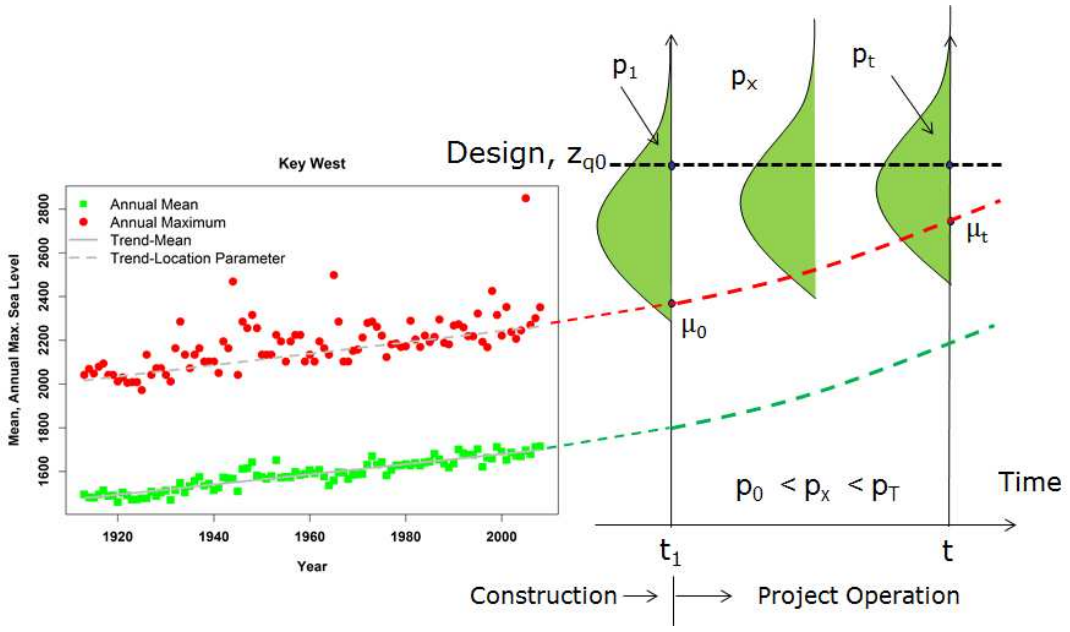

Figure 2 - Concept of Return Period and Risk, demonstrating paradigm shift in approach to assess vulnerability to designs based on a return period level developed using an assumption of stationarity (Obeysekera 2013)

Designs for existing built coastal infrastructure which were made under assumptions of stationarity may now been inadequate for present and future conditions due the recognition of the impact of non-stationarity on designs base on a fixed return period. Many studies in the past decades have shown that hydrological records exhibit some type of non-stationarity. Human intervention in river basins (e.g., urbanization), the effect of low-frequency climatic variability (e.g., Pacific Decadal Oscillation), and climate change due to increased greenhouse gasses in the atmosphere have been suggested to be the leading causes of changes in the hydrologic cycle of river basins in addition to changes in the magnitude and frequency of extreme floods and extreme sea levels (Salas 2013).

Understanding and recognition of the impact of global sea level rise and climate change design variables such as water level due to non-stationarity represents a paradigm shift in coastal engineering. Accounting for the impact of non-stationarity on the past and future performance of coastal infrastructure is rapidly becoming a priority in coastal areas and significant research opportunity.

1.2 Global Sea Level Rise

Design of coastal infrastructure requires the estimation of extreme sea-level at project locations. Global average sea level has been rising at the rate of 1.7 mm/year since the middle of the nineteenth century (Church and White 2011). Although the observed tide-gage data shown little or no acceleration above a linear trend (Houston and Dean 2011; Watson 2011), it is expected that the global mean sea level will be increasing at a faster rate during the 21st century and beyond (Bindoff et al. 2007; Houston 2012). Consequently, sea-level extremes will change accordingly. However, the projections of the future sea-levels are highly uncertain, which have

led coastal engineering specialists to suggest scenario-based approaches for mean sea-level increase (NRC 1987; USACE 2011a; Obeysekera and Park 2013).

1.2 The Role of Preparedness and Resilience in Vulnerability Assessments

President Barak Obama issued an executive order (EO) (Order 13653 2013) meant to prepare the United States for the impacts of climate change. EO 13653 defines three key terms:

1. *Preparedness* - means actions taken to plan, organize, equip, train, and exercise to build, apply, and sustain the capabilities necessary to prevent, protect against, ameliorate the effects of, respond to, and recover from climate change related damages to life, health, property, livelihoods, ecosystems, and national security.

2. *Adaptation* - means adjustment in natural or human systems in anticipation of or response to a changing environment in a way that effectively uses beneficial opportunities or reduces negative effects.

3. *Resilience* - means the ability to anticipate, prepare for, and adapt to changing conditions and withstand, respond to, and recover rapidly from disruptions.

Along with the changing paradigms in water resources engineering which recognize the impacts of non-stationarity on built coastal infrastructure, vulnerability assessments of US coastal infrastructure which account for climate change impacts become a part of preparations for the impacts of climate change. A framework which identifies coastal infrastructure vulnerability to global sea level rise informs preparedness actions, identifies adaptation potential and enhances resilience of existing infrastructure by identifying performance threshold windows.

1.3 Objectives

The overall research objective is to develop a framework which can assess current and future vulnerability and engineering performance of existing coastal infrastructure under the range of plausible global sea level rise predictions. Preparedness, adaptation and resilience actions will be informed and enhanced by implementing the framework in coastal vulnerability assessments. The framework is called the Climate Preparedness and Resilience Register (CPRR) to emphasize the contribution made by coastal infrastructure vulnerability assessments to climate preparedness, adaptation and resilience activities identified in EO 13653. Specific research objectives are to:

1. Define a framework to assess vulnerability. The framework should be applicable to a wide range of coastal infrastructure types and geographic areas.
2. Develop methodologies to execute the framework. The methodologies should account for the impact of non-stationarity in past and future water levels for the design and performance of existing coastal infrastructure.
3. Demonstrate the applicability of framework and conduct vulnerability assessments for two case studies with different infrastructure types in different geographic areas.

2.0: REVIEW OF LITERATURE

This chapter contains a review of literature. The literature review is designed to elaborate on the four main elements of the CPRR framework.

2.1 Climate and Sea Level Change Vulnerability Assessments

There exists a large amount of literature which proposes frameworks to conduct vulnerability assessments of coastal infrastructure and communities impacted by global sea level rise. This literature review compared vulnerability assessments reviewed to the four key elements of the proposed framework. The criteria for the comparison by framework element follows:

1 Scenarios – Does the reviewed vulnerability assessment include scenarios or scenario based analysis.

2 Common Tidal, Geodetic Vertical Datum Reference– Does the vulnerability assessment explicitly insure that a common reference or adjustment between tidal and geodetic vertical datums is exists.

3 Total Water Levels - Does the vulnerability assessment utilize analysis of extreme water level events, or utilize total water level models to define coastal forcing.

4 Performance - Does the vulnerability assessment explicitly attempt to account for performance changes caused by global sea level rise?

Table 1 - Review of Vulnerability Assessments

Author	Year	Main Focus	1	2	3	4
IPCC	1991	Common Methodology - Influential framework incorporating expert judgment and data analysis of socio-economic and physical characteristics to assist the user in estimating a broad spectrum of impacts from sea level rise.	Y	N	N	Y
Nicholls and Misdorp	1993	Synthesis of vulnerability analysis studies.	Y	N	N	Y
Nichols and Hoozemans	1996	Common Methodology (CM).	Y	N	Y	N
El-Raey	1997	Seven stage vulnerability assessment methodology.	Y	N	N	N
Klein and Nichols	1999	Identifies differences between the Common Methodology and IPCC Technical Guidelines.	Y	N	N	N
Kelly and Adger	2000	Focus on clarifying relationship between vulnerability and adaptation.	N	N	Y	N
Wu et al.	2002	This study demonstrates how sea-level rise increases the vulnerability of coastal communities to flooding associated with coastal storms.	Y	N	Y	N
Lewsey et al.	2004	Proposed sea level monitoring network and other measure to improve accuracy of climate forecasts.	Y	N	N	N
Ford and Smit	2004	Focus on arctic communities.	N	N	Y	N
Patt et al.	2005	Questions the validity of vulnerability assessments.	N	N	N	N
Patt and Dessai	2005	Focused on how to communicate uncertainty.	N	N	N	N
Tsimplis et al.	2005	Quantified the spatial and temporal dependency of sea level and wave heights on the North Atlantic Oscillation (NAO) for UK.	Y	N	Y	N
Smit and Wandel	2006	Adaptation in human communities are closely associated with adaptive capacity and vulnerability.	Y	N	Y	N
Füssel	2007	Defined two major interpretations of vulnerability end-point and starting point.	N	N	N	N
Johnson and Marshall	2007	Species specific vulnerability.	N	N	N	N
Tribbia and Moser	2008	Looked at what type of information is generally used.	Y	N	N	N
Snoussi et al.	2008	Mapping/GIS approach looked at broad area and used IPCC technical guidelines.	Y	N	N	Y
Sterr	2008	Suggested that vulnerability assessment changes are more accurate at smaller scales.	Y	N	Y	N
Dwarakish et al.	2009	Standard assessment using coastal vulnerability index (CVI).	N	N	N	N
Hinkel and Klein	2009	Presented the development of the DIVA (Dynamic and Interactive Vulnerability Assessment) tool.	Y	Y	Y	N
Rosati and Kraus	2009	Looked at RSLR and impacts to elements of coastal navigation projects – jetties, channels, dredged material disposal sites.	Y	Y	Y	Y
Ionescu et al.	2009	Applies mathematical expressions to IPCC definitions.	N	N	N	N
Kumar et al.	2010	Uses 9 risk variables to define vulnerability.	N	N	N	N

Preston et al.	2011	Defined framework types as Risk-Hazard (RH) models, Pressure-and-Release (PAR) models, and Expanded Vulnerability (EV) models.	N	N	N	N
Balica et al.	2012	Coastal City Flood Vulnerability Index (CCFVI).	Y	N	N	N
Hunter	2013	Technical paper deriving sea level change rates for vulnerability assessment planning.	Y	N	N	N
Hall and Marqusee	2013	Stressed the importance of the quality of elevation and location data.	Y	Y	Y	Y
Kriebel and Geiman	2014	Explores the definition of a generic coastal flood stage (FS), an elevation at which significant flooding of local infrastructure is initiated, for regional or nationwide use in flood hazard analysis for the US	Y	Y	Y	N
Ray and Brown	2015	Decision tree framework	Y	N	N	Y
Garster et al.	2015	Comprehensive Evaluation of projects with respect to Sea Level change (CESL).	Y	Y	Y	Y

2.2 Impact of Nonstationarity on Design Return Periods of Coastal Infrastructure

Olsen et al (1998) derives "expected waiting time" definition for return period for nonstationary conditions. Parey et al. (2007, 2010) and Cooley (2013) examine two definitions of return period under nonstationary conditions for hydrologic design. Salas and Obeysekera (2013) compare size of infrastructure needed to withstand a given design storm for stationary versus nonstationary return period.

Rootzen and Katz (2013) introduce a "Design Life Level" to relate risk over a planning period under nonstationary conditions. In a changing climate, risk assessment instead should include both a specification of the period when the construction will be in use, the design life period, and of the probability of exceeding a hazardous level during this period. Although some aspects of water resources management could continue to be based on an annual chance of occurring, adapting to its change from one year to the next, this would not be practicable for many design problems Besides Design Life Level, we also discuss a variant, termed Minimax Design Life Level, which focuses on the largest exceedance risk for any year of the design life

period. Further, the Risk Plots and Constant Risk Plots, as introduced below, may be used to follow how risk changes with time.

2.3 Impact of Nonstationarity on Coastal Water Levels

Current practice of assuming stationarity in hydrologic extremes may not be applicable for some future engineering designs (Salas and Obeysekera 2014). The non-stationarity in extremes such as floods may be due to human influences in watersheds such as land-use changes, construction of dams, and changes in the climatic regime. Recent advances in addressing non-stationarity of extreme events have allowed the extension of the concepts of return period and risk into a nonstationary framework

Over the last five decades, several different extreme value analysis methods for estimating probabilities of extreme still water levels have been developed. Arns et. al (2013), compared estimates of extreme water level probabilities using two of the main extreme value analysis methods and conducted a systematic sensitivity assessment of the different steps involved in setting up and using these statistical techniques.

2.4 Engineering Performance Metrics for Coastal Infrastructure, Reliability versus Return Period

Read, (Read and Vogel 2015) compared application of the average return period with the more common concept of reliability and recommended replacing the average return period with reliability as a more practical way to communicate event likelihood in both stationary and nonstationary contexts. Referring to a system's reliability directly conveys two pieces of information: the likelihood of no failure within a given number of years (i.e., over a planning horizon) and the accepted level of reliability that is implicit in the design.

Volpi et al. (2015) discuss the probabilistic concept of return period widely used in hydrology. Return periods are widely used, especially in engineering practice for design and risk assessment. Return period also rely on some basic assumptions that should be satisfied for a correct application of this statistical tool. The concept of Equivalent Return Period is introduced, which controls the probability of failure still preserving the virtue of effectively communicating the event rareness.

3.0: FRAMEWORK DEVELOPMENT–ELEMENTS AND STRUCTURE OF THE CLIMATE PREPAREDNESS AND RESILENCE REGISTER

The Climate Preparedness and Resilience Register (CPRR) framework outlines and categorizes procedures for an assessment of the historic and future design performance of existing coastal infrastructure. The CPRR framework may also be used to plan and assess new coastal infrastructure projects by applying the same methodologies in the planning and design process. The CPRR framework has four major elements (Figure 3) which are combined to create a framework which allows for accurate assessments of past and future coastal infrastructure design while considering the impact of global sea level change on coastal water levels. The major framework elements are developed in order starting with Datum Adjustment and ending with Performance Thresholds.

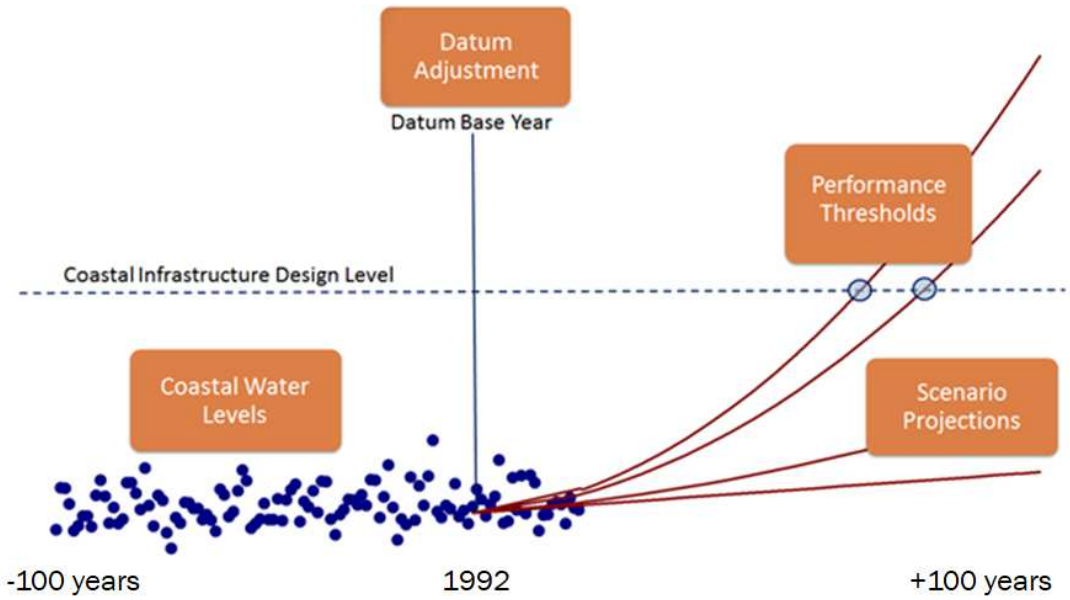

Figure 3 - CPRR framework, major elements

The elements of the framework are defined as:

1. Datum Adjustment. It is important to relate coastal forcing and current infrastructure performance to a common reference geodetic vertical datum, hence the need to convert local tidal datum to a geodetic datum. Tidal to geodetic datum adjustments are assumed to be at the midpoint of the current National Tidal Datum Epoch (NTDE). In the CPRR framework, the current year NTDE (1983-2001) midpoint, 1992 is referred to as the "datum base year".

2. Coastal Water Levels. The framework uses a component based model to define coastal water levels impacting infrastructure while accounting for past and future non-stationarity due to global sea level change. Component models such as the "Total Water Level" (TWL) (Ruggerio et al. 2001; Serafin and Ruggerio 2014) utilize coastal water level data from multiple sources; measured, computed and combinations to create a site-specific estimate of coastal forcing acting on coastal infrastructure. Coastal water levels are adjusted to the datum base year of 1992 for NOAA tidal stations to correctly reference the tidal datum to the geodetic datum.

3. Scenario Projections. A range of plausible scenarios are defined to examine future climate change and global sea level conditions. The relative rate of sea level change associated with the location of interest is applied to each of the future sea level change scenarios. Past and future water levels are adjusted for sea level change by scenario and normalized to the year 1992, the midpoint of the current NTDE (1983-2001).

4. Performance Thresholds. Performance functions are developed for one or several design component(s) of a coastal infrastructure which may be used to assess vulnerability.

> Performance thresholds are defined as the intersection of future projected coastal water level time series and a static infrastructure critical performance target. A time varying performance model is developed expressed in terms of elevation, function, and/or reliability. An elevation-based performance like flooding simply relates to the exceedance of a certain water level. The term function defines a non-elevation performance metric impacted by coastal water levels such as pump efficiency, wetland accretion and salinity, navigation gate closures, sedimentation, etc. A reliability-based performance metric allows for a significant refinement of vulnerability assessments by incorporating uncertainty into to critical performance targets typically based on design assumptions and other factors.

The reliability performance metric adds precision to the performance function by recognizing uncertainty within each scenario in the coastal water level and design (as built) inputs to the performance equation. The CPRR framework may inform the adaptive capacity or performance limit for existing coastal infrastructure once the performance threshold is found by revising the infrastructure critical performance elevation or function level.

The research goal is to define and categorize technical approaches and methods needed to develop the four primary elements of the CPRR framework. Performance is defined and tracked over time until a performance "threshold" is reached. Repeating the process under additional scenarios representing the range of plausible global sea level rise impacts provides a bounded estimate of when design performance will be negatively impacted or lost over time.

A CPRR analysis may utilize a tiered approach which begins using a simple elevation model in which performance is recognized as the static design or as-built elevation compared to a time series of a projected critical coastal water level based on a return level or some other key metric.

Using a distribution of possible values for analysis in both the coastal water level and infrastructure definitions will provide additional precision in computing performance thresholds. Because much of the coastal infrastructure in the United States was designed and constructed 50 to 100 years ago, the performance analysis period in CPRR may span 150 to 200 years when past and future performance is considered.

3.1 Datum Adjustment

A common vertical reference datum is necessary to convert the dynamic local tidal datum to a static, geodetic datum to account for non-stationarity in historical coastal forcing assumptions used to develop designs and to accurately assess performance over time. Accounting for past and future vertical datum adjustments and applying appropriate uncertainty to the adjustments is a key first step in a vulnerability assessment using the CPRR framework. In the United States, the current terrestrial vertical datum is NAVD88.

Perhaps the most critical foundation for a performance based assessment of coastal infrastructure is an understanding of the vertical datum in use at the time of design and construction, and the datum corrections (if any) made to coastal water levels used to support the design. In the United States, prior to the mid-1970s, the vertical datum used for many USACE projects was mean sea level (MSL) based on the Sea Level Datum of 1929, as defined by the U.S. Coast and Geodetic Survey in 1929. Sea Level Datum of 1929 served as a consistent national vertical datum and was referenced in various forms as “mean sea level”, “MSL”, or “MSL29”. In 1976, the Coast and Geodetic Survey formally changed the name of “MSL29” to National Geodetic Vertical Datum, or “NGVD29”. In doing so, the name “mean sea level” (referring to the vertical datum established in 1929) was changed, but the definition remained the same (NGS 2001). For national consistency in the United States, the vertical datum of NGVD29

has been replaced with the North American Vertical Datum of 1988 (NAVD88). Because NAVD88 and NGVD29 are defined using different methods, the two datums are vertically offset as shown in Figure 4 (USACE 2010).

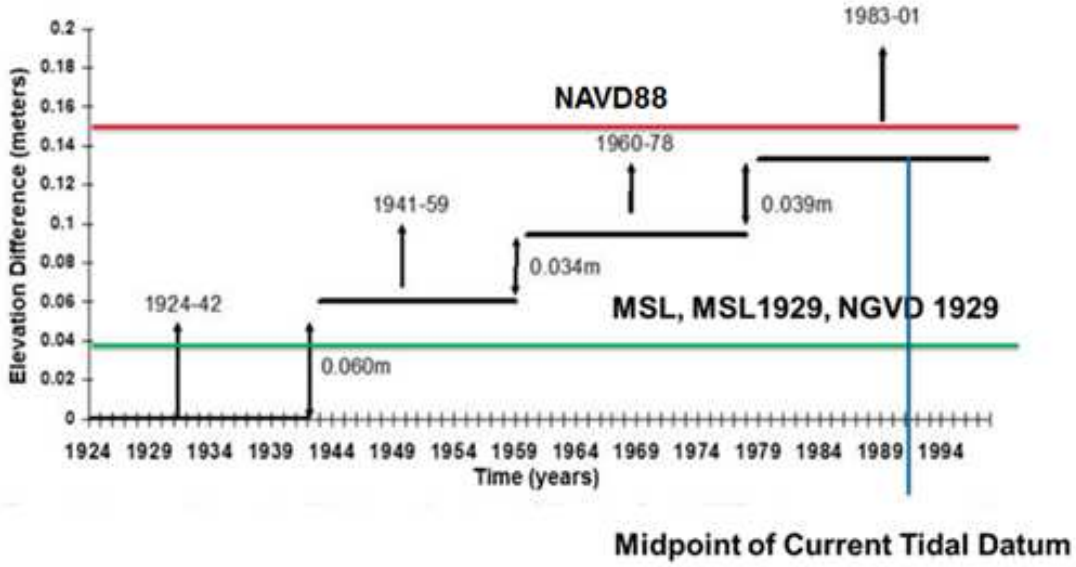

Figure 4 - Conceptual schematic depicting key relationships between tidal and geodetic datums

Sea level changes affecting coastal water levels are measured by tide gauges referenced to tidal datums. Tidal datums define a static mean sea level reference to the geodetic vertical datum NAVD88 or NGVD29 based on the current National Tidal Datum Epoch (NTDE). NTDE's are roughly 18 to 19 years and correspond to an 18.6-year astronomical cycle. In areas with high rates of vertical land movement impacting sea levels, such as Alaska and Louisiana, tidal datums are revised in 5-year cycles.

The CPRR is developed with the current NAVD88 vertical datum for vulnerability assessments made in the continental United States. The CPRR may be applied internationally using the same principles, changing the reference to the local geodetic datum. The CPRR framework utilizes a simplifying assumption that the current vertical, geodetic datum in use,

NAVD88 is static, and incorporates adjustments from the current tidal datum and older geodetic datum, NGVD29 to place coastal water levels adjusted for non-stationarity and existing coastal infrastructure elevations on the same baseline.

3.2 Coastal Water Levels

The key processes which impact design and performance of coastal infrastructure are tides, winds, precipitation and waves. Several researchers have described a component based or "Total Water Level" (TWL) approach (Ruggerio et al. 2001), (Serafin and Ruggerio 2014), and (Moritz et al. 2017). Since the TWL model components are process based, it is often used to design coastal infrastructure.

3.2.1 Methodology, Total Water Level Model

Coastal TWL's influenced by tides are the result of complex interactions between multiple oceanographic, hydrological, geological and meteorological processes that act over a wide range of spatial and temporal scales. Important components of the TWL model include astronomical tide, wave set-up, wind set-up, large-scale storm surge, precipitation, fluvial discharges, monthly mean sea level, and land subsidence/uplift. The contribution of each component of a TWL has the potential to significantly alter spatially and temporally varying flood hazards, resulting in a complex and non-linear problem. Local, site specific topography, bathymetry, shoreline type and presence engineered structures greatly influences the relative contribution and magnitude of individual components comprising a TWL. Under certain conditions, some TWL factors can be neglected, and linear superposition of various terms is appropriate, resulting in a relatively manageable problem from a hydrodynamic and statistical point of view (Moritz et al. 2017).

The TWL model allows for application of extreme value theory to individual components or combinations of TWL's representing combinations of separable physical processes. Application of a TWL model to design criterial may be targeted to address individual coastal processes. Figure 5 shows a TWL model of simple open coast profile with a coastal structure. The still or static water level is defined as

$$SWL = MSL + \eta_A + \eta_{NTR} \tag{3.1}$$

where MSL is the mean sea level, η_A is the deterministic astronomical tide, and η_{NTR} is the non-tidal residual η_{NTR} is given as

$$\eta_{NTR} = seasonal\_cycle + MMSLA + SS + Q \quad (3.2)$$

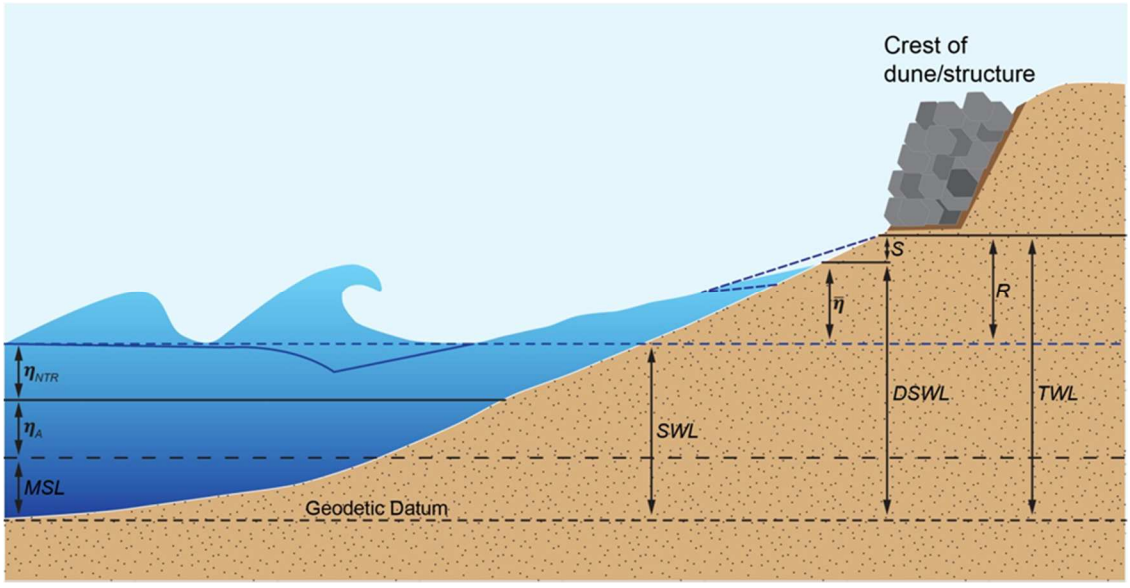

Figure 5 - Schematic, generalized elements of a coastal total water level impacting a coastal structure

and is defined as any elevation change in the SWL not related to the astronomical tide. The

seasonal cycle can be substantial (on the order tens of centimeters) due to cyclical changes in water temperature and other coastal forcing. The η_{NTR} also includes low frequency monthly mean sea level anomalies (MMSLA) associated with water level variability due to water temperature and the geostrophic effects of currents (e.g., processes associated with the El Niño-Southern Oscillation, ENSO), and/or relatively high frequency components due to the presence of winds and low atmospheric pressure (e.g. storm surge, SS). In sheltered environments, precipitation and river discharge, Q, also contribute significantly to η_{NTR} (Figure 3-4). (Moritz, et al. 2017)

The dynamic still water level, DSWL (Figure 6), combines the SWL as defined above (Equations 3.1 and 3.2) with wave induced changes to the mean sea surface and wave induced water level fluctuations on the order of minutes, and is defined as

$$DSWL = SWL + \bar{\eta} + \eta' \tag{3.3}$$

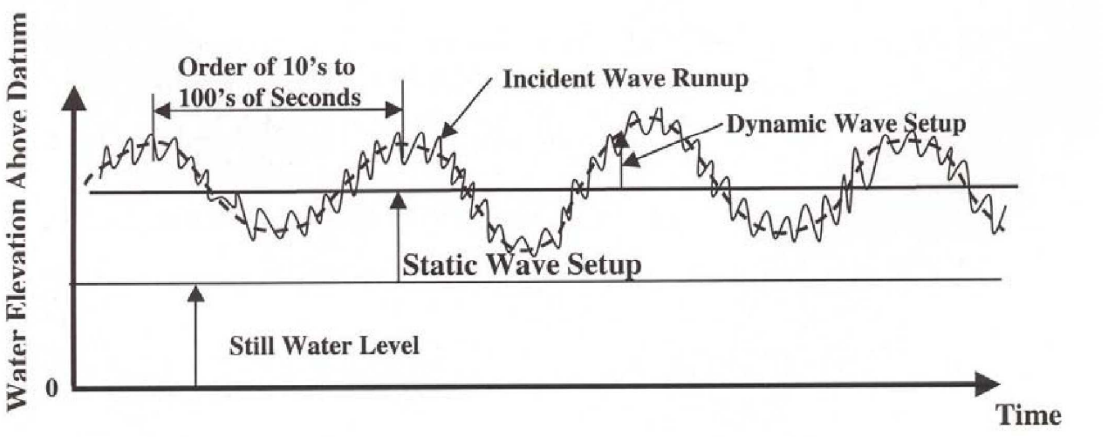

Figure 6- Dynamic, Static wave setup schematic diagram

$\bar{\eta}$ denotes the mean water level in the presence of waves including wave setup (a super elevation of the water level due to wave breaking which reaches its maximum at the shoreline, and set

down. η' indicates additional low frequency water level fluctuations due to waves caused by processes such as bound long waves and wave groups. In many situations, the DSWL should be used to compute depth limited breaking wave heights for project applications. In situations where swash processes are negligible (e.g., waves impinging directly on a breakwater), the TWL is equal to the DSWL. When waves run-up on coastal protection structures or beaches, swash processes are non-negligible and

$$TWL = DSWL + S \tag{3.4}$$

where swash, S, consists of contributions from both the incident band, S_{inc}, and the infragravity band, S_{ig}, as

$$S = \sqrt{S_{inc} + S_{ig}} \tag{3.5}$$

Existing condition TWL's may be modified and projected for the entire range of possible future rates of RSLR, represented a scenario describing a global sea level rise prediction. The methods for this adjustment and a discussion of scenarios is follows in section 3.3. The local RSLC rate is applied to the equations developed for various scenarios and projected from the datum base year of 1992. This procedure sets the start year for the three USACE scenarios at the datum base year 1992, and insures that the datum adjustment to NAVD88 is not over or under adjusted. Existing condition TWL's adjusted from the local tidal datum to NAVD88 reflect the datum base year of 1992 since the datum adjustment from the floating tidal datum to the static geodetic datum is reflected in the average shift of mean sea level over the 19-year tidal epoch. Figure 3 illustrates this concept, the changes to the tidal-geodetic datum reference are averaged out over the 19-year tidal epoch, creating a step-wise plot.

TWL's are adjusted for RSLC using the assumption of linear superposition, that is, a time-based increment of elevation change is added or subtracted to the static TWL. The dynamic TWL components are added to the revised static TWL. In some cases, the adjustment in the static TWL may result in a transition from a depth-limited condition for dynamic TWL, causing an abrupt change in the dynamic TWL or a non-linear shift. Thus, transitions in TWL's should be evaluated for significant elevation changes. More complex interactions with local topography and bathymetry may cause non-linear effects and additional calculation to account for the non-linear combinations.

TWL's may be categorized in probabilistic terms as annual exceedance probability (AEP) water levels, adjusted to the year 1992. In practical terms, as sea level increases with time, AEP will change as well. An AEP 10% 1992 datum base year TWL elevation will increase in frequency of occurrence as sea level increases. Thus, TWL AEPs adjusted for future SLC represent dynamic return periods with respect to the datum base year elevation and the scenario projection. This concept has implications for design performance assessment and future vulnerability.

Figure 7 below shows a graphical component based summary of the TWL model as applied to coastal water levels.

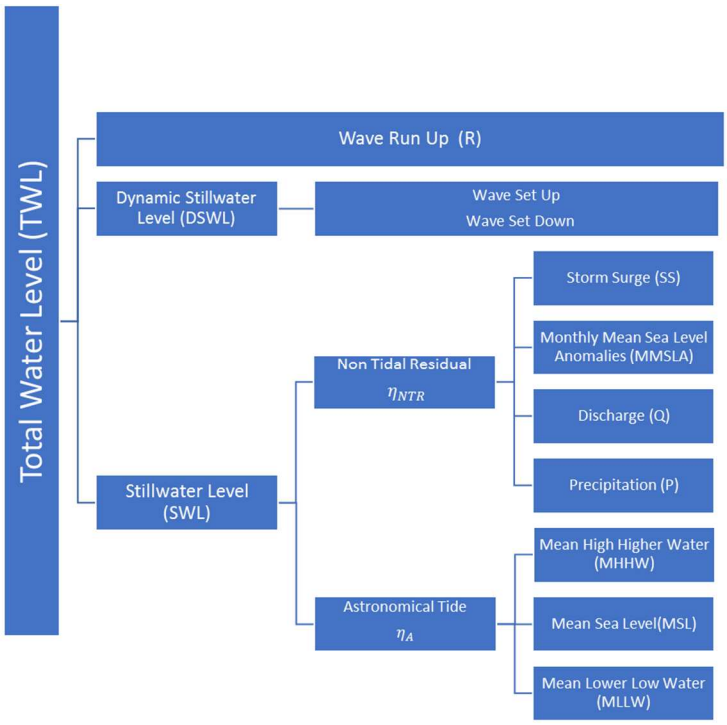

Figure 7 – Schematic of TWL model with individual components

3.2.1 Methodology, Applying Statistical Models to Coastal Water Levels

Time series data of measured water level data may be used to develop AEP estimates for a CPRR assessment using tide gauge records or tidally influenced gages. The proposed methodology to apply local tide gauge data at a coastal infrastructure site is to:

1. Convert data from local tidal datum to NAVD88 (geodetic datum) (Datum Adjustment)
2. Detrend data (remove historical linear mean sea level trend due to RSLC) to datum base year 1992.
3. Apply empirical distributions to detrended data set, typically Generalized Extreme Value (GEV)

4. Estimate parameters

5. Fit statistical model(s) to data, rank using goodness of fit tests

The detrended data set represents a stationary data set to which one or more statistical models may be fit as described in step 5. Table 2 lists common statistical models which may be used.

Table 2 - Statistical Models, Empirical Distributions, and Parameter Estimation Techniques recommended for Extreme Water Level analysis

Statistical Model Probability Density Function	Empirical Distribution Plotting Position	Parameter Estimation
Normal	Weibull (1939)	Maximum Likelihood Estimation (MLE)
Logistic	Gringorten (1963)	Method of Moments (MOM)
Lognormal	Hazen (1914)	L-Moments
Log Pearson III	Beard (1943)	Probability Weighted Moments (PWM)
Generalized Pareto Distribution (GPD)	Hirsh (1987)	
Generalized Extreme Value (GEV)	Cunnane (1978)	
Non-Parametric Techniques	Blom (1958)	
	California (1923)	
	Adamowski (1981)	
	Chegodayev (1955)	

Best practices for developing extreme water level probability using tide gauge or other coastal water level records are presented in (Arns, et.al. 2013). Figure 8 shows a workflow for developing extreme water level statistical models.

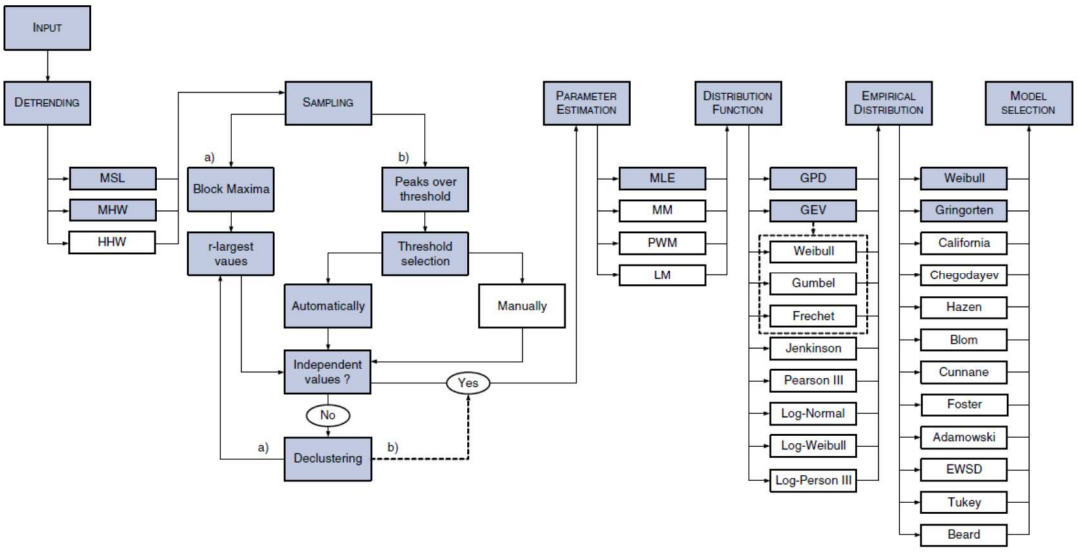

Figure 8 - Flow chart for processing extreme water level probabilities from nonstationary measured data impacted by global sea level rise. Graphic from Arns (2013)

The GEV model is most commonly used to develop extreme value statistics from coastal water levels from observed tide gauge data. These data are assumed to be SWL and may have to adjusted by adding dynamic TWL components for some vulnerability assessments.

3.3 Scenario Projections

Vulnerability assessments of existing coastal infrastructure rely on application of the most current science to prediction of changes induced by global sea level change and climate change. At this time, there is no consensus prediction of the magnitude of global sea level change with in the proposed assessment time frame of 100 years. Figure 9 shows the range of global sea level rise projections, 1987 to 2013 (NRC 1987), (IPCC 2001), (IPCC 2007), (Rahmstorf 2007), (Horton 2008), (Pfeffer 2008), (Vermeer and Rahnstorf 2009), (Jevrejeva et al. 2010).

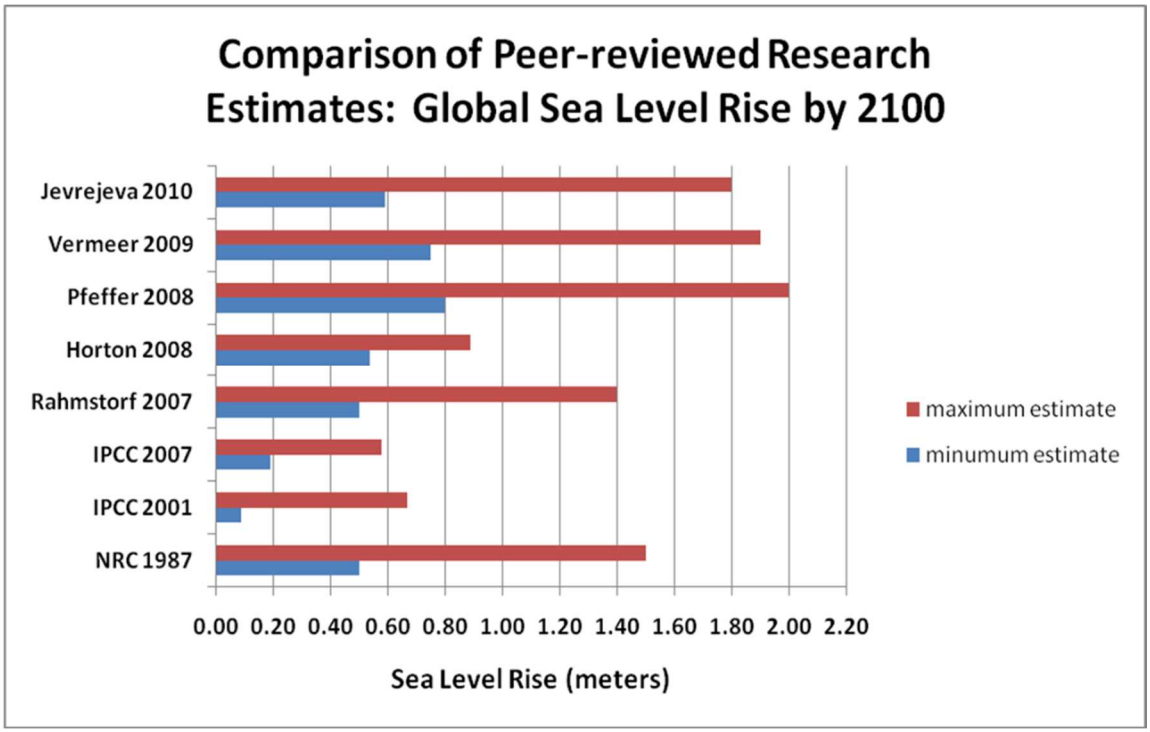

Figure 9 - Range of Global Sea Level Rise Projections, 1987 to 2013 (Graphic, Pers. Communication, White 2016)

The range of overall global sea level rise future projections is large, including the range within individual projections, suggesting that assigning probabilities to any one projection would not be useful. The range of estimates since 1987 confirm the paradigm shift from the recent past of stationarity or non-stationarity with predictable changes to a wider range of uncertainty requiring a shift in evaluation techniques for vulnerability assessments. In fact, prematurely down-selecting to one future or assigning probabilities a priori to any of these projections could result in inaccurate vulnerability assessments of coastal infrastructure.

The CPRR framework recommends that a scenario based approach be utilized to make coastal vulnerability assessments. The use of scenarios to make vulnerability assessments is supported by the following points (Pietrowsky 2011);

1. Scenarios are appropriate when uncertainties are large, the consequences are significant, and outcomes cannot be bounded.

2. Sea level change (and more broadly, broader climate change) meets the first and last of these three conditions.

For the second condition, sensitivity analysis may be used to determine the potential consequence of sea-level change, and the sensitivity test guides our scope of study and the rigor of the scenario analysis. The CPRR framework supports a tiered analysis approach, utilizing application of parametric, non-parametric, and reliability analysis techniques to adjust estimates of coastal water levels, design or existing performance within the constraints of a scenario. Additional analysis within the framework components may add precision a vulnerability assessment, and more importantly offer valuable information such as rates of performance loss under the range of global sea level rise scenarios analyzed.

Global sea level rise scenarios are related to global climate scenarios. Climate scenarios are plausible representations of the future that are consistent with assumptions about future emissions of greenhouse gases and other pollutants and with our understanding of the effect of increased atmospheric concentrations of these gases on global climate. A range of scenarios can be used to identify the sensitivity of an exposure unit to climate change and to help policy makers decide on appropriate policy responses. It is important to emphasize that, unlike weather forecasts, climate scenarios are not predictions (Carter 2007).

The choice of climate scenarios and related non-climatic scenarios is important because it can influence the outcome of a coastal infrastructure vulnerability assessment 100 years into the future. Extreme scenarios can produce extreme impacts; moderate scenarios may produce more

modest effects (Smith and Hulme 1998). It follows that the selection of scenarios can also be controversial, unless the fundamental uncertainties inherent in future projections are properly addressed in the impact analysis (Carter 2007). When evaluating results of a vulnerability assessment developed with the CPRR framework, conceptually, the scenario based analysis informs the potential timing, so that question comes down "when, not it "performance will be impacted.

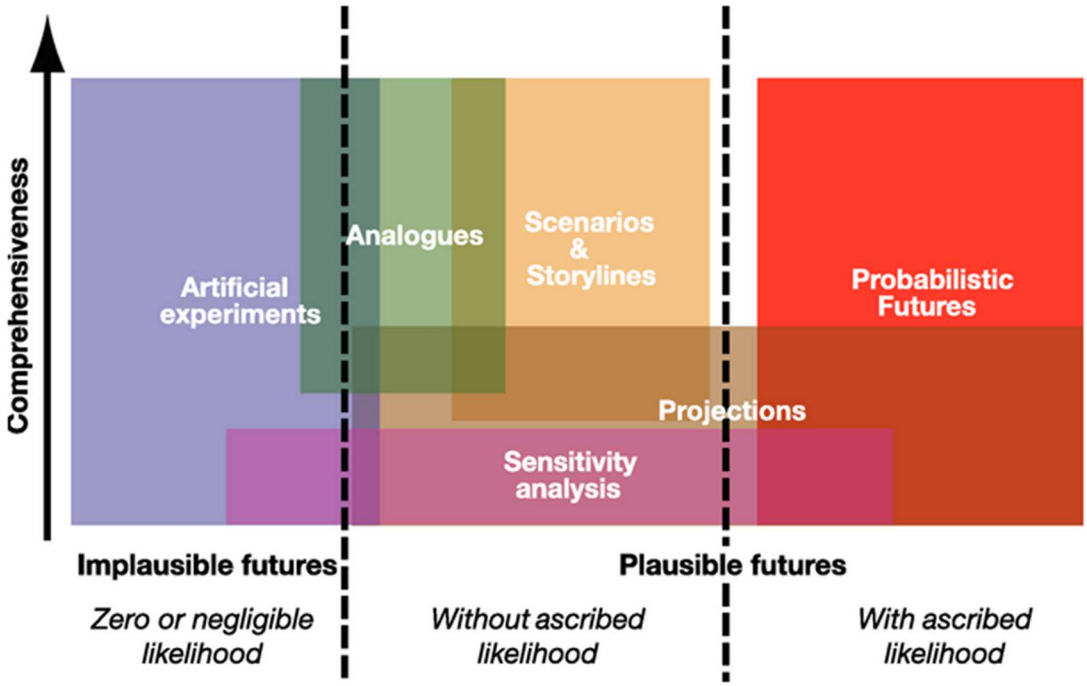

Figure 10 –– Diagram describing types of information with corresponding uncertainty against level of detail

Carter (2007), provides definitions and guidelines for commonly used terms used in developing coastal water level data for analyses (Figure 10).

Projection. The term "projection" is used in two senses in the climate change literature. In general usage, a projection can be regarded as any description of the future and the pathway

leading to it. However, a more specific interpretation has been attached to the term "climate projection" by the IPCC when referring to model-derived estimates of future climate.

Forecast/Prediction. When a projection is designated "most likely" it becomes a forecast or prediction. A forecast is often obtained using physically-based models, possibly a set of these, outputs of which can enable some level of confidence to be attached to projections.

Scenario. A scenario is a coherent, internally consistent and plausible description of a possible future state of the world (IPCC 1994). It is not a forecast; rather, each scenario is one alternative image of how the future can unfold. A projection may serve as the raw material for a scenario, but scenarios often require additional information (e.g., about baseline conditions). A set of scenarios is often adopted to reflect the range of uncertainty in projections. Other terms that have been used as synonyms for scenario are "characterization", "storyline" and "construction". The use of multiple scenarios is recommended for vulnerability assessments of coastal infrastructure in the CPRR framework.

Baseline/Reference. The baseline (or reference) is any datum against which change is measured. It might be a "current baseline", in which case it represents observable, present-day conditions. It might also be a "future baseline", which is a projected future set of conditions excluding the driving factor of interest. Alternative interpretations of the reference conditions can give rise to multiple baselines. Establishment of a common vertical datum with a time stamp lead to using the term datum base year as the common starting point for past, present and future performance analysis, one of the key principles in the CPRR framework.

3.3.1 Methodology, Developing Scenario Based Relative Sea Level Change Projections

Future global mean sea level change projections are applied to coastal water levels using equation 3.6, from (NRC 1987) and (USACE 2011a).

$$E(t) = 0.0017t + bt^2 \tag{3.6}$$

where

t - time in years, starting in the datum base year 1992

E(t) - the eustatic SLR in meters as a function of t

b - a constant, which applies an acceleration factor to non-linear global SLR future trajectories

For projections after the datum base year 1992, the equation 3.6 is modified

$$E(t_2) - E(t_1) = 0.0017(t_2 - t_1) + b(t_2^2 - t_1^2) \tag{3.7}$$

where t_1= time is the time between the beginning year of interest and 1992 and

t_2 is the time between the ending year of interest and 1992 (USACE 2011a, Flick et al. 2012). Table 3 lists coefficients for commonly used global sea level rise scenarios for the United States developed by USACE and NOAA.

Table 3 - United States and Global Sea Level Change Scenario "b" coefficients

Source	Scenario	"b"
NRC	Observed	0
USACE	Low	0
NRC	modified NRC Curve I	0.0000271
NRC	modified NRC Curve III	0.000113
USACE	Intermediate	0.0000271
USACE	High	0.000113
NOAA	Intermediate-Low	0.0000271
NOAA	Intermediate-High	0.0000871
NOAA	Highest	0.000156

Eustatic sea level rise (USACE, 2013) is caused by the global change in the volume of water in the world's oceans in response to three climatological processes:

1. ocean mass change associated with long-term forcing of the ice ages ultimately caused by small variations in the orbit of the earth around the sun, density changes from total salinity and

2. changes in the heat content of the world's oceans

Relative (local) sea level change (RSLC) is the local change in sea level relative to the elevation of the land at a specific point on the coast. RSLC is a combination of both global and local SLC caused by changes in estuarine and shelf hydrodynamics, regional oceanographic circulation patterns (often caused by changes in regional atmospheric patterns), hydrologic cycles (river flow), and local and/or regional vertical land motion (VLM), subsidence or uplift. Relative SLC or RSLC refers to the combination of the global eustatic SLR and vertical land motion downward or subsidence. Equation 3.2, does not contain local VLM. Local RSLC rates are developed by combining the eustatic rate of 0.0017 meters plus the VLM. In practice, RSLC rates are determined from the linear trend of mean sea level from tide gauge records near a location of interest where a CPRR will be developed. In the US, RSLC rates are published from

NOAA tide gauge records, and a rate from a tide gauge close to the site of interest may be used. Equation 3.2, is modified, replacing the 0.0017 with the published tide gauge rate in meters as:

$$RSLC(t) = Mt + bt^2 \tag{3.8}$$

t = time in years, starting in 1992

RSLC(t) is the RSLC in meters as a function of t

b is a constant, which applies an acceleration factor to non-linear future trajectories.

M = RSLC (meters), published rate from tide gauge data or developed from linear trend of tidal component of tidally influenced gauges

3.3.2 Methodology, Applying Scenario Projections to Coastal Water Level Statistical Models

Future projections are developed using the nonstationary GEV model (Coles et al. 2001) modified using the global sea level rise scenario equations (Equation 3.8 $E(t) = Mt + bt^2$). For any future year t, water levels adjusted for RSLR may be described by

$$\mu(t) = \mu_{1992} + Mt + bt^2 \tag{3.9}$$

where μ = GEV location parameter developed from data detrended to the year 1992

t = future year (subtracted from 1992)

M = RSLR rate in meters/year

b = RSLR acceleration factor (equation 3.6)

Equation 3.9 can be applied to develop AEP data for future years under any scenario. The GEV developed from 1992 detrended data is adjusted for future years by adding RSLR to the location parameter. The shape and scale parameters are held constant.

3.4 Performance Thresholds

The performance threshold element of the CPRR framework is designed to identify a non-performance condition based on a coastal water level. The TWL model is used to describe the dominant processes and frequency of occurrence which controls infrastructure performance being investigated. Table 4 shows a list of common processes with frequency of occurrence. Frequency of occurrence under RSLC is variable since the base condition is changing.

Table 4 - Performance categories, frequency of occurrence, process. (adapted from Moritz et al. 2017)

Performance Category	Process	Frequency	Typical Return Period
Inundation	Short-term flooding Long-term flooding	High frequency Low frequency	5 to 20 year 20 to 1000 year
Erosion	Short-term erosion Long-term erosion	High frequency Low and high frequency	5 to 20 year 10 to 50 year
Wave Damage	Structure damage Stability	Low frequency	50 to 100 year
Hydrostatic Loading	Differential loading	Low and high Frequency	5 to 50 year
Hydrodynamic Efficiency	System drainage	Low and high frequency	5 to 50 year
Operating Conditions	Wave run-up, overtopping, transmission	High frequency	2 to 20 year
Water Quality	Water quality	High frequency	2 to 20 years
Water Management	Operational Criteria	Low and High Frequency	Sub 1 to 500 year

3.4.1 Methodology, Elevation-Based Performance Model

To assess performance using an elevation-time performance model, several pieces of information must be developed for the infrastructure being assessed.

1. Define the critical design elevation based on a static (geodetic) elevation
2. Performance criteria based on original design
3. Performance criteria based on current design or existing condition

The critical elevation is defined as the elevation at which performance is measured. In the lowest tier of analysis, it may be defined as the elevation at which a water level crosses a structural elevation threshold, such as a levee crest or top dike. Performance may be tied to the water level crossing which is a significant if not a damaging event. Critical elevations are often tied to specific physical processes for which the infrastructure is designed to perform against coastal forcing defined by water levels. Typically, an elevation based metric will be defined as a limit state or performance/non-performance metric, such that a water level exceeding the critical elevation is defined as non-performance. This elevation may be defined as the crest of a coastal levee, or some elevation above or below the crest at which will trigger a process which represents a condition at which the design fails or does not perform. For example, a water level elevation above the crest of a coastal dike which meets and exceeds the defined critical elevation when combined with a duration may represent an overtopping flow rate which is exceeds design standards causing a process such as erosion which can lead to failure. Similarly, a water level which meets and exceeds a defined critical elevation which is below the coastal dike crest may trigger a different process leading to non-performance or failure such as seepage or flow transmission through the dike. In practice, a coastal structure may have one or more critical elevations which are tied to specific processes which are triggered by water levels meeting or exceeding those critical elevations.

Figure 11 shows two performance metrics for an armored coastal structure. Rear side or back slope erosion performance is measured by overtopping rate, which would be a CPRR analysis which is based on a process – overtopping rate. While it is possible to convert the critical or non-performing overtopping rate to an elevation, since the performance metric is based on a flow rate, it is clearer to present the performance analysis using function based parameter such as flow rate. The second performance metric in Figure 11, armor stability, would be a CPRR analysis which is based on an on an elevation based performance threshold. In this case, the critical water level metric is wave height at the structure.

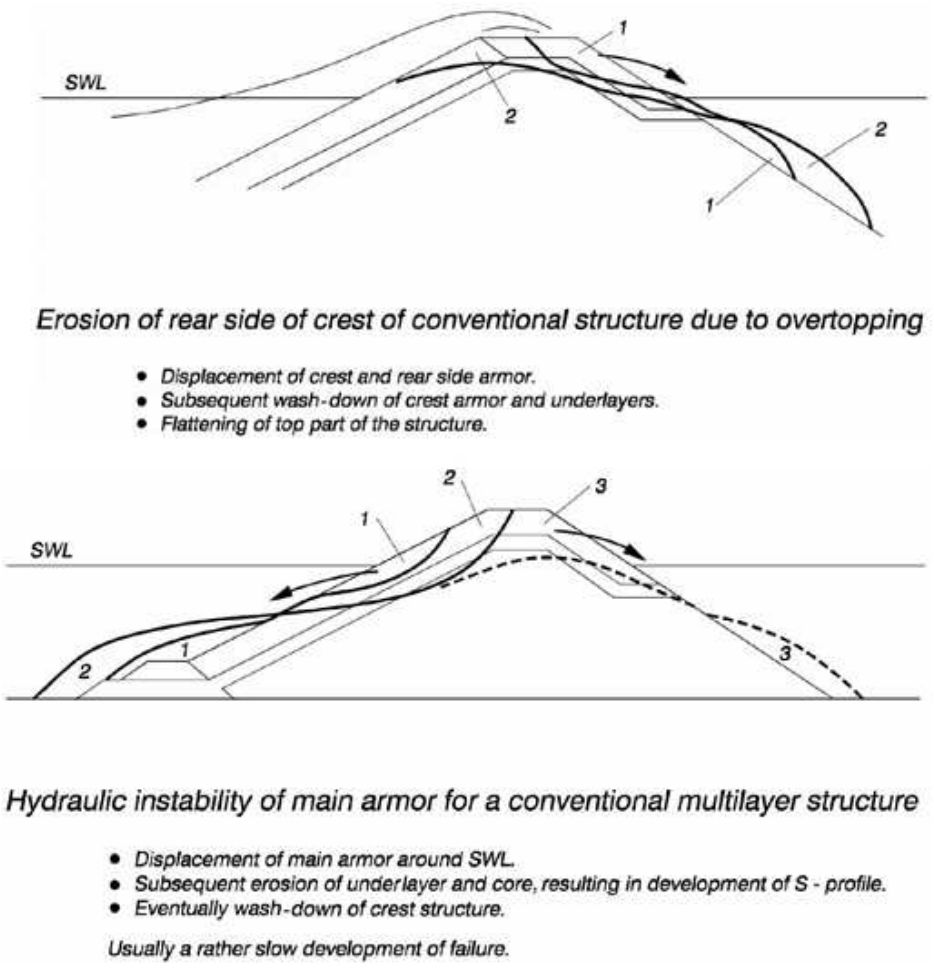

Figure 11 - Non-performance (failure) modes for an armored coastal structure, (USACE 1984)

Figure 12 shows a coastal structure showing failure or non-performance of an armor stone design. The photo shows displacement of some of the large armor stone, several feet of sand cover the area of armor stone displacement. Waves are visible around armor stone loss which has created a gap or low area vulnerable to additional wave overtopping.

Figure 12 – Example of non-performance, armored coastal structure, Humboldt Jetties, Aug 2016. Photo by Patrick O'Brien

3.4.2 Methodology, Function-Based Performance Model

A function based performance assessment is used to where the design purpose of the infrastructure is more readily defined as a function rather than a static elevation. To apply a function based performance metric, a critical performance threshold must be defined based on the function being assessed. An example of functional performance are gate closures for a

coastal navigation project. The closure frequency is tied to a coastal water level and duration of the closure tied to interior drainage. Another example of a function based performance assessment is pump station efficiency for an interior drainage system whose outfall is impacted by coastal water levels (USACE 2014b). The pump station was sized at 1800 cubic feet per second (cfs). In this example, there was no performance threshold defined, and efficiency, expressed in horsepower (HP), was evaluated against RSLC at the project site at 50 and 100 years into the future (Figure 12). A more comprehensive evaluation would have established a performance threshold in HP and computed a time series of efficiency in HP.

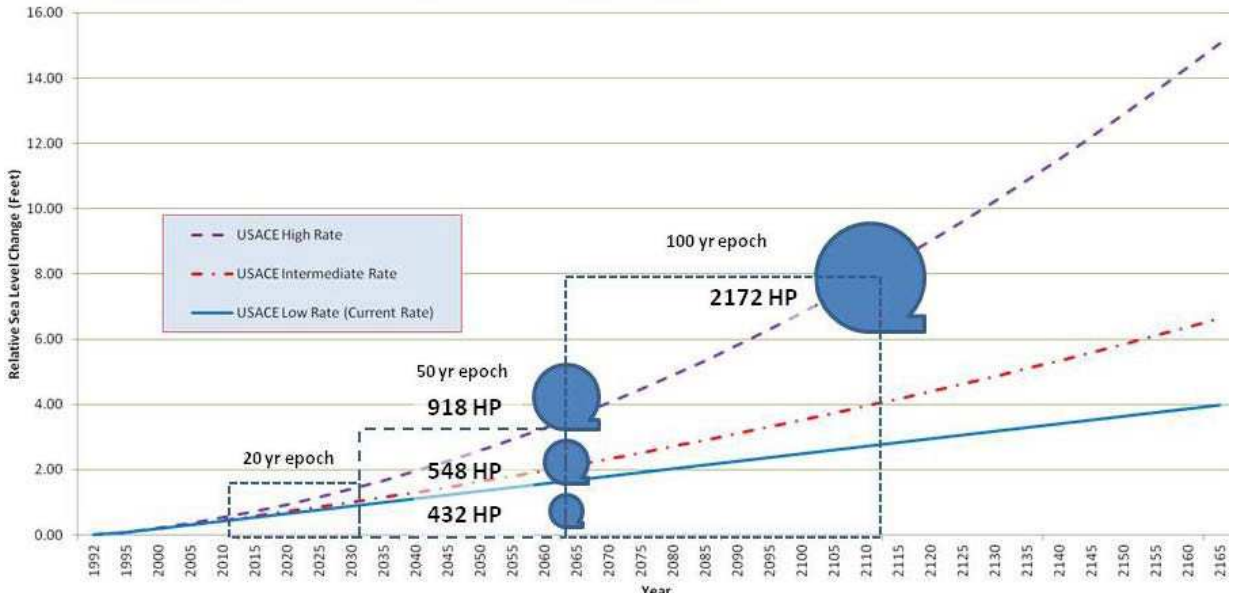

Figure 13- Example function-based performance model for an 1800 cfs pump station

3.4.3 Methodology, Reliability-Based Model

The highest level of analysis in the CPRR framework is based on reliability. A reliability based time series is created for one or more scenarios and performance may be assessed.

Performance thresholds for reliability are based on risk tolerance. Typically, satisfactory performance is defined as 0.5 which means that loading and forcing are equal.

Applying reliability is a significant refinement of the lower level assessment allowing parametric and non-parametric uncertainty to be applied. Reliability is computed for each time step with RSLC applied to the coastal water level being assessed. A benefit of using a reliability-based model is that it provides an improved performance window estimate as well as how fast performance declines as it nears a defined reliability threshold.

Performance of existing coastal infrastructure is defined using a limit state approach borrowed from reliability engineering which defines unsatisfactory performance. Kamphuis, (Kamphuis 2010) describes a probabilistic design technique defined by:

$$R = \Gamma S \tag{3.10}$$

where R is the resistance or strength of the structure, S is the design load (typically related to a AEP water level), and Γ is the factor of safety (Reeve 2006, 2009, Kamphuis 2010).. Failure is a binary or step function, when $R > \Gamma S$ the probability of failure is 0, when $R < \Gamma S$, the probability of failure is 1. The Limit State Equation, is an expression which grossly represents the design equation, defines the failure function as:

$$G = R - S \tag{3.11}$$

Where G is called the failure function. When G > 0, the design condition fails or does not perform. Using this basic model, we can use it to define performance with G representing the performance variable. The CPRR framework uses the term non-performance instead of failure. One of the goals of a CPRR analysis is to assess infrastructure performance across a wide range of plausible futures and define performance thresholds for one or more scenarios

which define a time window, allowing for a planned intervention in the future before a non-performance condition leads to failure.

Performance in the CPRR framework is represented using this equation, holding R constant representing the design or modified to represent the existing condition. The S side of the equation with RSLC added over time is represented as a time series representing a distribution of coastal water levels representing a design or ad-hoc load on a coastal infrastructure design element, typically a water level defined as an AEP. The time series of elevations representing S is dynamic and rises or falls when the impact of RSLC is accounted for in both the past and future water levels. S is defined using the component based coastal water level model, and the TWL may also be represented by a parametric distribution function fit to data. For example, observed tide gauge data is usually considered still water (SWL). The representative distribution is shifted to the right, by adding or subtracting RSLC to the measure of central tendency or location parameter, creating a snapshot of the performance function at a future date. Figure 14 illustrates this concept, as sea level rise component is added to the distribution creating a new stationary distribution of coastal water levels, adjusted for RSLC.

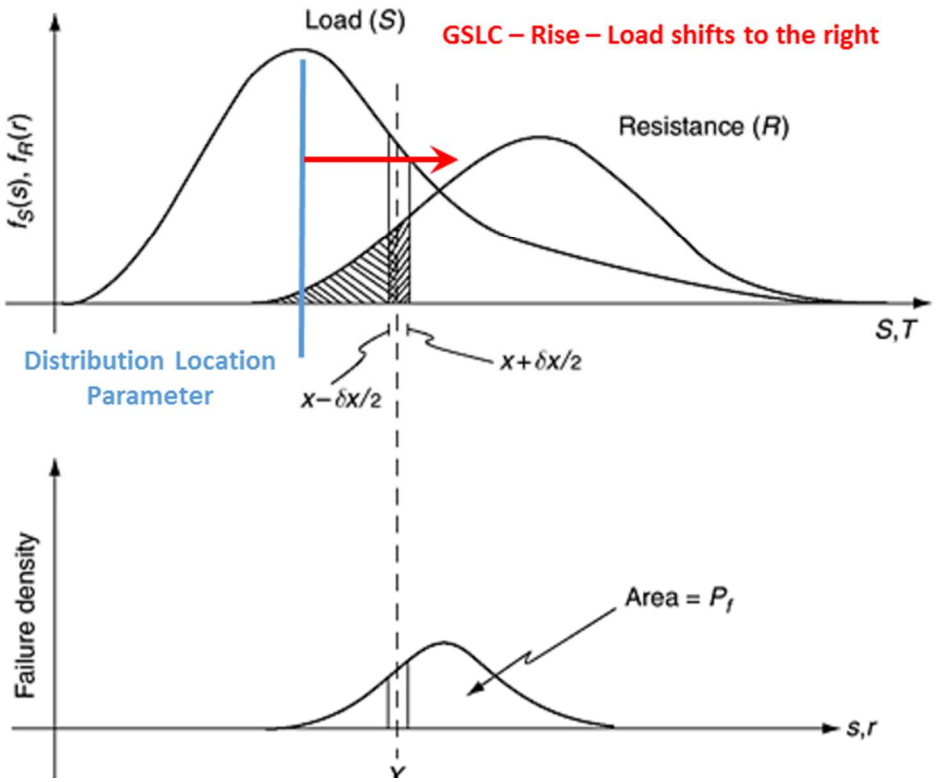

Figure 14 - Modification of the basic reliability model for reliability-based performance model under RSLC, adapted from Reeve (2009)

Older coastal infrastructure may have been designed using equations or methods which have now been superseded. A CPRR analysis may explore performance under the original, older design assumptions and refine the analysis based on current design standards. Original design assumptions may be impacted by current practice on both sides of the performance equation, on the load side, non-stationarity was not recognized in water level analysis used to develop extreme water level probabilities which resulted in an under estimation of return period estimates. On the resistance side, many design equations for coastal structures have been revised or replaced with new ones. Despite these factors, resulting from lack of information, engineers designing coastal infrastructure in the last 100 years used an effective factor of safety which

accounts for the continued satisfactory performance of coastal infrastructure despite significant levels of sea level rise over the last 100 years.

The CPRR framework is designed to assess performance using increasing levels of detail in a tiered approach. Owing to the large variety, and complexity of coastal infrastructure types and subcomponents, the CPRR framework utilizes three performance models:

1. Elevation-based
2. Function-based
3. Reliability-based

The two performance categories may be analyzed in greater detail by applying parametric uncertainty to key design elements in reliability analysis. Refinement of the performance function will cause the performance threshold estimate to adjust and add precision to the CPRR analysis. Many coastal structure designs are based on physical model tests which have produced empirical performance ranges for design elements. These performance ranges may be incorporated into the performance function using parametric distributions. The highest level of analysis converts the two performance categories to a reliability function. There are several advantages of using reliability in a CPRR analysis:

1. The reliability function uses the same basic load-resistance model, with uncertainty defined on both sides of the equation.
2. Reliability analysis may be conducted at additional levels of detail, including stochastic simulation of both load and resistance elements.

3. Reliability is a better metric for evaluating risk and vulnerability (Read and Vogel 2015) than the traditional return period concept which is not well suited to non-stationarity.

Applying reliability to continuous time series representing a future global sea level change scenario may provide added resolution and understanding of future performance. A time series of reliability representing performance will provide information on the trajectory of performance change under a range of accelerating global sea level rise scenarios.

4.0: CASE STUDIES DEMONSTRATING APPLICATION OF THE CPRR FRAMEWORK; ELEVATION AND RELIABILITY-BASED PERFORMANCE MODELS, SAN FRANCISCO WATERFRONT

4.1 San Francisco, California, USA Waterfront CPRR

4.1.1 Background

The San Francisco seawall delineates the boundary between San Francisco's landside and San Francisco Bay. It provides coastal flood protection to the City's landside infrastructure, including the Embarcadero, the Financial District, local and regional light rail transit systems, and key utility infrastructure, including the City's combined sewer system. The seawall, including the historic bulkhead wharfs and adjoining finger piers are part of the Embarcadero Historic District, was listed on the National Register of Historic Places in 2006.

The seawall was designed and built in the mid to late 1800's to convert the irregular coastline of sandy cover and rock outcrops to a deep-water waterfront with associated infrastructure to provide for increased shipping traffic and commerce. The seawall was constructed from 1879 to 1916 by the California Board of State Harbor Commissioners, hundreds of feet bayward of the natural shoreline atop Young Bay Mud (Figure 15). The seawall supports land built of fill material that is prone to liquefaction in an earthquake.

The seawall and waterfront were selected for a demonstration of the CPRR technique because of it is a well-known location and contains many critical infrastructure elements for which vulnerability assessments would be performed for impacts to sea level change in the near and long term as part of overall all urban planning activities. The critical infrastructure elements are easily separable and identifiable.

Figure 15 -Map of San Francisco Waterfront and Seawall (image from Los Angeles Times, April 2016)

The seawall supports major infrastructure such as roadways, buildings and underground mass transit systems by providing a raised elevation which provides protection from tidal driven water levels in San Francisco Bay (Figure 16).

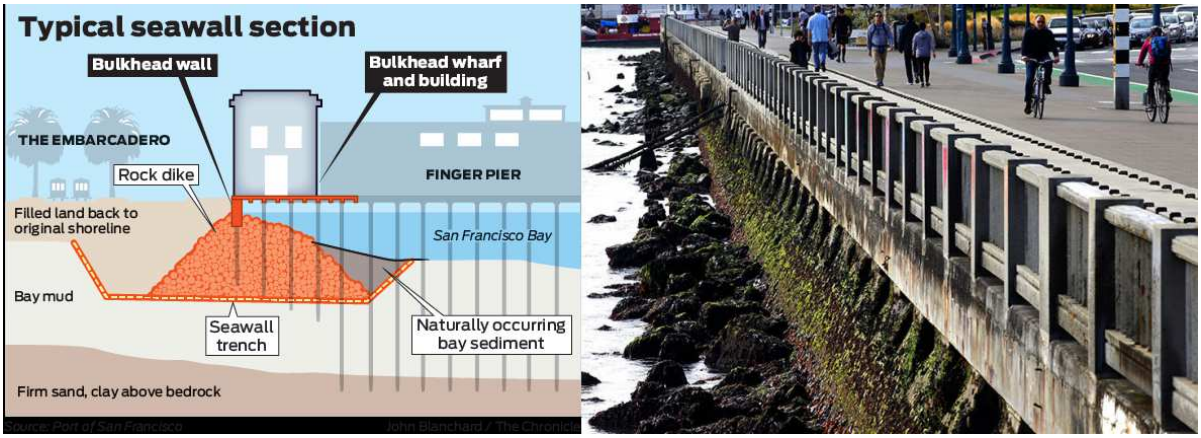

Figure 16-– Typical Seawall section showing major infrastructure elements (left), exposed seawall section along Embarcadero at low tide with exposed foundation (image from San Francisco Chronicle, July 2016).

The NOAA tide gauge network around San Francisco Bay (Figure 17) has been in existence for many years and provides key information needed to develop a CPRR analysis, measured water level data and concurrent astronomical tidal predictions which support the total water level approach used in the CPRR. The tide gauge network also provides a tidal datum along with conversion to the geodetic datum NAVD88. The NOAA tide gauge, No. 9414290 San Francisco, CA is located near the Golden Gate Bridge has a very long observed data record having been established in 1854. Data from this tide gage will be used to develop the CPRR for the San Francisco Waterfront.

Figure 17 - NOAA tide gauge network in North San Francisco Bay (image from NOAA tides and currents website)

4.1.2 Applying CPRR to the San Francisco Waterfront

The CPRR framework will be applied to assess the vulnerability of significant and critical infrastructure at the San Francisco Waterfront to future water levels impacted by Relative Sea Level Change. The analysis will utilize the observed water level record from NOAA tide gauge 9414290 to develop extreme water level statistics at the area of interest. Development of the information for a CPRR follows a linear process in order as described by the main framework elements shown in Figure 18.

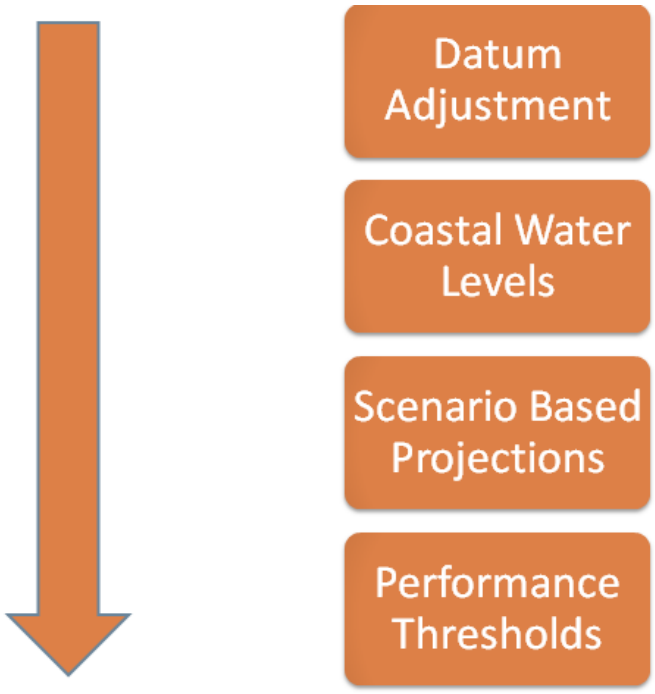

Figure 18 -Flow chart for San Francisco Waterfront CPRR analysis

Development of the San Francisco Waterfront CPRR will begin with selection of tide gauge(s), identifying the local tidal datum and adjustment to NAVD88 at the area of interest and follow the flow chart order in Figure 18.

4.2 Datum Adjustment, San Francisco Waterfront

The process for developing the datum adjustment for a CPRR follows the flow chart found in Figure 19.

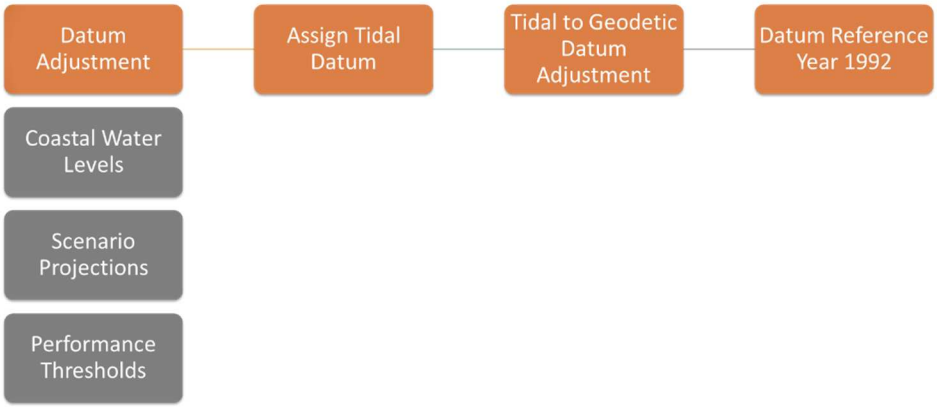

Figure 19 – Workflow for Datum Adjustment element of CPRR framework

A NOAA tidal prediction station, 9414317 Pier 22½, San Francisco is in the waterfront area where the CPRR framework will applied to several critical waterfront infrastructure elements. The station provides astronomical tide predictions only and has a tidal datum adjustment to NAVD88 which will provide a reliable local tidal datum adjustment. Figure 20 shows the location of the tidal station relative to the San Francisco Waterfront and Seawall.

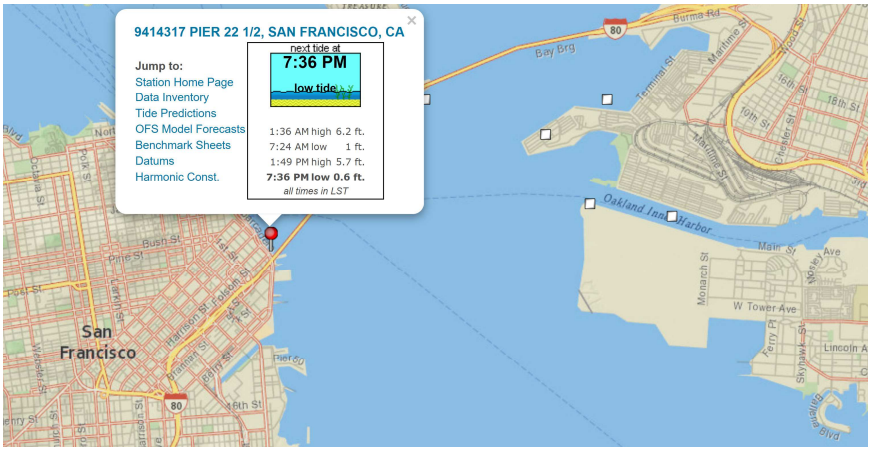

Figure 20 - NOAA station 9414317, Pier 22 ½, San Francisco, CA

Table 5 shows the datum adjustment to NAVD 88 for NOAA, 9414317 Pier 22½, San Francisco, CA.

Table 5 -NOAA station 9414317, Pier 22 ½ Tidal Datum

Tidal Datum	Description	Station Datum	NAVD88
MHHW	Mean Higher-High-Water	9.74	6.24*
MHW	Mean High Water	9.12	5.62
MTL	Mean Tide Level	6.86	3.36
MSL	Mean Sea Level	6.75	3.25
DTL	Mean Diurnal Tide Level	6.61	3.11
MLW	Mean Low Water	4.60	1.10
MLLW	Mean Lower-Low Water	3.48	-0.02
NAVD88	North American Vertical Datum of 1988	3.50	0.00
STND	Station Datum	0.00	

**These elevations represent the midpoint of the current NTDE (1983-2001), 1992.*

4.3 Coastal Water Levels, San Francisco Waterfront

Coastal water level information was developed for the Pier 22 ½ site from the observed record at the adjacent gage, NOAA 9414290, near the Golden Gate Bridge. Figure 21 shows the process and steps needed to create an observed record at the Pier 22 ½ site.

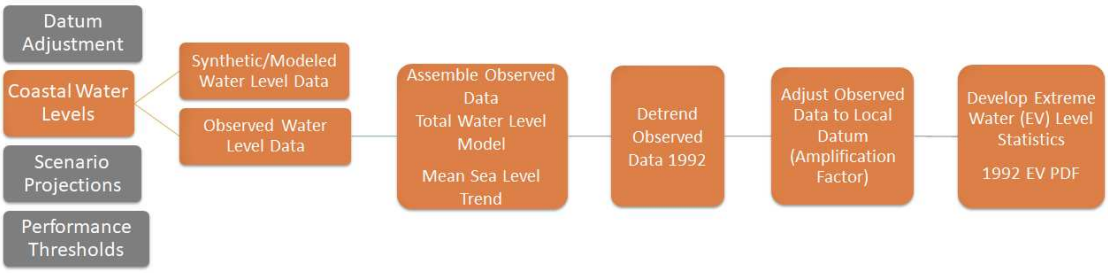

Figure 21 – Workflow for Coastal Water Levels element of CPRR framework

The goal of the Coastal Water Levels section in the CPRR framework is to develop extreme water level statistics or other specific water level data tied to performance at the location of the coastal infrastructure being assessed. Extreme water level statistics or water level information may be either extreme high or low water levels, instantaneous water levels or water levels of specific duration. The water level statistics may be developed for observed data which generally represent combinations of the elements described in the total water level model for classification of coastal water levels. The San Francisco Waterfront CPRR assumes a SWL instantaneous peak based on the data set used to develop the extreme value statistics.

4.3.1 Methodology, Analyzing Observed Tide Gauge Records

NOAA tide gage 9414290, San Francisco is nearest to the area of interest, and the tidal datum at the area of interest defined by NOAA tide prediction station 9414317, Pier 22½, San Francisco, CA. Figure 22 shows the relative locations of both stations. The Pier 22½ station provides astronomical tide predictions only and has a defined tidal to geodetic datum adjustment.

Figure 22- Locations of NOAA tide datums 9414290 and 9414317

The NOAA tide gage 9414290 located near the Golden Gate Bridge has a very long data record, back to 1854. Monthly peak water levels from 1900 to 2015 were used to develop extreme water level statistics. The observed monthly data represent still water (SWL) levels.

4.3.2 Methodology, Relative Sea Level Change Trend, San Francisco Waterfront

Monthly observed water levels of mean sea level from August 1897 through January 2017 were available for NOAA tide gage 9414290 and used to compute the RSLC rate associated with the tide gage. This rate will be used at the Pier 22½ tidal datum and the scenario projections will use this rate. The assumption is that the underlying geology is similar due to the proximity of the gage and therefore the mean sea level trend for 9414290 is representative at the Pier 22 ½ location.

A linear regression was computed on NOAA tide gage 9414290 record of mean sea level data 1897-2017 (Figure 23) to determine the most current long term RSLC rate.

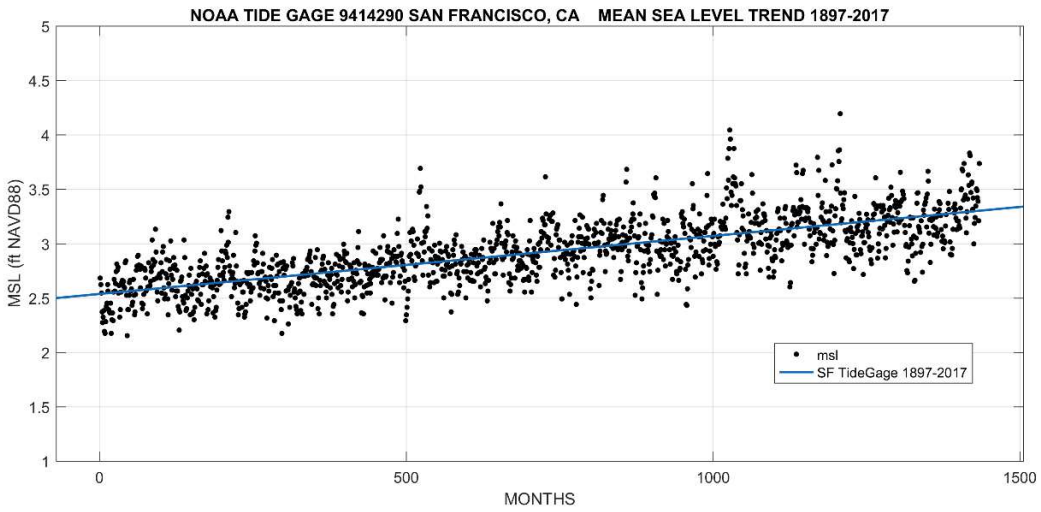

Figure 23- Linear trend, mean sea level. NOAA tide gauge 9414290, 1897-2017

The linear regression model used to compute the RSLC rate at NOAA tide gage 9414290 is given by Equation 4.1:

$$f(x) = p1(x) + p2 \tag{4.1}$$

where p1 is in feet/month and p2 is in feet

The fitted coefficients with 95% confidence bounds are

$$p1 = 0.0005334 \ \ (0.0005065,\ 0.0005603)$$

$$p2 = 2.537 \ \ (2.515,\ 2.559)$$

Goodness of fit: SSE: 65.67, R-square: 0.5147

The RSLC rate is the slope of the linear fit coefficient p1 in feet/month, as the data is monthly:

$$p1 = 0.0005334 \ feet \ / \ month$$

The monthly RSLC rate is annualized to provide an annual rate in Equation 4.2. RSLC rates are typically expressed in feet or mm/year:

$$RSLC_{NOAA9414290} = 0.0005334 \frac{feet}{month} \times 12 \frac{month}{year} = 0.0064 \frac{feet}{year} \tag{4.2}$$

The conversion to mm/year is given below by Equation 4.3 including the 5/95% confidence level:

$$RSLC_{NOAA9414290} = 0.0005334 \frac{feet}{year} \times 304.8 \frac{mm}{year} = 1.96 \pm 0.1 \frac{mm}{year} \tag{4.3}$$

The RSLC rate used in the San Francisco Waterfront CPRR for future projections will be 1.96 mm/yr.

4.3.3 Methodology, Detrending Observed Data Record, San Francisco Waterfront

The NOAA tide gage 9414290 observed data, from August 1897 through January 2017, is nonstationary due to the gradual increase in the base tidal datum due to RSLC. To remove the bias due to RSLC, the observed data set is converted to a stationary data set by detrending the data using the RSLC trend developed from the long term linear regression of mean sea level data. The trend of the monthly peak water level data is slightly higher; the mean sea level trend is used because the tidal datum correction to the geodetic datum (NAVD88) is based on mean sea level.

For monthly data records, the formula to adjust observed water levels is given by:

$$y_t = [(1992 \times 12month) - (t \times 12month)] \times RSLC \tag{4.4}$$

where y_t is the adjustment factor in feet for a water level at time *t* and is added to data before June 1992, the midpoint of the current NTDE (1983-2001) and subtracted from data after June 1992.

The datum adjustment procedure in the CPRR assumes that tidal datum elevations also represent the midpoint of the NTDE, so data adjustments in the Coastal Water Level step of the CPRR are also tied to the same date. Therefore, the observed data record form NOAA 9414290 is detrended to the year 1992, so that the data set corresponds to the tidal datum adjustment to NAVD88. This enables future RSLC projections in the Scenario Projections step to be made from a concurrent starting point accounting for the tidal datum adjustment. This is important since the observed data record includes the astronomical tidal range which is part of the tidal datum. An example detrending adjustment for NOAA tide gage 9414290 is presented below:

Observed monthly peak water level for August 1897 = 5.78 feet NAVD88, *t* = 1897.667

Detrending adjustment factor:

$$y_{1897.667} = [(1992.5 \times 12 month) - (1897.667 \times 12 month)] \times 0.0005334 \frac{feet}{month} \quad (4.5)$$

$$y_{1897.667} = (1137.996 month) \times 0.0005334 \frac{feet}{month} = 0.607 feet \quad (4.6)$$

The August 1897 observed water level detrended to 1992 is then computed by 4.7:

$$5.78 feet + 0.607 feet = 6.48 feet NAVD88 \quad (4.7)$$

From a practical perspective, this conversion also shows the impact of relative sea level change on historical water levels, a water level of 5.78 feet in 1897 is equivalent to 6.48 feet in

1992 terms and even higher in 2017 terms (6.48 + 0.16 = 6.64 feet), with the addition of RSLC from 1992-2017 at the RSLC rate of 1.96 mm/year. The impact of the detrending adjustment is shown in Figure 24. The histograms in Figure 24 representing the observed data and detrended data show a shift to the right representing higher elevations created by adding the detrending adjustment to the observed data. Detrending the observed record enables the impact of RSLC to be reflected in storms which occurred many years ago. Detrending removes bias due to RSLC and allows the observed dataset to be made stationary and adjusted to the datum base year of 1992. Detrending adjustments are necessary to correct for observed RSLC in the record and assure an accurate tidal to geodetic adjustment.

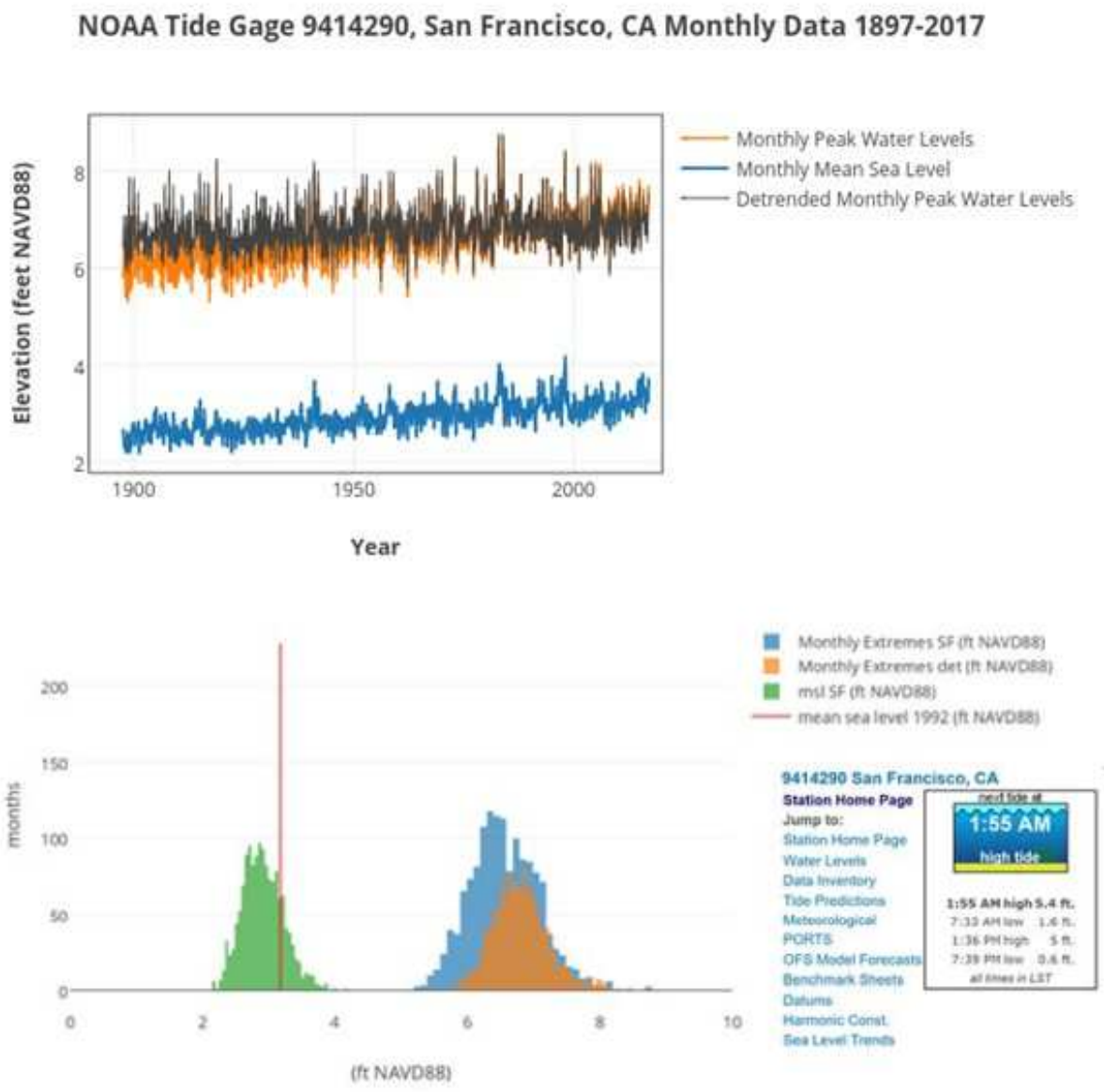

Figure 24 - Monthly peak water levels 1897-2017, NOAA 9414290 San Francisco near Golden Gate Bridge, showing the impact of the detrending adjustment on the historical water levels

4.3.4 Methodology, Adjust Observed Water Level Data to Local Tidal Datum, San Francisco Waterfront

Tidal datums and ranges (Figure 25) in San Francisco Bay reflect both dissipation north of the Golden Gate Bridge and amplification south of the Golden Gate Bridge (AECOM 2016). A simplistic data adjustment based on the difference between MHHW levels was used to transfer

the observed record of monthly peaks from NOAA 9414290 which are at or above MHHW to the San Francisco Waterfront area represented by the NOAA 9414317. The adjusted record may be then used to develop extreme water level statistics at the San Francisco Waterfront. Figure 4.11 depicts the tidal amplification phenomena south of the Golden Gate Bridge and tidal dissipative phenomena in the north Bay, north of the Golden Gate Bridge.

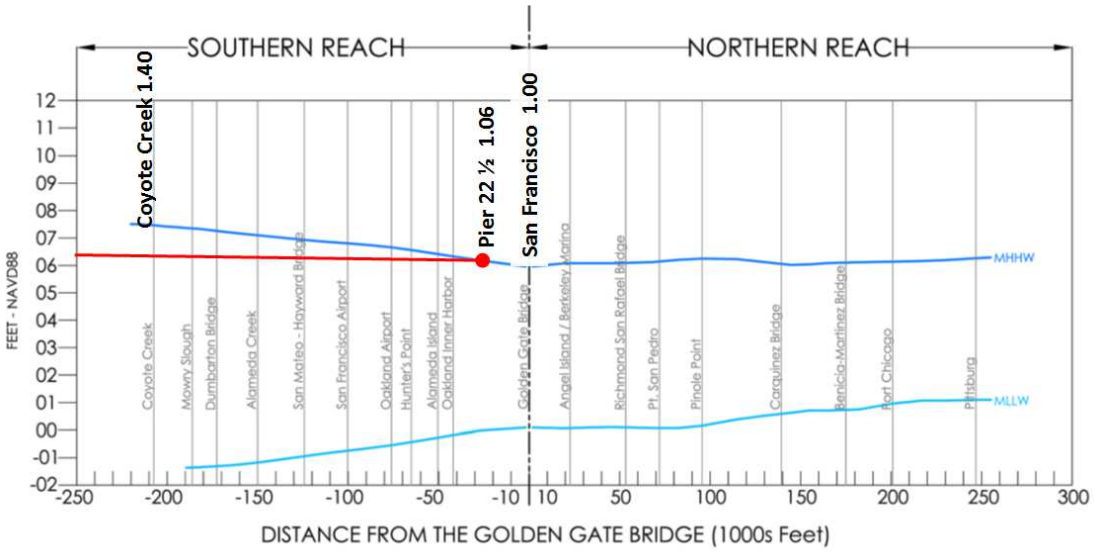

Figure 25 - Tidal datums in San Francisco Bay adapted from AECOM (2016)

For reference in this simplified method, NOAA station 9414290 is the baseline data set and assigned an amplification factor of 1.0, while the Pier 22 ½ and Coyote Creek locations (NOAA stations 9414317 and 9414575 respectively) have amplification factors of 1.06 and 1.40. The tidal datums for NOAA stations 9414290 and 9414317 were compared (Table 6) and a transfer function was developed to adjust the observed, detrended water level data record to the area of interest at the San Francisco Waterfront, defined by NOAA 9414317 Pier 22½.

Table 6 - Tidal Datums, NOAA 9414290 and 9414317

	NOAA 9414290, SAN FRANCISCO			NOAA 9414317, PIER 22 ½	
Tidal Datum	Station Datum	NAVD88	Amplification Factor	Station Datum	NAVD88
MHHW	11.82	5.90	1.06	9.74	6.24
MHW	11.21	5.29	1.06	9.12	5.62
MTL	9.16	3.24	1.06	6.86	3.36
MSL	9.10	3.18	1.06	6.75	3.25
DTL	8.90	2.98	1.06	6.61	3.11
MLW	7.11	1.19	1.06	4.60	1.10
MLLW	5.98	0.06	1.06	3.48	-0.02
NAVD88	5.92	0.00	1.06	3.50	0.00

An amplification factor was developed for water levels at or above MHHW and applied to the monthly maximum water level record for NOAA tide gage 9414290 to create a proxy data set of observed water levels at NOAA 9414317, Pier 22½. A comparison of the adjusted water levels based on the amplification factor is shown in Figure 26. Application of this methodology requires adoption of simplifying assumptions stating that the magnitude of the non-tidal residuals is the same between the two stations and that the overall shape of the tidal stage hydrograph is similar except for the shift caused by the amplification effect. While in practice, the water levels would be shifted temporally and possibly have slightly greater or lesser non-tidal residuals, the simplifying assumption is reasonable for obtaining a record of instantaneous annual peak water elevations from which extreme value statistics may be calculated.

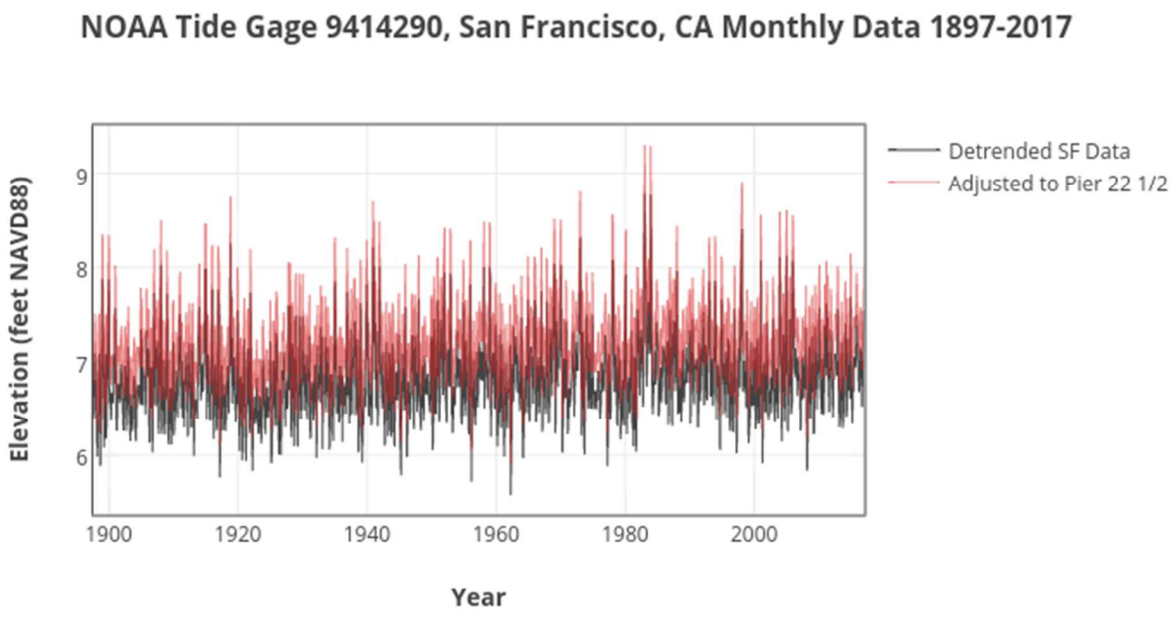

Figure 26 - Adjusted, detrended time series for NOAA 9414317 (Pier22½), showing impact of amplification factor

Computation of the amplification factor between NOAA 9414290 and 9414317 follows.

The amplification factor is the ratio between MHHW at the two locations:

$$A = \frac{MHHW_{NOAA9414317}}{MHHW_{NOAA9414290}} \tag{4.8}$$

$$MHHW_{NOAA9414317} = 6.24\,feetNAVD88 \tag{4.9}$$

$$MHHW_{NOAA9414290} = 5.90\,feetNAVD88 \tag{4.10}$$

Amplification Factor

$$A = \frac{6.24\,feetNAVD88}{5.90\,feetNAVD88} = 1.06 \tag{4.11}$$

The factors used to amplify the predicted tide at San Francisco are assumed to be linear and were computed by comparing predicted tide and tidal datums at the baseline NOAA 9414290 tide station to other tidal stations throughout San Francisco Bay. Use of amplification factors are an appropriate surrogate method for developing accurate water levels and developing extreme water level statistics in areas where local mean sea level and tidal datum have been defined. (USACE 2014)

4.3.5 Methodology, Apply Statistical Model to Coastal Water Levels, San Francisco Waterfront

The observed water level record from the San Francisco tide gage was used to develop a data record at the Pier 22½ tide prediction station by applying an amplification factor. The adjusted record was used to develop extreme water level statistics. The adjusted monthly data record was converted to an annual series (Figure 27).

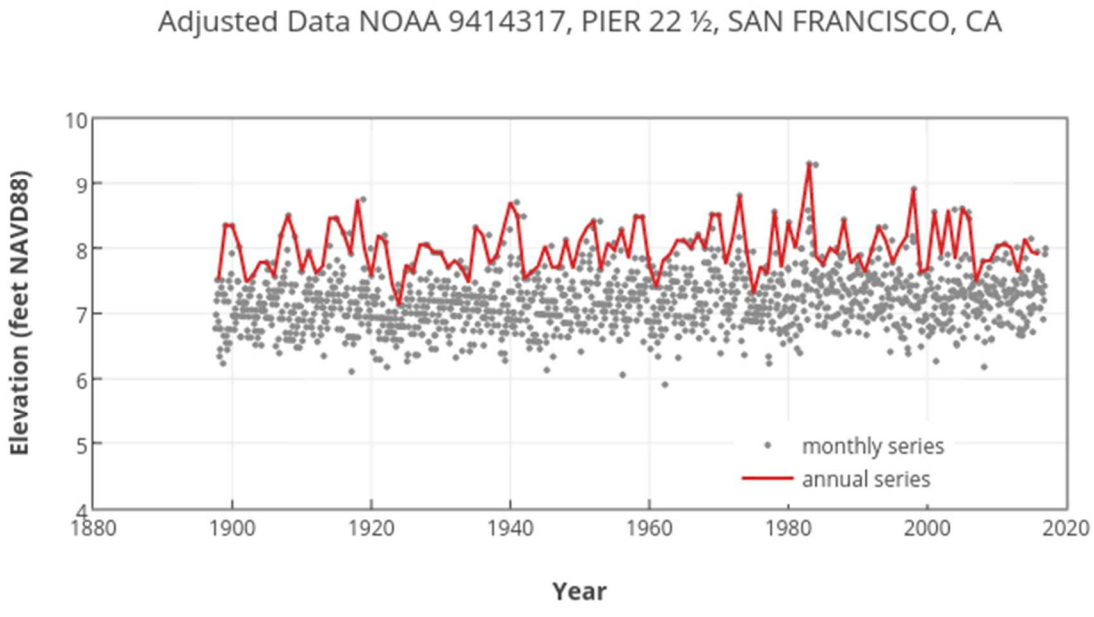

Figure 27 - Annual peak water levels at NOAA 3414317 Pier 22½, from monthly series derived from amplification factor adjustment

The monthly data set of maximum observed water levels for NOAA tide gage 9414290 (1897-2017) was converted to annual data utilizing a block maxima approach to create a data set of annual maximums from 1898 to 2016, 118 years. Figure 28 shows a box plot comparison between NOAA 9414290 and 9414317 reflecting the amplification factor of 1.06.

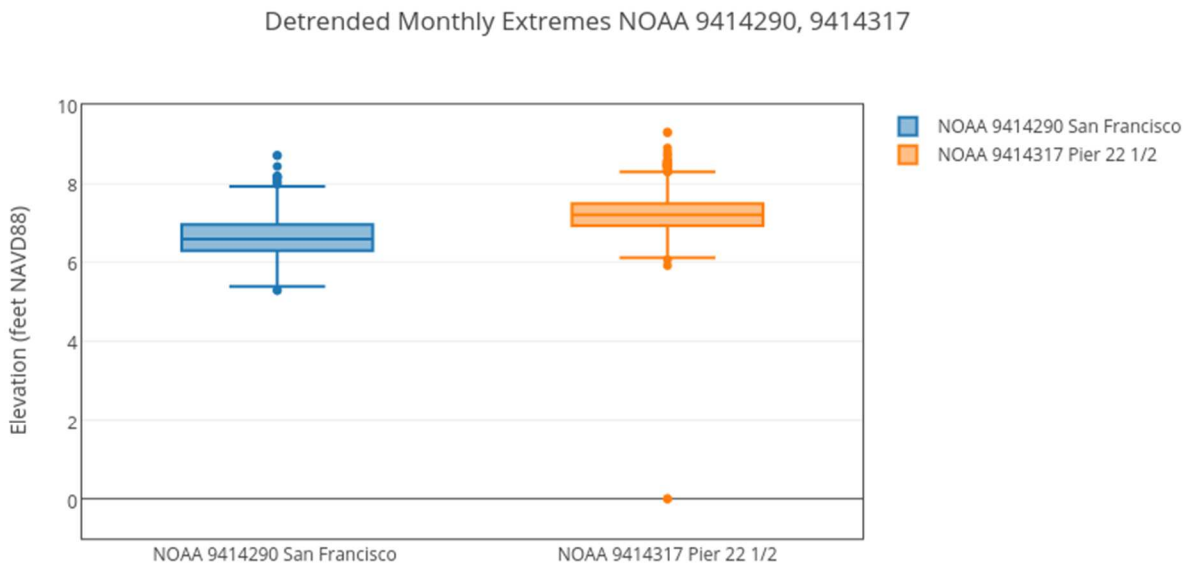

Figure 28 - Box Plot comparison showing the shift of the monthly water level statistics in caused by San Francisco Bay tidal amplification in the South Bay

An empirical distribution of the adjusted annual peak data at Pier 22½ was developed and several distributions were fit to the data, with the computed log likelihood parameter and visual inspection of the fitted data used to select the distribution which best fit the data. As expected the GEV distribution produced the best fit and was used to develop extreme value statistics from the adjusted annual maximum data set created from NOAA tide gage 9414290. Table 7 presents the distribution parameters and comparison of the fits and their corresponding log likelihood factors.

Table 7 - Distributions fitted to Pier 22½ adjusted data

Distribution Type	Parameters	Mean, Variance	Log likelihood
GEV	7.85, 0.33, -0.122	8.005, 0.136	-47.4057
Gamma	474.145, 0.0169	8.005, 0.136	-49.6879
Normal	8.005, 0.3718	8.005, 0.136	-50.6144

Figure 29 compares the distributions in Table 7 to the detrended data.

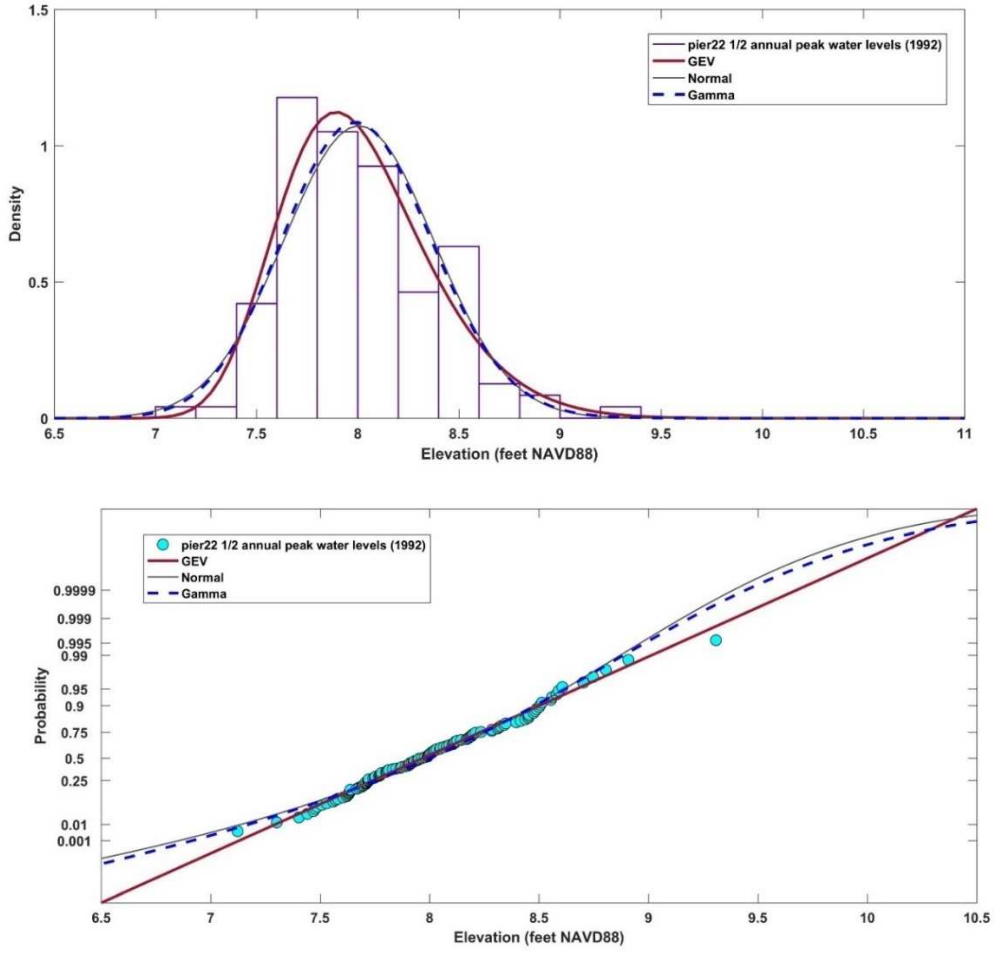

Figure 29 -Comparison of distributions to detrended, adjusted data set created for the Pier 22½ tidal datum

4.4 Scenario Projections, San Francisco Waterfront

The third step in the CPRR framework is to develop future water level projections under a range of scenarios which represent the range of plausible future conditions. Figure 30 shows the workflow for this element.

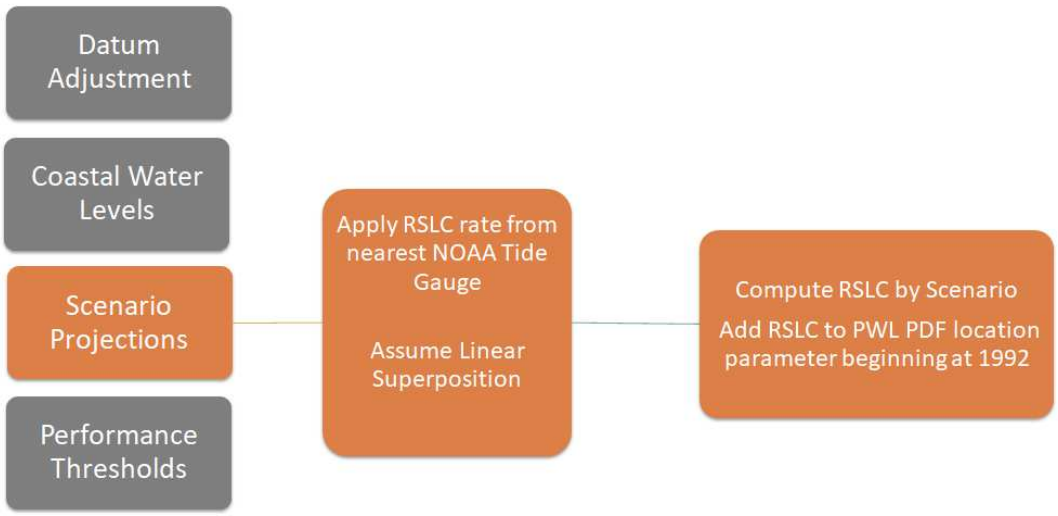

Figure 30 – Workflow for scenario projections, San Francisco Waterfront CPRR

The annual peak water level data used for the San Francisco Waterfront CPRR was developed and transformed to the time and location of interest using methods associated with the first two CPRR framework items, Datum Adjustment and Coastal Water Levels.

4.4.1 Methodology, Applying RSLC Scenario Projections to Coastal Water Level Statistical Model, San Francisco Waterfront

The annual peak water level data described by a GEV distribution (μ, σ, ξ), the Pier 22½ GEV (7.85, 0.33, -0.122), is referenced to a static geodetic datum (NAVD88), representing the year 1992. The data record from the San Francisco tide gage was detrended by the mean sea level trend (1.96 mm/year) and adjusted to the Pier 22½ tidal datum using an amplification factor (1.06) based on the ratio of MHHW between the two tidal datums.

Projections of the annual peak water level data are made by adding RSLC for time *t* to the location parameter, μ for the projected future time *t* associated with a scenario. The GEV distribution representing annual peak still water levels at Pier 22½ is given by:

$$Z_t = GEV(\mu(t), \sigma, \xi) \tag{4.12}$$

where *t* = number of years starting in 1992, the location parameter projection, μ*(t)* is given by:

$$\mu(t) = \mu_{1992} + M(t) + b(t)^2 \tag{4.13}$$

where M, RSLC is in meters and a conversion to feet must be applied if the GEV parameters are in feet. The projected location parameter preserves the stationarity of the annual peak SWEL record created by detrending the observed record at NOAA 9414290 by the mean sea level trend (+ 1.96 mm/year).

Table 8 shows discrete values of the projected location parameter at years 2017, 2040 and 2100 for four scenarios. Specific annual exceedance probability (AEP) events may be derived from the GEV cumulative frequency distribution function. The MATLAB function *gevinv* was used to develop future AEP values from projected GEV distributions:

$$Z = gevinv(P, \xi, \sigma, \mu(t)) \tag{4.14}$$

where *Z* = AEP value in feet NAVD88

P = 1-AEP, ξ = shape factor = -0.122, σ = scale factor = 0.33, $\mu(t) = \mu_{1992} + 0.0017(t) + b(t)^2$

A 10%/ 10-year AEP at Pier 22 ½ is computed as follows for the year 2040 based on the USACE High Scenario using the MATLAB function gevinv:

$$Z = gevinv[(1-0.1), -0.122, 0.33, 9.01) \quad (4.15)$$

$$Z = gevinv(0.99, -0.122, 0.33, 9.01) \quad (4.16)$$

A 10-year AEP for the year 2040 based on the USACE High Scenario is then equal to:

$$Z = 9.66\, feetNAVD88 \quad (4.17)$$

Table 8 - Projected values of GEV location parameter, AEP for Pier 22½

Year	Scenario	RSLC (feet)	GEV Location Parameter (feet NAVD88)	10% / 10year AEP (feet NAVD88)	1% / 100year AEP (feet NAVD88)
1992			7.85	8.50	9.01
2017	USACE Low	0.161	8.01	8.66	9.17
2040	USACE Low	0.309	8.16	8.81	9.32
2040	USACE Int.	0.514	8.36	9.01	9.52
2040	USACE High	1.163	9.01	9.66	10.17
2040	NOAA High	1.488	9.34	9.99	10.50
2100	USACE Low	0.695	8.55	9.20	9.71
2100	USACE Int.	1.732	9.58	10.23	10.74
2100	USACE High	5.019	12.87	13.52	14.03
2100	NOAA High	6.665	14.52	15.17	15.68

Specific water levels representing a storm event, or some other significant water level may be projected into the future under the range of available scenarios, provided the water elevation of interest is first referenced to 1992 by the detrending procedure using the mean sea level trend.

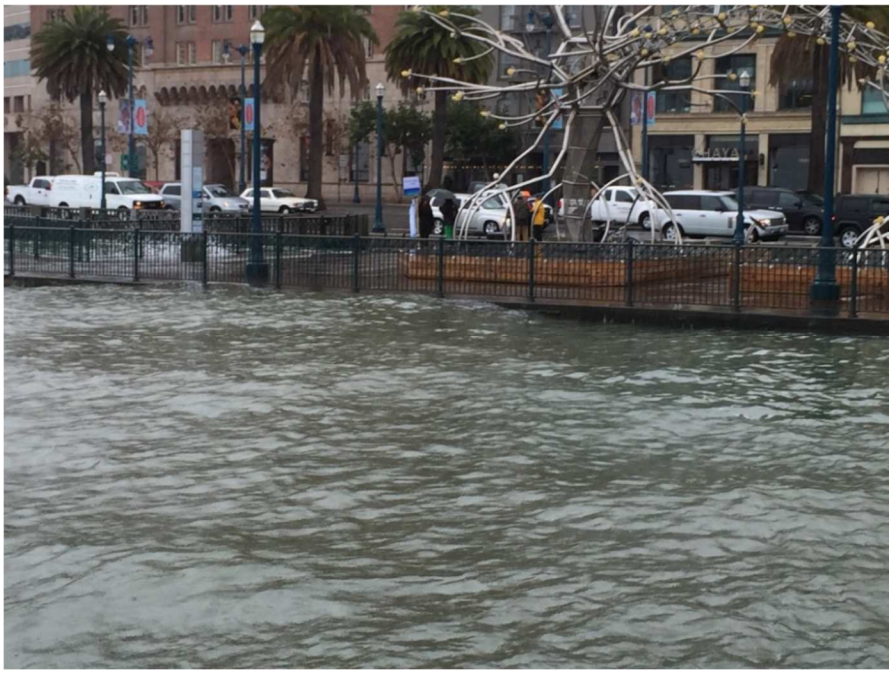

Figure 31 - San Francisco Bay waters overtopping the seawall and spilling onto the adjacent walkway immediately southeast of the Agricultural building November 24, 2015 (USACE 2016)

The king or spring tide is commonly used as a proxy for future sea level change impacts. The photograph shown in Figure 31 was taken November 24, 2015 during a king tide event at the San Francisco waterfront adjacent to the Pier 22 ½ location. The measured water level at the NOAA San Francisco Tide Gage was 7.54 feet NAVD88. Using the amplification factor for converting the measured San Francisco tide gage water levels to Pier 22 ½ water levels, the king tide at the San Francisco Waterfront is computed by:

$$7.54\,feetNAVD88 \times 1.06 = 7.99\,feetNAVD88 \tag{4.18}$$

The November 2015 king tide water level adjusted to Pier 22 ½ is detrended back to 1992 so the water level may be projected into the future:

$$7.99\,feetNAVD88 - (2015 - 1992.5) \times 0.000643 \frac{feet}{year} = 7.84\,feetNAVD88 \tag{4.19}$$

4.5 Performance Thresholds, San Francisco Waterfront

Two performance models will be used to determine performance thresholds for the San Francisco Waterfront CPRR, an elevation-based, and a reliability-based.

4.5.1 Methodology, An Elevation-Based Performance Model, San Francisco Waterfront

The process for determination of performance thresholds using an elevation-based performance model is shown in Figure 32 below.

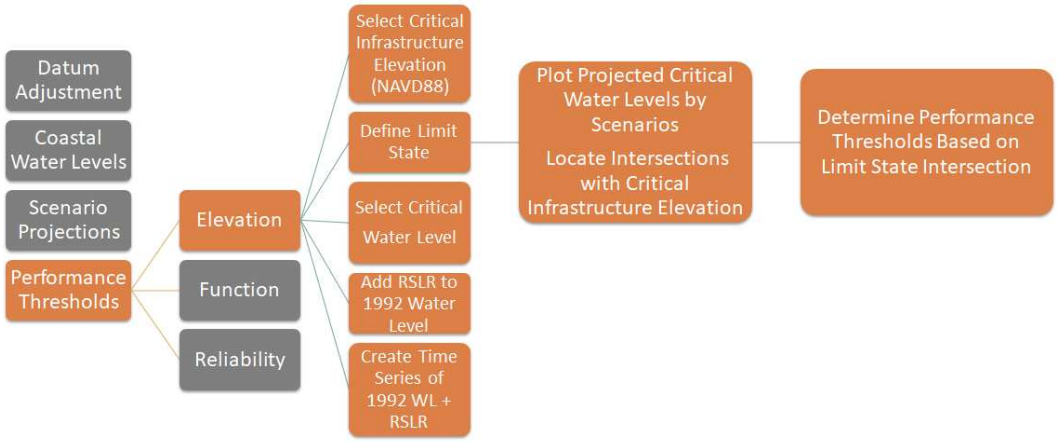

Figure 32 – Workflow to apply an elevation-based performance model to determine performance thresholds at the San Francisco Waterfront

Elevations of critical infrastructure locations subject to flooding on the San Francisco Waterfront are shown in Figure 33. Table 9 presents the critical infrastructure locations, elevations and AEP level selected for elevation based performance threshold determination.

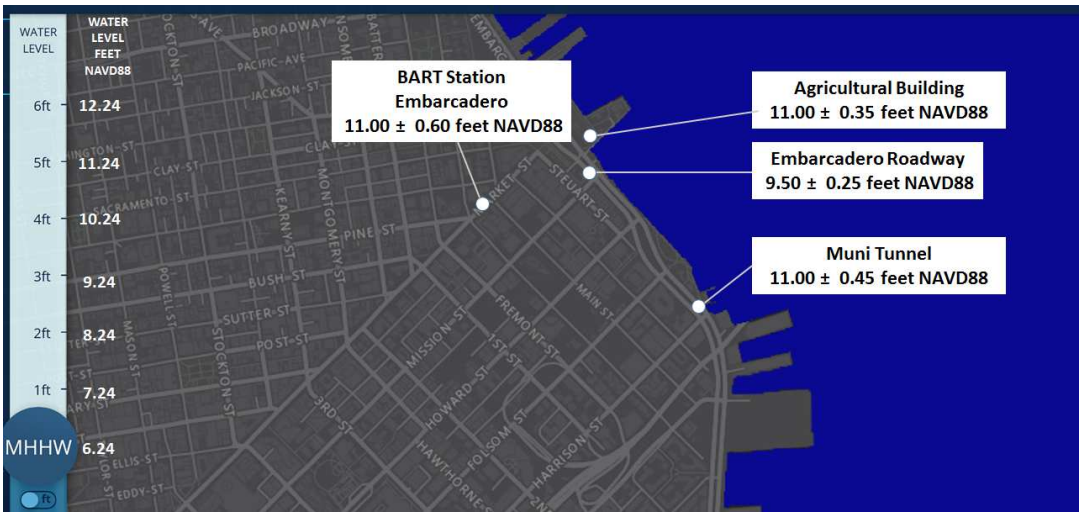

Figure 33 - Critical infrastructure locations, elevations, San Francisco waterfront. Displayed water level is at MHHW or 6.24 feet NAVD88

Table 9 - Existing Conditions Water Levels, San Francisco Waterfront

Infrastructure Element	Elevation (feet NAVD88)	ACE/Significant Water Level (feet NAVD88)	1992 SWL (feet NAVD88)	2017 SWL (feet NAVD88)
Embarcadero Roadway	9.50	King Tide 10% ACE 1% ACE	7.84 8.50 9.01	7.99 8.66 9.17
Embarcadero BART station	11.00	King Tide 10% ACE 1% ACE	7.84 8.50 9.01	7.99 8.66 9.17
Agricultural Building	11.00	King Tide 10% ACE 1% ACE	7.84 8.50 9.01	7.99 8.66 9.17
Muni Tunnel	11.00	King Tide 10% ACE 1% ACE	7.84 8.50 9.01	7.99 8.66 9.17

4.5.2 Methodology, Performance Thresholds from Elevation-Based Performance Model, San Francisco Waterfront

The three water levels selected for performance threshold determination represent a king tide, 10 year and 100-year future water levels respectively for four scenarios (USACE Low, Intermediate, High and NOAA High). Two AEP water levels determined from extreme value statistical analysis from section 4.3 are selected for evaluation, a 10 and 100-year AEP. These specific water levels will be projected into the future as a time series representing each scenario. The point where time series for each scenario crosses the elevation defining the specific infrastructure element is a performance threshold representing a specific time in the future. Table 10 shows the performance thresholds for the San Francisco Waterfront Elevation-Based performance model.

Table 10 - San Francisco Waterfront – Elevation-Based performance model

			Threshold Range/Scenarios			
Infrastructure Element	Performance Metric (feet NAVD88)	Performing Water Level (feet NAVD88)	USACE Low (year)	USACE Int. (year)	USACE High (year)	NOAA High (year)
Embarcadero Roadway	SWL > 9.50	King Tide	> 2120	2097	2051	2043
	SWL > 9.50	10-year AEP	> 2120	2068	2036	2031
	SWE > 9.50	100-year AEP	2068	2038	2021	2018
Agriculture Building, Muni Tunnel, BART Embarcadero	SWL > 11.00	King Tide	> 2120	> 2120	2076	2065
	SWL > 11.00	10-year AEP	> 2120	> 2120	2065	2056
	SWL > 11.00	100-year AEP	> 2120	2109	2057	2047

Time series plots of the San Francisco Waterfront Elevation based CPRR at Pier 22½ are shown in Figure 34. Performance thresholds indicated by crossings of the King Tide and AEP

projected time series and the static elevation lines representing the critical infrastructre locations are shown in Figure 34 and correspond to the values in Table 10.

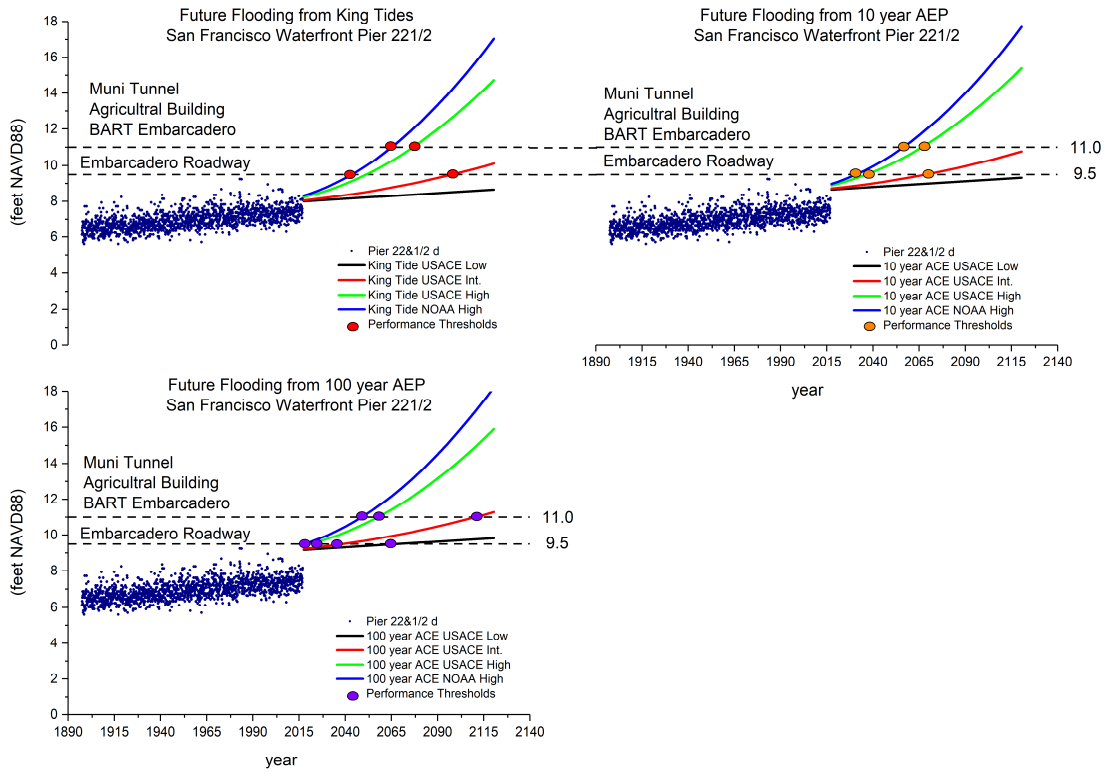

Figure 34 – Elevation-based performance model with performance thresholds, San Francisco Waterfront

4.5.3 Methodology, A Reliability-Based Performance Model, San Francisco Waterfront

A reliability-based performance model was applied after the elevation-based model was completed. The reliability-based performance model was developed to provide additional vulnerability information and to incorporate uncertainty into the significant and critical infrastructure performance elevations. A flow chart is presented in Figure 35 below showing the analysis steps to develop a reliability based performance model.

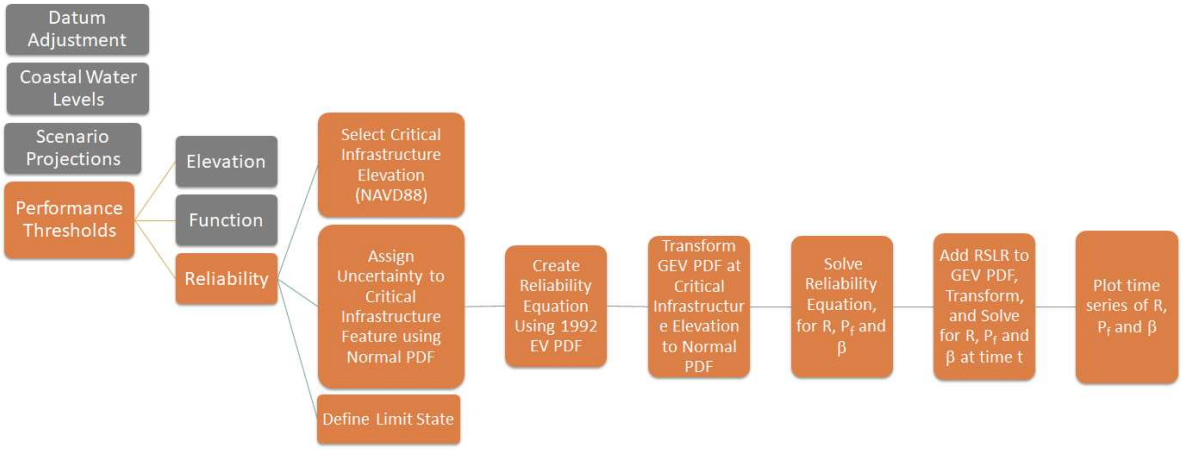

Figure 35 – Workflow for Reliability-based performance model

There are several advantages to a reliability-based performance model, the most important one is that uncertainty connected with the infrastructure elevation or some other aspect of the infrastructure's exposure to current and future coastal water levels may be evaluated with uncertainty within each scenario projection. The reliability-based performance model was applied to each of the four infrastructure elements in the San Francisco Waterfront vulnerability assessment. Each infrastructure element was assigned an uncertainty value which assumed a normal distribution. Table 11 lists the infrastructure elements analyzed along with their respective uncertainties. The limit state was defined as a simple exceedance of the infrastructure elevation for a water level, water levels are assumed to be SWL.

Table 11 – Infrastructure elevations with uncertainty, San Francisco Waterfront

Infrastructure Element	Elevation (feet NAVD88)	Limit State/Performance Metric (feet NAVD88)
Embarcadero Roadway	9.50 ± 0.25	SWL > 9.50
Embarcadero BART station	11.00 ± 0.60	SWL > 11.00
Agricultural Building	11.00 ± 0.35	SWL > 11.00
Muni Tunnel	11.00 ± 0.45	SWL > 11.00

The information developed for the reliability-based performance model uses the same basic information as the elevation-based performance model. The analysis follows these steps:

1. Define limit state for reliability analysis. Performance for initial flooding of the Ferry Building is defined as annual exceedance of water levels at elevation 9.5 feet NAVD. Water levels will be based on the cumulative distribution function of the annual peak water level series developed at the Pier 22 and ½ tidal datum.

2. The reliability analysis is developed by assigning uncertainty to significant and critical infrastructure performance elevation(s). Performance elevations with uncertainty are assumed to be normally distributed.

3. Create performance function using 1992 water levels.

4. Determine 1992 probability of failure (P_f based on limit state definition at significant and critical infrastructure performance elevation(s) using GEV.

5. Adjust non-normal coastal water level distribution (GEV) to equivalent normal distribution at significant and critical infrastructure performance elevation(s).

6. Solve performance equation for reliability index using the equivalent normal distributed parameter for coastal water levels and infrastructure elevation with uncertainty described by a normal distribution. Convert reliability index to Pf and reliability (inverse Pf). Create plot of projected time series of reliability index, Pf and reliability to find performance thresholds.

4.5.4 Methodology, Applying Reliability Equations to develop a Reliability-Based Performance Model, San Francisco Waterfront

Limit state definitions are used to define performance and nonperformance for infrastructure elements in the CPRR framework. For the San Francisco Waterfront (from Table 11), the limit states are defined as:

$$SWL > 9.50\, feetNAVD88 \tag{4.20}$$

$$SWL > 11.00\, feetNAVD88 \tag{4.21}$$

The general performance equation adapted to the CPRR framework is given as:

$$G = R - S \tag{4.22}$$

where G = Performance in feet, R = Resistance (static infrastructure elevation) in feet, S = Load (coastal water levels) in feet

For future scenario projections 4.1.22 becomes:

$$G(t) = R - S - RSLC(t) \tag{4.23}$$

where t = time

R = Resistance (Coastal Infrastructure) PDF

S = Coastal Water Level PDF

RSLC(t) = Cumulative relative sea level change

Probability of failure or non-performance without uncertainty is found using the cumulative probability distribution point (CDF) equivalent to where the GEV function defining the water levels is equal to one of the SWL elevations defining the limit states for the infrastructure functions, 9.5 or 11.00 feet NAVD88 respectively. The probability of failure at time t is defined by the GEV function developed for Pier 22 ½ which defines the distribution of water levels having a location factor of $\mu(t)$

$$P_f(t) = 1 - GEVCDF(9.5, -0.122, 0.33, \mu(t)) \tag{4.24}$$

where $P_f(t)$ = probability of failure at time t, defined by $\mu(t)$

The variables R and S in equation 4.22 are assumed to be defined by a normal or lognormal distribution. Observed and synthetic coastal water levels typically obey the Generalized Extreme Value (GEV) distribution. To apply 4.23 which assumes that the variables R and S are independent and normally distributed, S is transformed into an equivalent normally distributed variable in the form (μ, σ) at the limit state values of 9.5 and 11.0 feet NAVD88 respectively. When applied at time t, the equivalent normal distribution becomes variable with time t in the form $(\mu(t), \sigma(t))$. This is shown graphically in Figure 36.

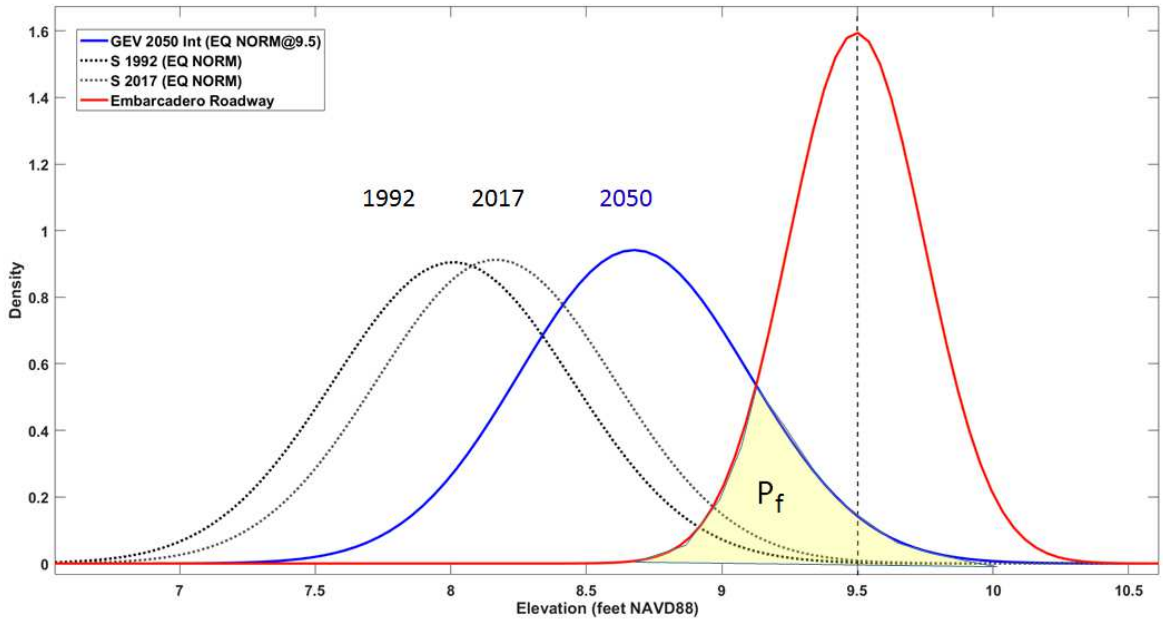

Figure 36 - Graphical depiction of equation 4.23 showing Equivalent Normal Distributions

For the equivalent projected normal distribution parameters $\mu(t)$ and $\sigma(t))$, $\mu(t)$ is simply the expected value or mean of the projected distribution and may be obtained from the projected GEV function at time t. $\sigma(t)$ is solved by iteration as an equivalent CDF value at the defined limit state or critical elevation. For a limit state of 9.5 feet NAVD88 corresponding to the Embarcadero Roadway elevation, using a projected GEV location parameter $\mu(t)$ = 8.521, for the GEV function (-0.122, 0.33, 8.521) the CDF value for 9.5 is 0.97516. The equivalent normal distribution parameter $\mu(t)$ = 8.675, $\sigma(t)$ is solved for by iteration. The computation is easily accomplished using the MATLAB function *disttool* as shown in Figure 37.

- GEV (8.521, 0.33, -0.122)
- X = 9.5 P = 0.97516

- Normal (8.675, 0.42033)
- X = 9.5 P = 0.97516

Figure 37- Solving for equivalent normal distribution parameter σ(t) from GEV distribution using MATLAB function *disttool*

Using the normally distributed parameters for *R* and *S*, the reliability index β is computed, when applied as a projected time series based om *R* and *S(t)*, β becomes $\beta(t)$. The equations are given as:

$$\mu_G(t) = \mu_R - \mu_S(t) \tag{4.25}$$

where μ_R = infrastructure elevation, $\mu_S(t)$ = mean of water level distribution at time *t*

Standard deviation is computed by:

$$\sigma_G(t) = \sqrt{\sigma_R^2 + \sigma_G^2(t)} \tag{4.26}$$

The reliability index at time *t* is given by:

$$\beta(t) = \frac{\mu_G(t)}{\sigma_G(t)} \tag{4.27}$$

The reliability index be used to compute P_f, since G is a normal random variable, P_f is given by:

$$P_f = \Phi(-\beta) \tag{4.28}$$

P_f *is* obtained from tables of standard normal probabilities or computed directly using the Microsoft EXCEL function *NORMSDIST* (-β).

T_f, is the return period in years or the annual exceedance probability in years given by:

$$T_f = \frac{1}{P_f} \tag{4.29}$$

Reliability is given by:

$$R = 1 - P_f \tag{4.30}$$

AEP's defining specific risk levels may be expressed as reliability indices (β), Table 12 shows AEP - P_f - β relationships for the San Francisco CPRR.

Table 12 - AEP, Probability of Failure and Reliability Index relationships

AEP (year)	Probability of Failure (P_f)	Reliability Index (β)
2	0.50	0
10	0.10	-1.38
100	0.01	-2.33

4.5.5 Methodology, Reliability-Based Performance Model, Embarcadero Roadway, San Francisco Waterfront

A reliability-based performance model was applied to the Embarcadero Roadway at the San Francisco Waterfront. Performance thresholds shown in Figure 38, top left and may be determined by inspection of the three remaining graphs.

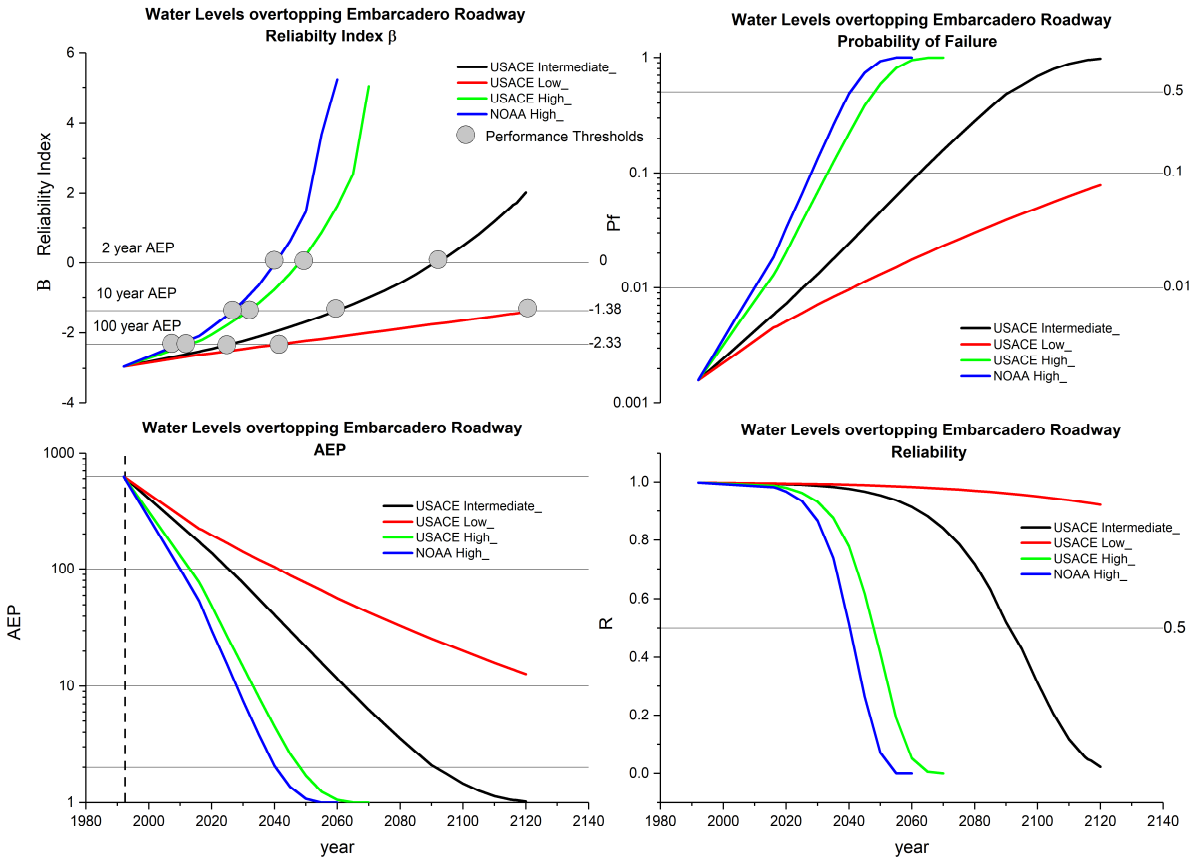

Figure 38 - Reliability-based performance model for Embarcadero Roadway (elevation 9.5 NAVD88), San Francisco Waterfront

Reliability-based performance models are typically applied as an additional tier of analysis following function or elevation-based performance models. The utility of a reliability-based performance model is shown in Figure 38, flood risk levels may be displayed as static levels on the y axis versus time on the x axis, the plot shifts from an elevation metric on the y

axis to a probability based measure on the y axis. In this tier, it is possible to plot a time series of AEP with uncertainty for a range of plausible scenarios, which is a very powerful vulnerability assessment, design and planning tool.

Tabular results of the reliability-based performance model for the San Francisco Waterfront, are given in Table 13 below. The Embarcadero Roadway at elevation 9.5 NAVD88 was assessed under the same four scenarios used in the elevation-time series performance model in section 4.5.1.

Table 13 - San Francisco Waterfront, Reliability-based performance model for Embarcadero Roadway

			Threshold Range/Scenarios			
Infrastructure Element	Performance Metric (feet NAVD88)	Reliability Metric (β)	USACE Low (year)	USACE Int. (year)	USACE High (year)	NOAA High (year)
Embarcadero Roadway	SWL > 9.50	0	> 2120	2090	2047	2040
		- 1.38	> 2120	2060	2032	2029
		- 2.33	2040	2025	2014	2010

Tables 14 and 15 present comparison of performance thresholds computed using elevation and reliability-based performance models.

Table 14 - Performance Threshold Comparison using elevation and reliability based performance models.

Performance Metric	Elevation-based				Reliability-based			
SWEL > 9.50	USACE Low (year)	USACE Int. (year)	USACE High (year)	NOAA High (year)	USACE Low (year)	USACE Int. (year)	USACE High (year)	NOAA High (year)
10-year AEP	> 2120	2068	2036	2031	> 2120	2060	2032	2029
100-year AEP	2068	2038	2021	2018	2040	2025	2014	2010

Table 15 -Performance life for 10, 100-year AEP SWL greater than Embarcadero Roadway, elevation 9.5 feet NAVD88

Performance Metric	Elevation-based Performance Life				Reliability-based Performance Life			
SWL > 9.50	USACE Low (years)	USACE Int. (years)	USACE High (years)	NOAA High (years)	USACE Low (years)	USACE Int. (years)	USACE High (years)	NOAA High (years)
10-year AEP	> 103	51	17	14	> 103	43	15	12
100-year AEP	51	21	4	1	23	8	-3	-7

Comparison of the performance thresholds obtained using the two performance models show performance thresholds shifting to the right or occurring sooner, an expected result when elevation and other uncertainty factors are factored in. The overall uncertainty is not reduced significantly under the range of scenarios, but within a scenario projection, additional accuracy is obtained by factoring in uncertainty. The rate at which performance is lost is also more clearly assessed by using suite of reliability metrics and the inverse of reliability, probability of non-performance. Loss of performance information within the scenario projections provides another piece of valuable time sensitive information on when remediation actions to maintain

performance or adapt the infrastructure element should commence. Finally, useful, additional information about the infrastructure may be incorporated into the uncertainty estimate through more robust, higher order reliability techniques.

4.5.6 Methodology, Reliability-Based Model, Additional Infrastructure Elements, San Francisco Waterfront

A reliability-based performance model was developed for the four infrastructure elements in Table 11 for the NOAA high scenario, to demonstrate the impact of uncertainty on the performance thresholds. The results are shown in Table 16.

Table 16 – Reliability-based performance model, NOAA high scenario, San Francisco Waterfront.

Infrastructure Element	Elevation with Uncertainty (feet NAVD88)	Limit State Performance Metric (feet NAVD88)	AEP / Performance Threshold
Embarcadero Roadway	9.50 ± 0.25	SWL > 9.50	1 2060.0 2 2063.5 100 2011.0
Embarcadero BART Station	11.00 ± 0.60	SWL > 11.00	1 2080.0 2 2063.5 100 2035.5
Agricultural Building	11.00 ± 0.35	SWL > 11.00	1 2080.0 2 2063.5 100 2043.5
Muni Tunnel	11.00 ± 0.45	SWL > 11.00	1 2080.0 2 2063.5 100 2040.3

The results show the impact of the elevation uncertainty on the 11-foot infrastructure elements, with uncertainty ranging from 0.35 to 0.60 feet. This uncertainty range resulted in

performance thresholds from year 2035.5 to 2043.5 for a 100-year AEP. Figure 39 shows a comparison of the infrastructure elements by a time series of the reliability index.

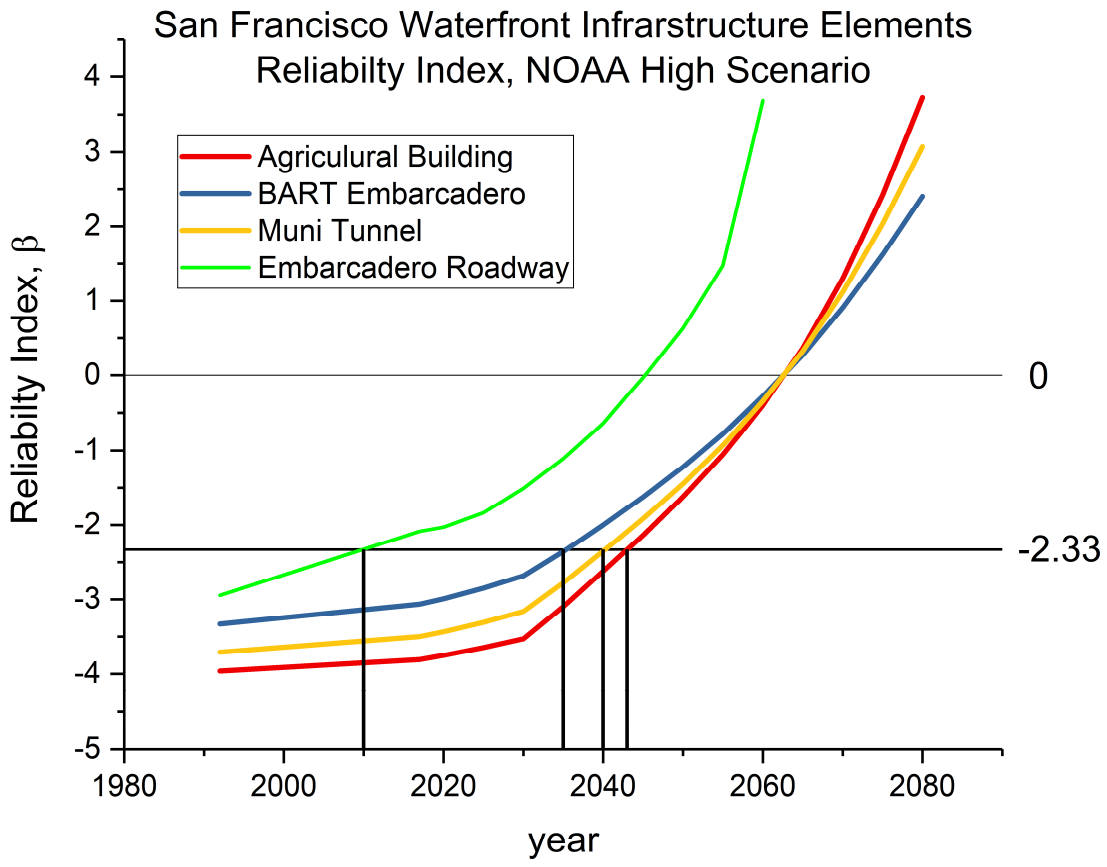

Figure 39 - Reliability Index form reliability-based performance model, San Francisco Waterfront, NOAA high scenario

It was expected that the impact of the uncertainty would be greater on the lower frequency events due to the flattening of the frequency curve. This result can be confirmed by inspection of the AEP time series plot shown in Figure 40.

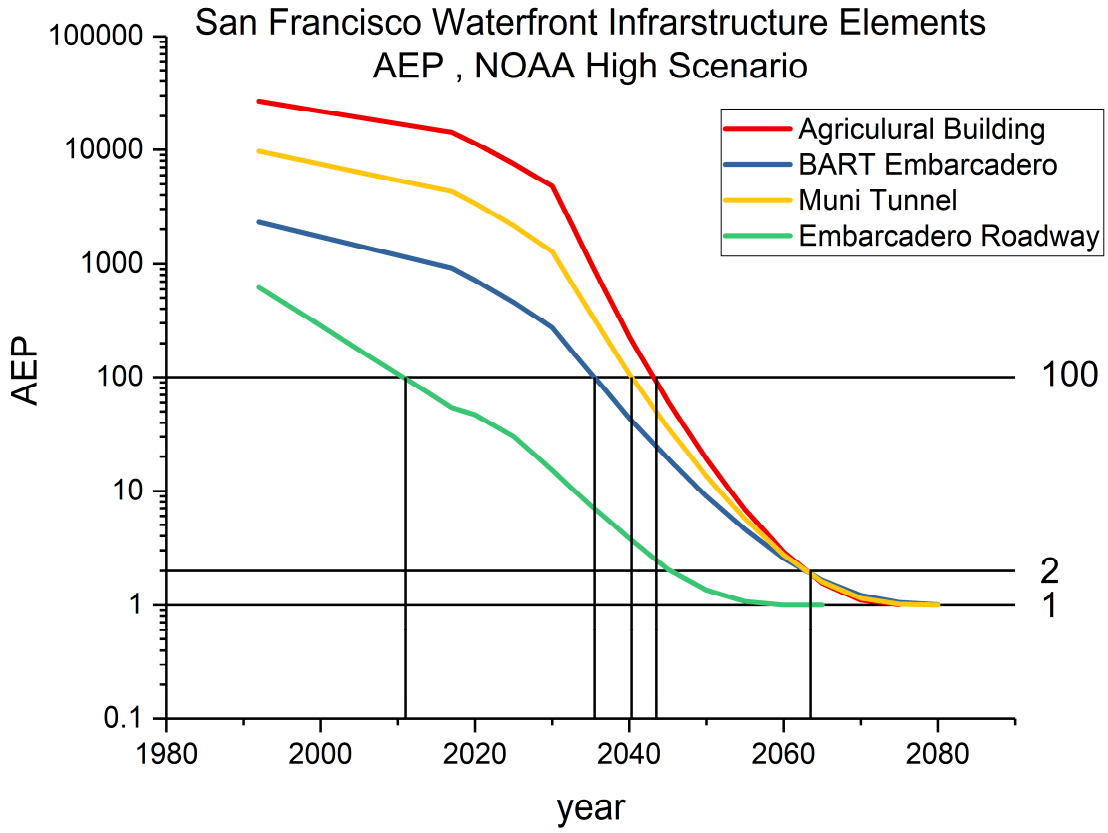

Figure 40 - Time series of AEP developed from reliability-based performance model, showing 2 and 100-year AEP performance thresholds, San Francisco Waterfront, NOAA high scenario

4.5.7 Methodology, Mapping Future Coastal Water Levels, San Francisco Waterfront

The NOAA sea level rise viewer beta version, https://coast.noaa.gov/slr/beta/ produces effective visualizations which may be used in conjunction with the CPRR framework to visualize impacts of sea level change. Figure 41 shows a water surface of 9.24 feet NAVD88, beginning to impact the Embarcadero Roadway at 9.5 feet NAVD88. The map shows a small area flooded which makes sense since the assigned uncertainty of 0.25 feet was applied. The water surface in the viewer is computed by adding 3 feet to MHHW. MHHW at Pier 22½ is 6.24 feet NAVD88, so the displayed flooding represents 9.24 feet NAVD88.

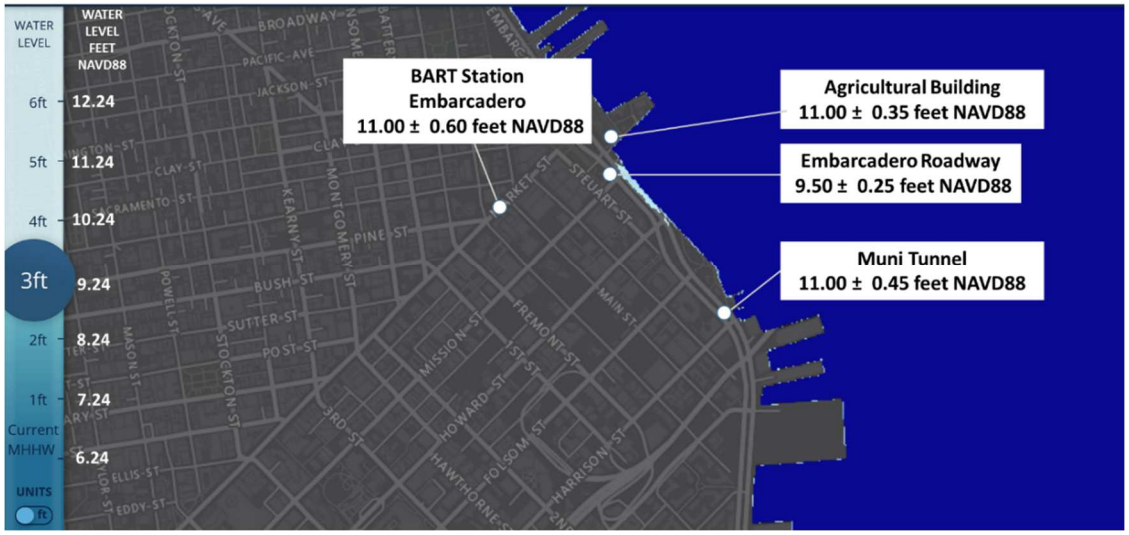

Figure 41 - NOAA sea level rise viewer, 9.24 feet NAVD88

Figure 42, 4 feet sea level rise + MHHW is an equivalent water level elevation of 10.24 feet NAVD88, shows the Embarcadero Roadway fully impacted and the other 11-foot elevation infrastructure elements are still dry, and outside the largest uncertainty estimate of 0.60 feet which would potential impacts at 10.40 feet.

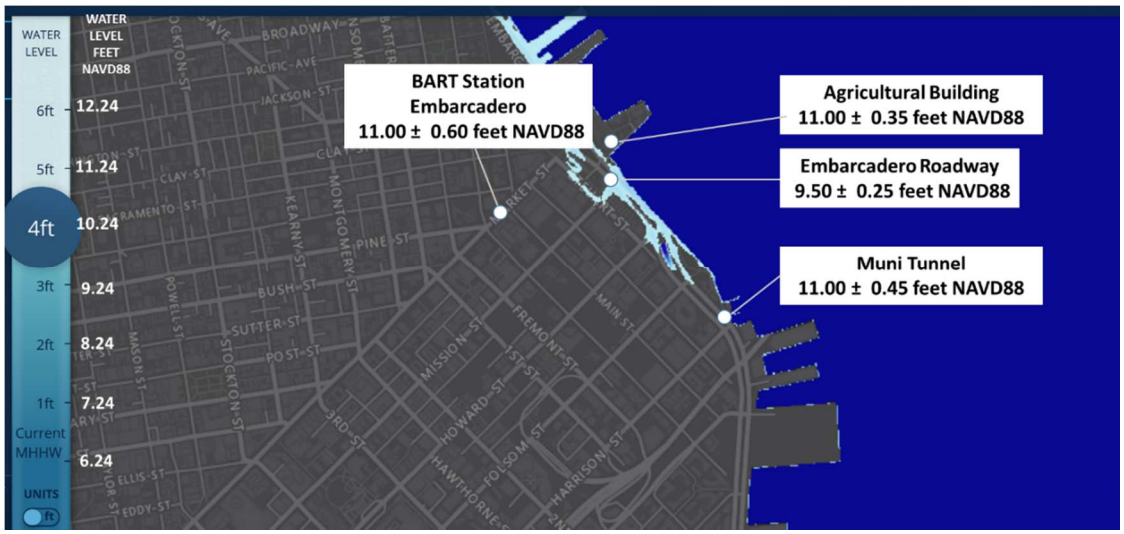

Figure 42 - NOAA sea level rise viewer, 10.24 feet NAVD88

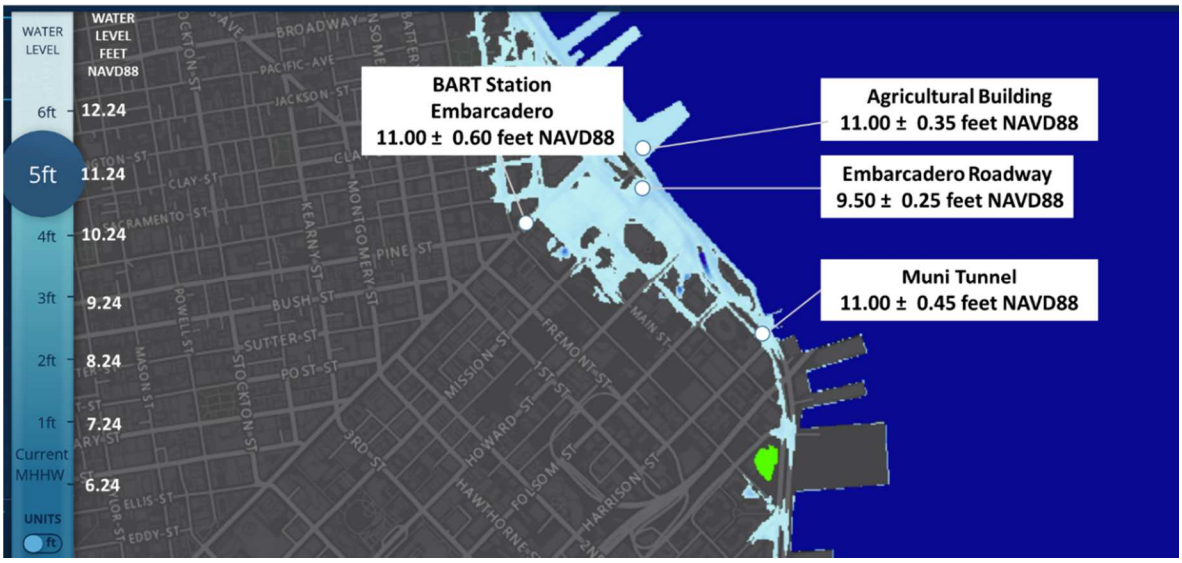

Figure 43 - NOAA sea level rise viewer, 11.24 feet NAVD88

Figure 43 shows the area impacted within 0.24 feet of the limit state of 11.00 feet NAVD with all elements impacted. The BART Embarcadero Station shows the least impact, which is why it was assigned the highest uncertainty given its location farther from the edge of the seawall with uncertain flooding pathways. Finally, Figure 44 shows the impact of 6 feet of sea level rise above MHHW, resulting in a water surface elevation of 12.24 feet NAVD88.

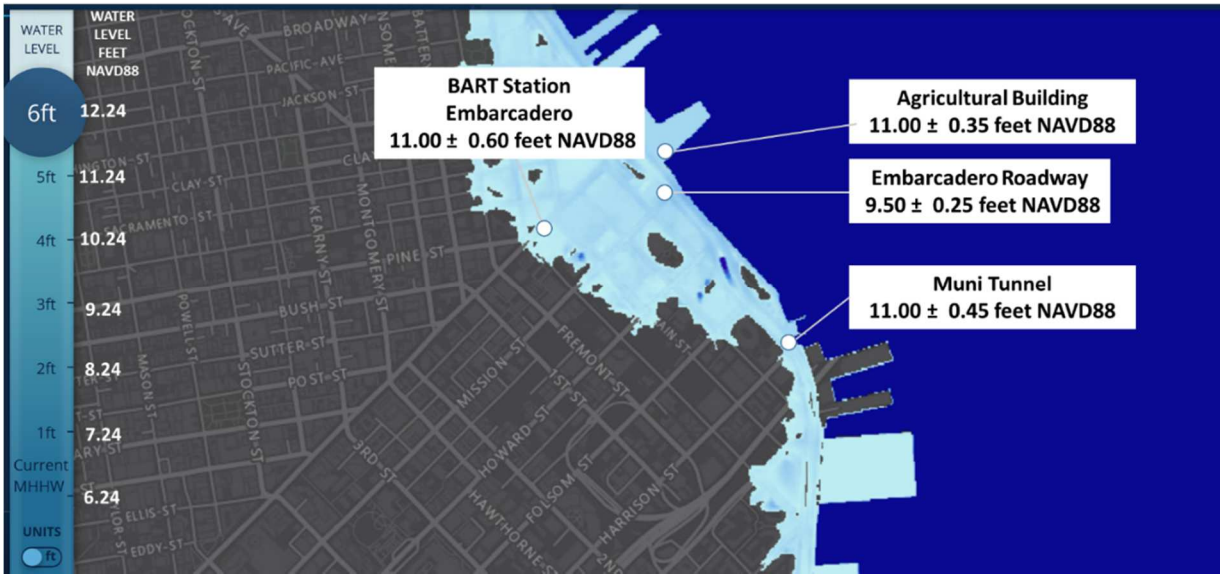

Figure 44 - NOAA sea level rise viewer, 12.24 feet NAVD88

The NOAA sea level rise viewer has limitations in that it can only map RSLC in one-foot increments above MHHW up to 6 feet. More control over the water level mapping would provide a more accurate plan view of conditions at the performance thresholds identified in the elevation and reliability-time series performance models.

5.0: CASE STUDIES DEMONSTRATING APPLICATION OF THE CPRR FRAMEWORK; FUNCTION AND RELIABILITY-BASED PERFORMANCE MODELS, STAMFORD HURRICANE BARRIER, NAVIGATION GATE CLOSURES

5.1 Stamford Hurricane Barrier, Stamford, Connecticut

A USACE project, the Stamford, CT Hurricane Barrier Project (SHB) was selected to apply the CPRR framework. The SHB extends from the West Branch eastward across the East Branch of Stamford Harbor, in the City of Stamford, Fairfield County, CT. The SHB was designed in 1962 to provide navigation and flood and coastal storm damage reduction (FCSDR) benefits to the harbor and approximately 600 acres consisting of the principal manufacturing plants of the city, residential sections, and a portion of the main commercial district). Construction of the SHB started in May 1965 and was completed in January 1969.

The project consists of three elements. The first, a barrier at the east branch of Stamford Harbor, is composed of a 2,850-ft-long earth fill dike with stone slope protection. It has an elevation of 17 feet 1962 mean sea level (MSL). A 90-ft-wide opening is provided for navigation, and a pump station discharges interior drainage (Morang 2007). The project is designed so that closures of the navigation gate will keep coastal tidal flooding from impacting the inner harbor. The navigation gate is opened during low tide to allow any high water that has collected in the harbor due to precipitation, runoff, and/or storm water to drain. Figure 45 shows the navigation gate in closed position. Navigation Gate closures (NGC) have averaged 11 per year over the period of record from 1969 through 2014. The project provides navigation benefits to the harbor as well as FCSDR. Changes in operation and performance of the SHB due to relative sea level change (RSLC) could result in longer or more frequent closure times, potentially decreasing the reliability of regular navigation traffic in and out of the small harbor.

Higher water levels on the ocean side and the land side of the SHB could stress both the project performance and that of critical infrastructure within the FCSDR area.

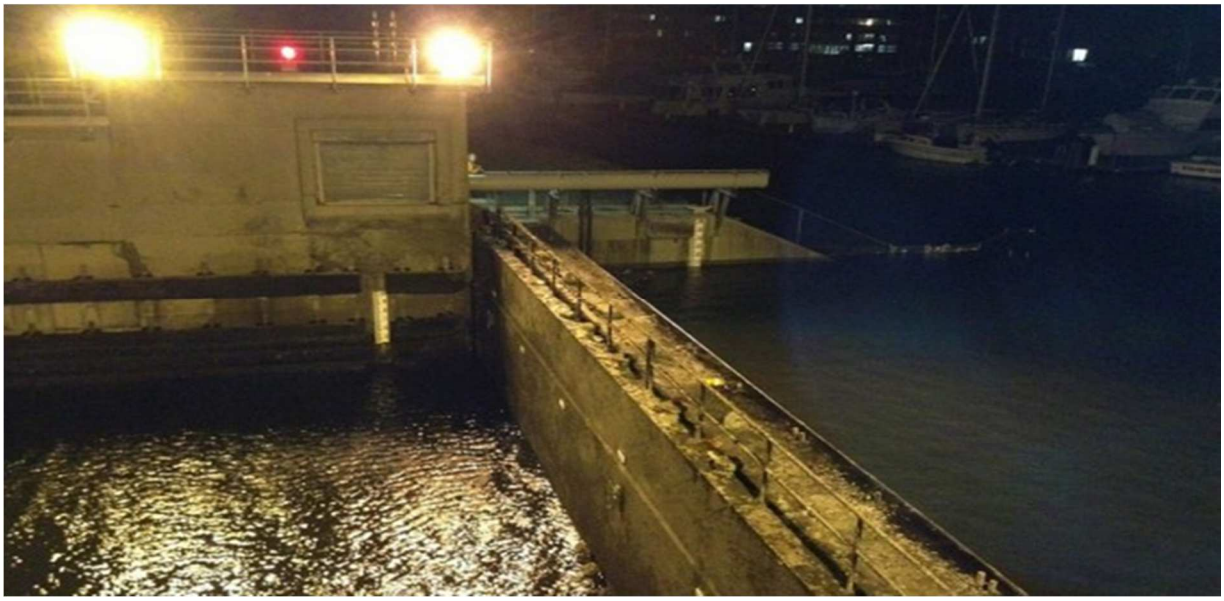

Figure 45 - Stamford Hurricane Barrier Navigation Gate in closed position

The second element is a barrier that provides protection at the west branch of the harbor. This barrier, which has an elevation of 17 feet, is composed of a 1,350-foot-long concrete wall; 2,950 feet of earth fill dike with stone slope protection and a pumping station.

The third element provides protection at Westcott Cove. This barrier is a 4,400-foot earth fill dike with stone slope protection having a maximum elevation of 19 feet. It also has two pumping stations. (USACE 1962) The main features are shown in Figure 46.

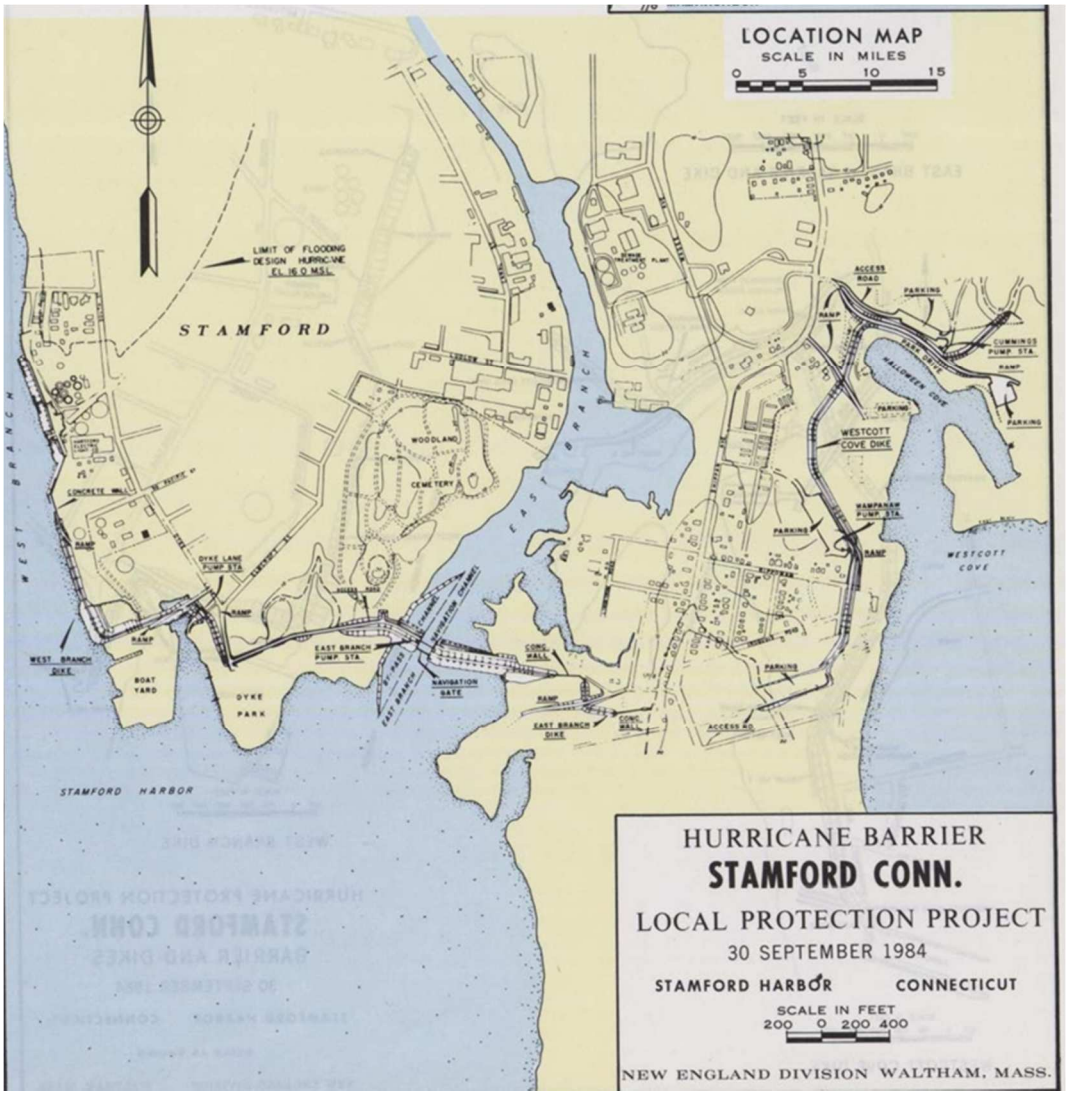

Figure 46 - Project Map, Stamford Hurricane Barrier

An analysis of the navigation function and how it will be impacted with RSLC will be the focus of this case study and provide a vulnerability assessment of navigation access to East Branch Harbor. The analysis will follow the same basic steps in the CPRR framework shown in Figure 47 below.

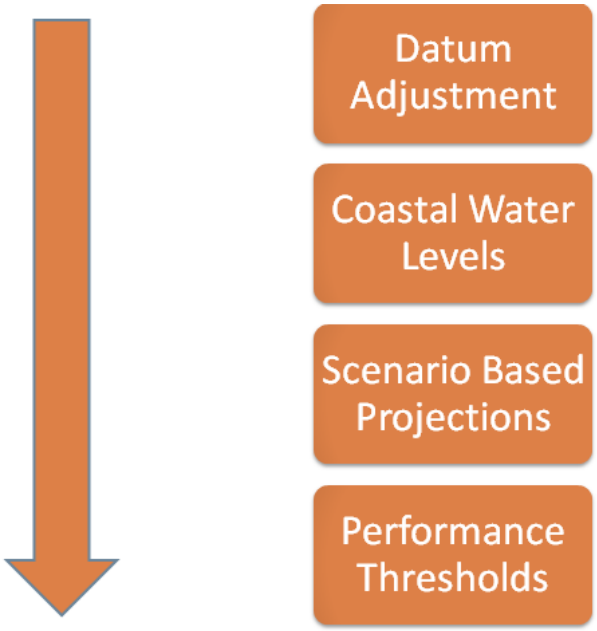

Figure 47 – CPRR framework for SHB Navigation Vulnerability Assessment

Development of the SHB CPRR will begin with selection of tide gauge(s), identifying the local tidal datum and adjustment to NAVD88 at the area of interest and follow the framework workflow order in Figure 48.

5.2 Datum Adjustment, Stamford Hurricane Barrier Navigation Gate Closures

The workflow for the Datum Adjustment is shown in Figure 48. The project documentation and current operation are referenced to the older geodetic datum, NGVD29, requiring an additional datum adjustment.

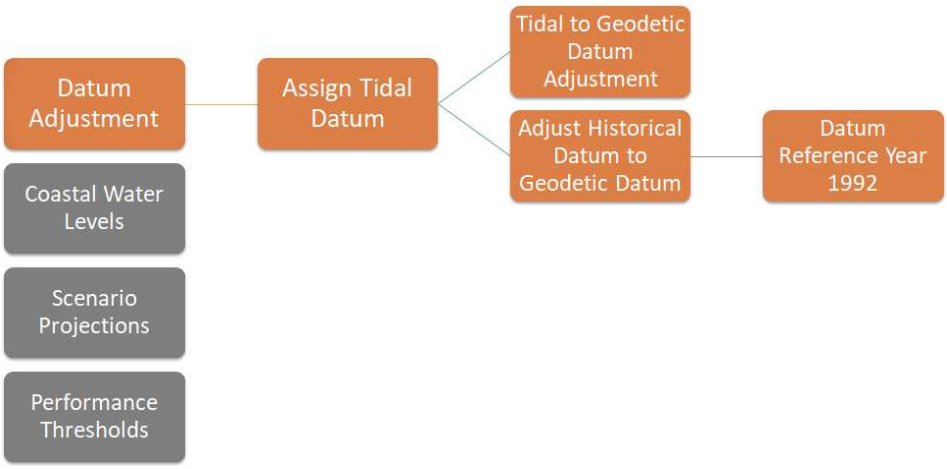

Figure 48 – Workflow for Datum Adjustment element in Stamford Hurricane Barrier Navigation Gate function-based performance model

5.2.1 Historical Background on Datums in Stamford Hurricane Barrier Design Documents

The original SHB design documents (USACE 1962) and operational manual elevations were in mean sea level (msl). Prior to the mid-1970s, the vertical datum used for many USACE projects was mean sea level (msl) based on the Sea Level Datum of 1929, as defined by the U.S. Coast and Geodetic Survey in 1929. Sea Level Datum of 1929 served as a consistent national vertical datum and was referenced in various forms as "mean sea level", "msl", or "MSL29". In 1976, the Coast and Geodetic Survey formally changed the name of "MSL29" to National Geodetic Vertical Datum, or "NGVD29".

When examining SHB project documents produced prior to 1976, it is assumed that the reference to "msl" was in relation to the 1929 vertical datum (not a local tidal datum). In this sense, "msl" is equivalent to NGVD29 prior to 1976. It is also noted that prior to 1976, local tidal datums such as mean high water (MHW) were often referenced to the vertical datum of "msl". Using the current documentation (post 1976), the term "msl" can introduce ambiguity as

"msl" is often assumed to represent mean sea level based on a local tidal datum; not the vertical datum of NGVD29 which represented a static geodetic datum.

5.2.2 Methodology, Assign Tidal Datum, Adjust Historical Geodetic Datum, Stamford Hurricane Barrier Design Navigation

The vertical datum of NGVD29 has been replaced with the North American Vertical Datum of 1988 (NAVD88). Because NAVD88 and NGVD29 are defined using different methods, the two datums are vertically offset. Given that present-day terrestrial surveys use NAVD88 as the basis to establish vertical control, it is advantageous to reference a project's legacy datum to NAVD88. Table 17 contains both the tidal datum adjustment and the both the current and legacy geodetic datum adjustment.

Figure 49 shows the locations of NOAA tide stations used in the SHB CPRR. Both stations are referenced to NAVD88 as shown in table 17.

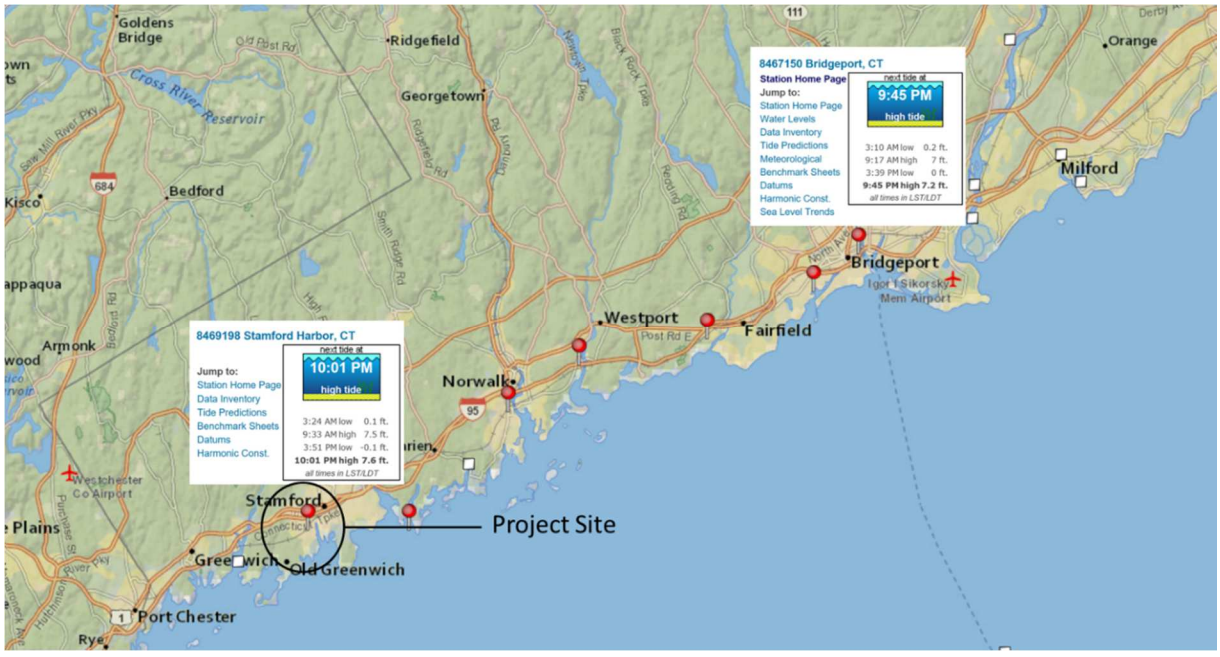

Figure 49 - Stamford Harbor, Bridgeport NOAA tidal stations

Table 17 - Tidal to Geodetic Datum adjustments Stamford Harbor, Bridgeport, CT

Tidal Datum (feet)	Stamford Project Design Manual (feet)	Stamford 1965-1969 (feet)	Stamford Harbor NOAA 8469198 (feet)	Bridgeport NOAA 8467150 (feet)
MHHW			3.73	3.48
MHW	3.80	4.20	3.38	3.15
MSL	0.00		-0.19	-0.22
MLW	-3.40	-3.00	-3.80	-3.60
MLLW		-3.30	-4.04	-3.84
NAVD88	-3.40	1.10	0.00	0.00
NGVD29	0.00	0.00	1.10	1.09

5.3 Coastal Water Levels, Stamford Hurricane Barrier, Navigation Gate Closures

The work flow to develop Coastal Water Level data for the SHB CPRR is shown in Figure 50. For analysis of gate closures, the performing water level used was the daily peak Stamford Harbor level at SHB.

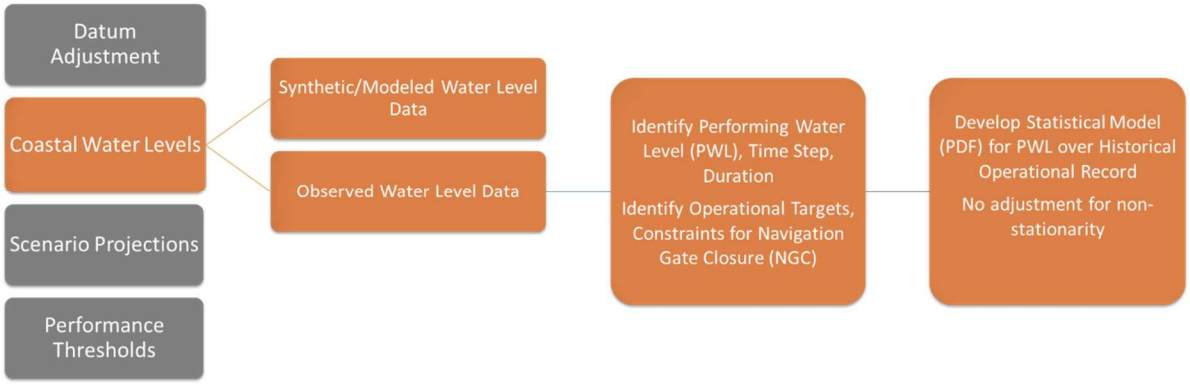

Figure 50 - Workflow for Coastal Water Levels used in the CPRR for NGC at Stamford Hurricane Barrier, Stamford, CT

The tide is diurnal at Stamford Harbor meaning two high tides or two low tides are possible in a 24-hour period. Therefore, two gate closure operations are possible within a 24-hour period. Because the long-term water level record is at a daily time step, the functional modeling of future gate closures will use a daily time step and assume a single closure in a daily time step. Since the primary goal of CPRR analysis is to locate performance thresholds, the assumption of one closure per day will be an accurate estimate for threshold targets which are determined by operational factors and cost of operation.

Continuous gauge records at SHB are available starting in 2001. To estimate daily peak water levels at SHB prior to 2001 the data adjustment technique used in the San Francisco Waterfront Elevation CPRR in Chapter 4 was utilized to adjust daily peak water levels from the NOAA gauge at Bridgeport, CT (NOAA 8467150). The adjustment is based on the ratio between MHHW at the Bridgeport, CT (NOAA 8467150) tide gauge and MHHW to the Stanford Harbor, CT (NOAA 8469198), the ratio is given by an amplification factor, *A*:

$$A = \frac{MHHW_{StamfordHar\,8469198}}{MHHW_{Bridgeport\,8467150}} = 1.07 \tag{5.1}$$

An average adjustment to obtain daily maximum water levels at Stamford was used to develop equation 5.2 and is given by the following formula,

$$StamfordDailyMaximum = BridgeportDailyMaximum + 0.3 \tag{5.2}$$

Water levels prior to 2001 were adjusted by 0.3 feet to complete the record of daily maximums at Stamford, 0.3 feet was added as a general adjustment to the Bridgeport data based on the estimate developed with equation 6.1. Additional data on water levels above 5.9 feet was

available from the SHB operational records, so the bulk adjustment was used on Bridgeport water levels between MHHW and 5.6 feet NAVD88.

A functional analysis of gate closure operations requires a more refined application of the statistical model approach used for a performing water level based on annual peak water levels. For the gate closure function, the daily ocean side peak water level governs the gate closure decision. The long term operational record shows a high degree of variability on daily peak water levels which trigger gate operation in monthly, seasonal, and interannual time scales. This variability is reflected in the long-term operational record by water year in Figure 51. While the variability is significant year to year, the record does not show a clear increase in NGC from RSLR.

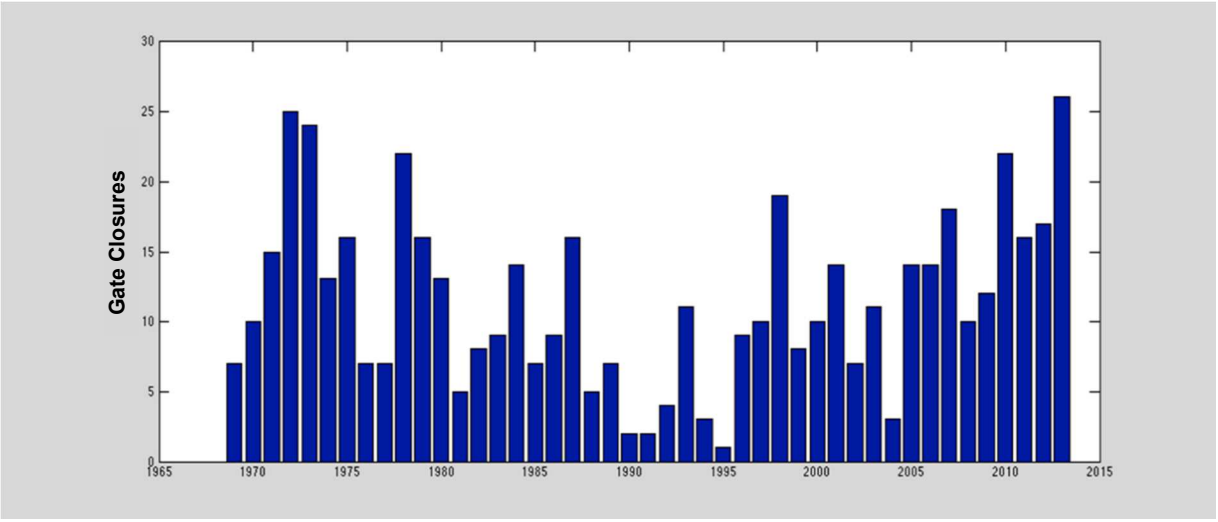

Figure 51 - Stamford Hurricane Barrier, Navigation Gate Closures by Water Year 1969-2014

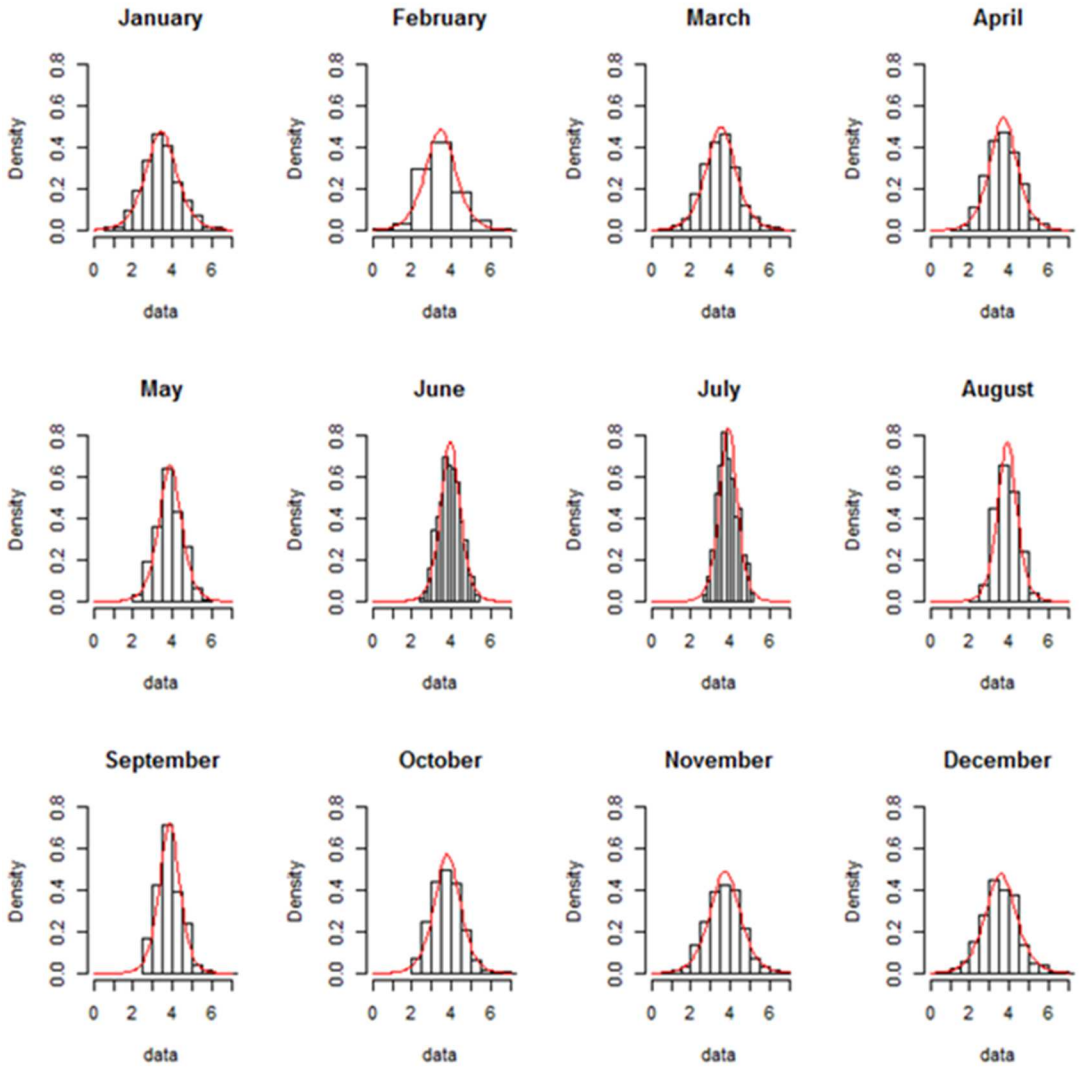

Figure 52 - Probability Density Function (PDF) for daily peak water levels (1969-2014) by month at Stamford Harbor

An examination of the monthly PDF's in Figure 52 shows significant monthly and seasonal variability in daily peak water levels by month and season. This variability controls NGC in the operational record.

5.4 Scenario Projections, Stamford Hurricane Barrier, Navigation Gate Closures

Figure 53 shows the workflow for application of RSLC scenarios. For the SHB CPRR, the three USACE SLC scenarios were used, Low, Intermediate and High.

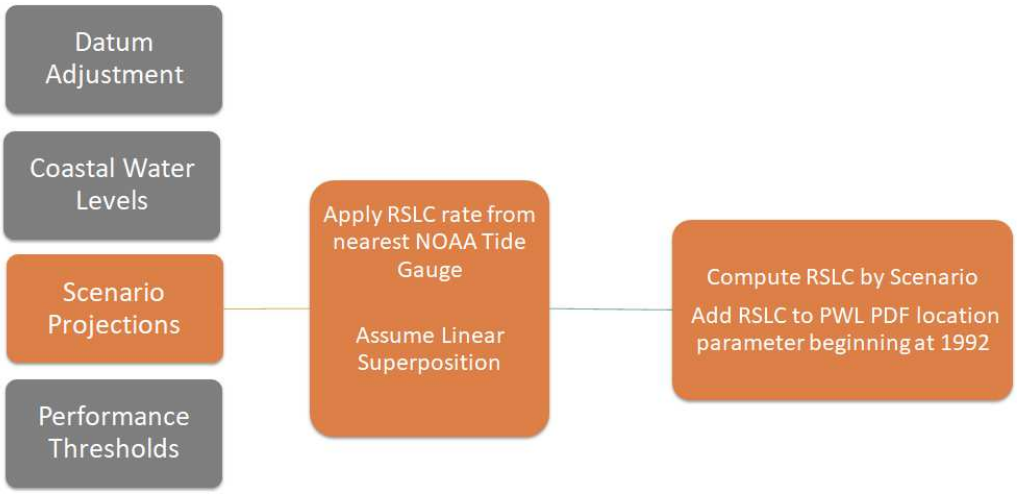

Figure 53 - Workflow for Scenario projections, Stamford Hurricane Barrier Navigation Gate Closures

To capture the seasonality in water levels at Stamford Harbor, the modified data set representing observed daily peak water level data was fit to 12 individual monthly logistic distributions (Table 18). Normally the observed record would be detrended to remove the impact of non-stationarity on the record, however to create the predictive model for functional performance, the record was not adjusted for sea level change. Since operation of the navigation gate is determined by forecasted water levels and potential for rainfall, the actual daily peak water level in Stamford Harbor corresponding to the gate closure operation is highly variable. Because the predictive model is based on the observed Stamford Harbor water levels in the operational record, adjustment of the water level record for relative sea level change would result in an inaccurate predictive model. The model will add RSLR based on the three SLC scenarios in the forecast period.

Table 18 - Monthly location parameters (feet NAVD88) for logistic distribution of SHB Gauge at Stamford Harbor

Month	Location Parameter 1992	Location Parameter 2015	Scale Parameter
January	3.43	3.65	0.52
February	3.45	3.67	0.51
March	3.53	3.75	0.50
April	3.72	3.94	0.46
May	3.88	4.10	0.38
June	3.96	4.18	0.32
July	3.91	4.13	0.30
August	3.91	4.13	0.32
September	3.85	4.07	0.34
October	3.80	4.02	0.43
November	3.74	3.96	0.51
December	3.58	3.80	0.52

All distributions, plots, and diagnostics were generated using the *fitdistrplus* library in the R statistical programming language (Delignette-Muller and Dutang 2015).

To compute the RSLC adjustments, the 2015 RSLC rate from the Bridgeport, CT (NOAA 8467150) tide gauge, 2.87 mm/year (NOAA 2015). The 1992 location parameters in Table 18 were adjusted to 2015 levels by adding RLSC from 1992 to 2015 in equation 5.3:

$$23 year \times 2.87 \frac{mm}{year} \times 0.0033 \frac{feet}{mm} = 0.22 feet \quad (5.3)$$

Scenario projections of RLSC at Stamford Harbor are based on the Bridgeport, CT 2015 rate of 2.87 mm/year and given by the following equations:

$$t = year - 1992 \tag{5.4}$$

$$RSLR_{USACELow} = RSLR_{Bridgeport} \times t \tag{5.5}$$

$$RSLR_{USACEInt} = RSLR_{Bridgeport} \times t + 0.0000271 \times t^2 \tag{5.6}$$

$$RSLR_{USACEHigh} = RSLR_{Bridgeport} \times t + 0.000113 \times t^2 \tag{5.7}$$

$$RSLR_{Bridgeport} = 0.00287m \tag{5.8}$$

where RSLR is in meters. The computed RSLR is converted to feet and added to the monthly location parameters in Table 18.

5.5 Performance Thresholds, Stamford Hurricane Barrier, Navigation Gate Closures

The CPRR for SHB Navigation utilized function and reliability based performance models to determine performance thresholds. Performance thresholds were based on a level of NGC which would cause a significant shift in operational cost or availability of East Branch Harbor to Navigation traffic. For the function-based performance model, 52 NGC/Water Year was chosen, under the assumption that a closure frequency of one NGC/week would cause the SHB project to be staffed with a crew to operate the NGC operation. Staffing the project would represent a significant increase in Operations and Maintenance costs. The effect of increased NGC on maintenance and long-term durability is not quantified in this analysis, though assumptions could be worked into the analysis and an additional threshold defined.

5.5.1 Operational Background, Stamford Hurricane Barrier

Figure 54 shows the workflow for development of a functional threshold defined by navigation gate closures (NGC) per water year. NGC/Water Year is an example of a functional metric whose value is determined or influenced by Coastal Water Levels.

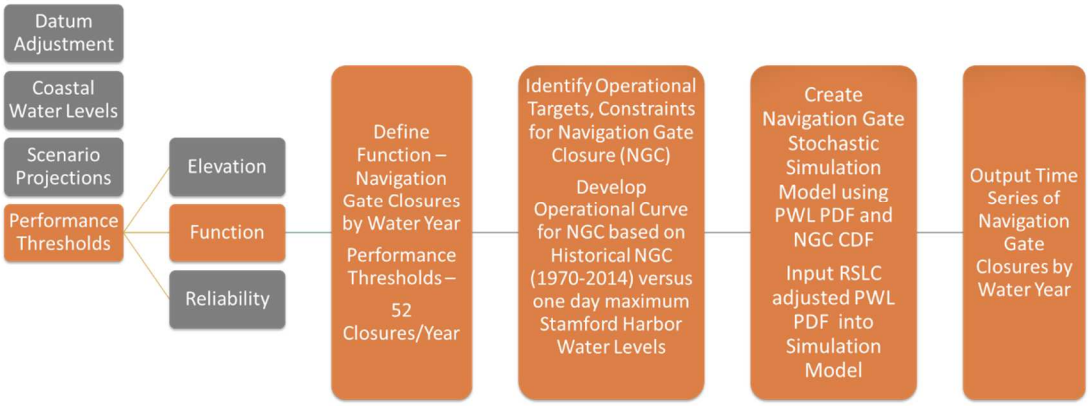

Figure 54 - Workflow for Function-Time series performance model (NGC/Water Year) for the Stamford Hurricane Barrier

Most functional metrics require a model or equation to incorporate performing water level defined in the Coastal Water Level section of the CPRR framework. The operational goals relating to closure of the navigation gate are to prevent combinations of flood tide and rainfall to reach an elevation of 5.9 feet NAVD88 (7.0 feet NGVD29) within East Branch Harbor. The design of the project must allow for interior drainage of the enclosed catchment of 1200 acres to drain into the harbor while the navigation gate is closed without causing the harbor level to rise over elevation 5.9 feet NAVD88 which would cause flooding in the immediate area and reduction of gravity drainage efficiency from the catchment stormwater drainage infrastructure. To provide sufficient storage for stormwater runoff entering East Branch Harbor behind the navigation gate when closed, the operational goal of the project is to keep the water levels in the harbor at or below 4.7 feet NAVD88 (5.8 feet NGVD29) when the navigation gate is closed.

Figure 55 shows daily maximum elevations at Stamford Harbor with the operational targets over the period 1969-2014. These elevations represent the East Harbor water levels with the navigation gate open.

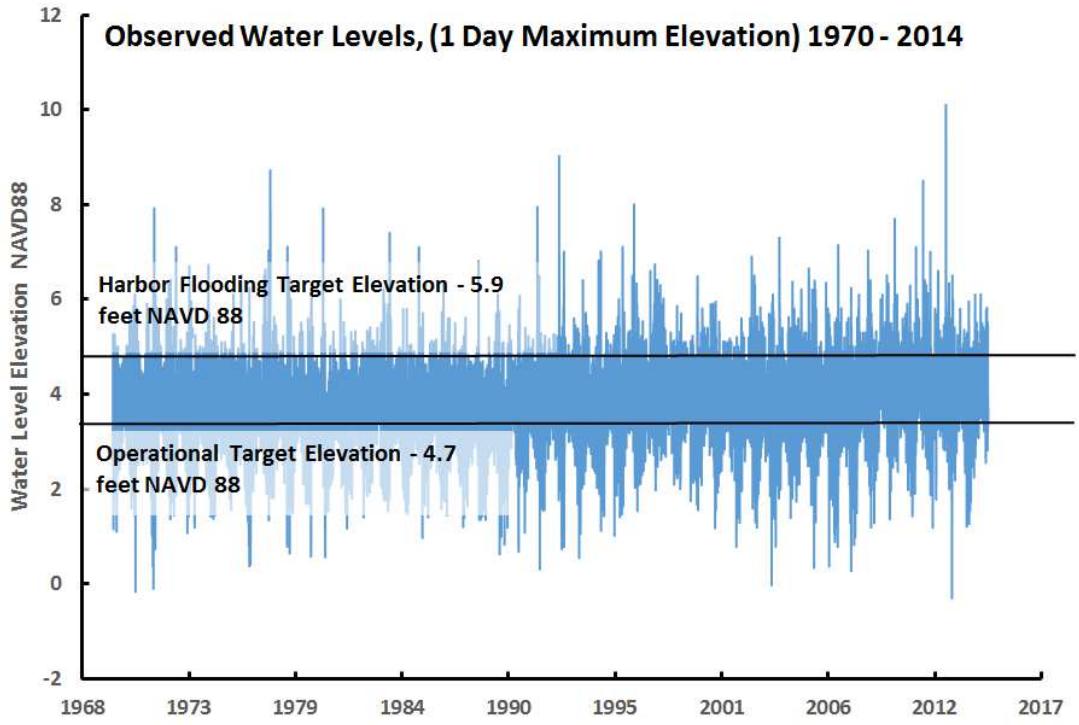

Figure 55 - One Day Maximum Water Levels, Stamford Harbor, CT

The SHB project (Figure 56) at East Branch Harbor includes a small pump station with a 100 cfs pump which allows for stormwater runoff volume to be discharged outside the barrier during closure periods. There is also an 8 x 8 bypass gate built into the gate which may be used to release water on falling tides while the gate is closed or more rapidly equalize water levels for a gate operation. A 1200-acre catchment drains into the East Branch Harbor and the interior drainage for the catchment relies on storage provided by the harbor at water levels below 5.9 feet NAVD88. Interior drainage of the 1200-acre catchment is augmented by a combination of pump capacity and harbor storage which are part of the SHB project.

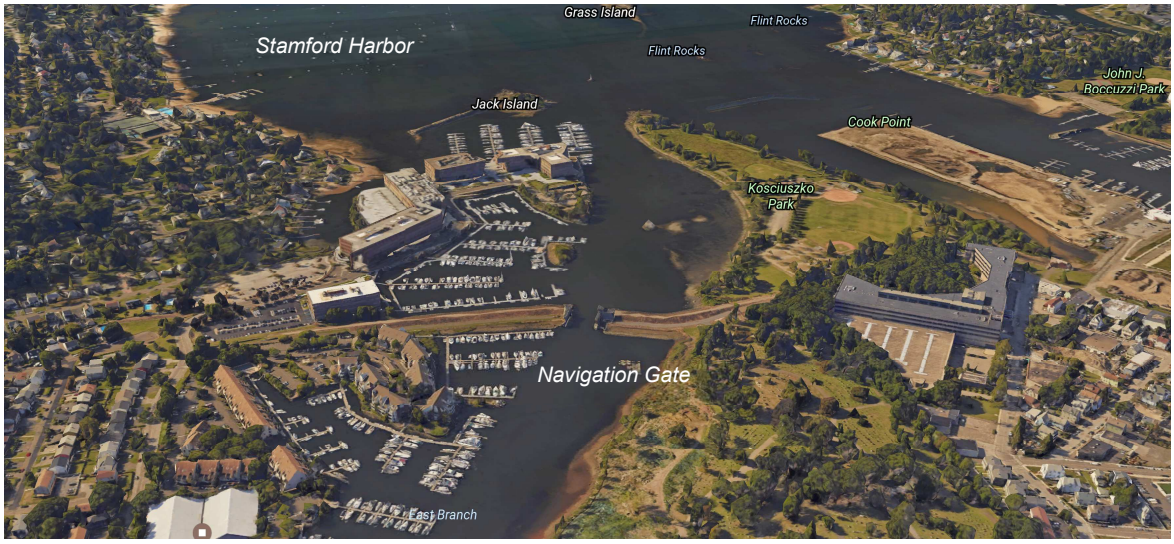

Figure 56 - Aerial view of the SHB Navigation Gate, Stamford Harbor, East Branch Harbor

The operational decision to close the navigation gate is made with consideration of several factors including the weather forecast, time to deploy a crew to operate the gate, public notice to marine interests through the coast guard and judgement of the USACE Reservoir Regulation staff in making the decision to close the navigation gate. Figure 57 shows the key Stamford Harbor elevation operational targets.

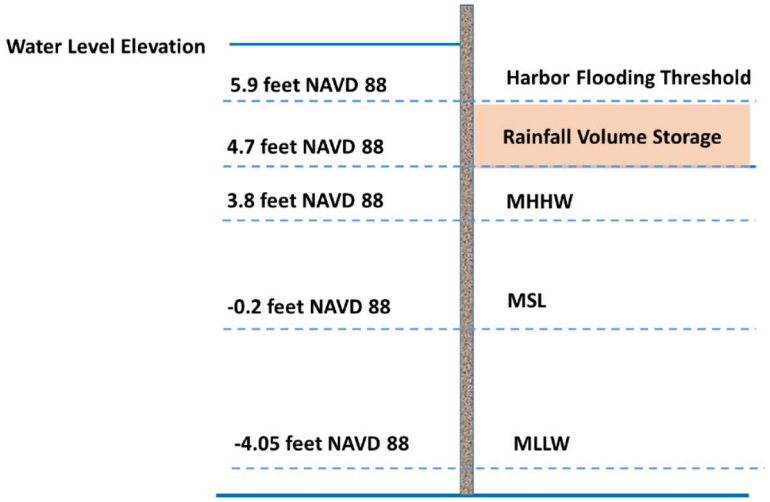

Figure 57 – Tidal Datum and significant elevation targets for Navigation Gate Closure operation

Qualitatively, NGC will increase with increasing RSLR. Development of a function based CPRR of NGC will provide insight on how current operations will be impacted by the magnitude and rate of RSLR at the SHB. The number of NGC per water year since the project opened has been highly variable over a year to year basis, and even seasonally. Over the period of 1970 to 2014, there were 522 gate closures, or an average of 11.9 per year (Figure 58).

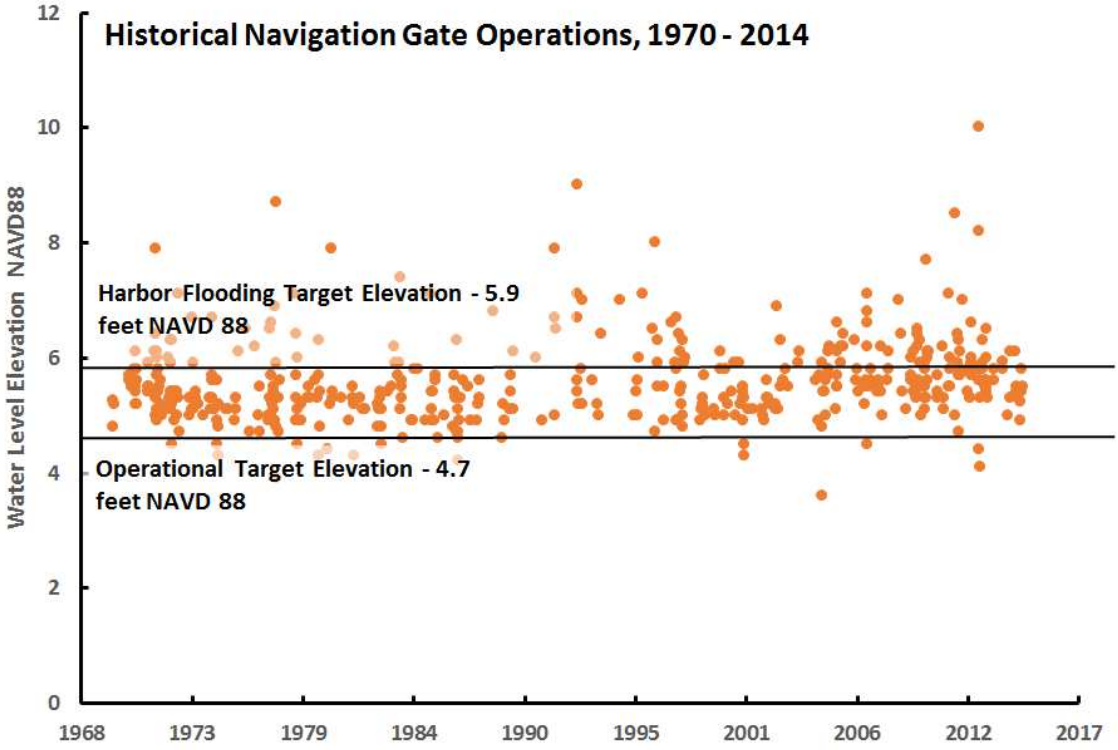

Figure 58 - Navigation Gate Closures versus Stamford Harbor elevation, Stamford Hurricane Barrier (1970-2014)

Several approaches for projecting future NGC impacted by RSLR were considered including a simplistic method applying observed gate closure rates to shifted stage duration curves under RSLR. These methods would not reflect the wide variability seen in annual operations by water year which ranged from 0 to 26 closures per year between 1970 and 2014. A goal of the function based CPRR for NGC is to capture the year to year variability in NGC

while providing an accurate projection of future NGC under a range of SLC scenarios. The variability in NGC projections is captured by providing confidence intervals representing the historical variability.

5.5.2 Methodology, Computational Model, Stamford Hurricane Barrier Navigation Gate Closures

A computational model based on the historical operational record was developed in the R computer code (R core team 2016) to create an unbiased projection which is based on the current and past operation at the SHB project, while preserving the factors which influence the decision to close the gate. Under a perfect foresight assumption, the gate closure decision would be triggered by simply closing the gate at elevations equal or greater than 5.9 feet NAVD88. The average elevation of Stamford Harbor for NGC based on the long term operational record is 5.3 feet NAVD88, 0.6 feet lower than the flooding threshold of East Harbor. Figure 59 shows an operational decision curve of NGC derived from the 1970-2014 operational record.

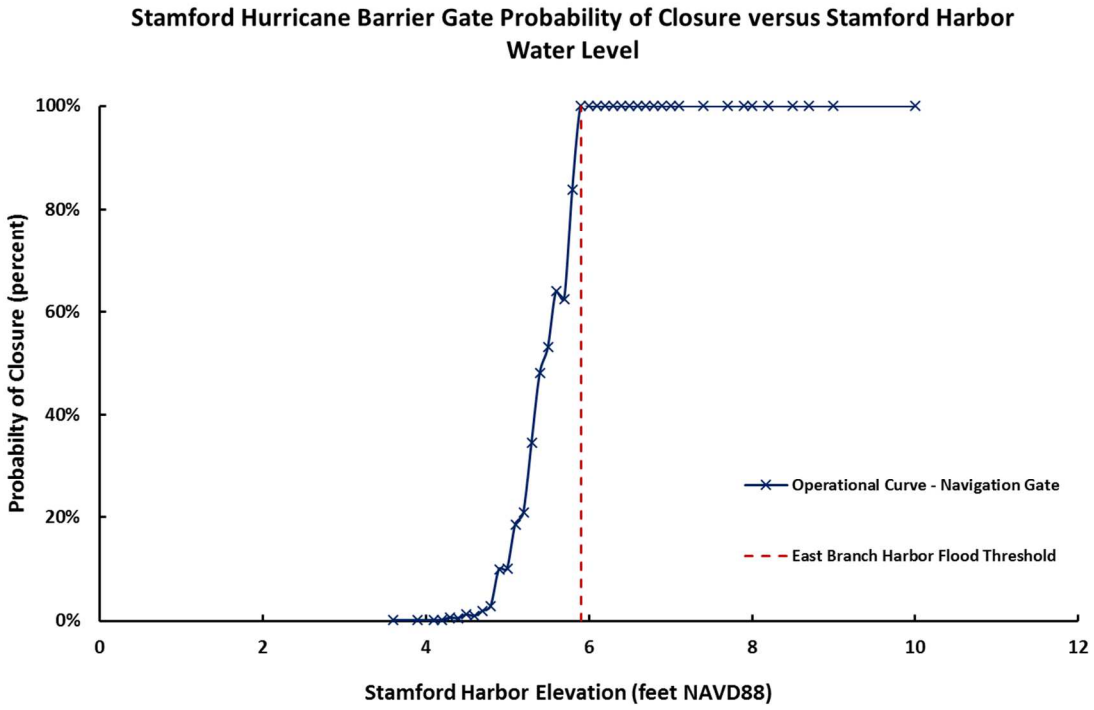

Figure 59 - Operational curve for the SHB navigation gate closures versus peak daily Stamford Harbor elevation developed from operational records 1970-2014

The operational curve is based on NGC over the period 1970-2014, with water levels occurring at or above 5.9 feet NAVD triggering a NGC 100 % of the time.

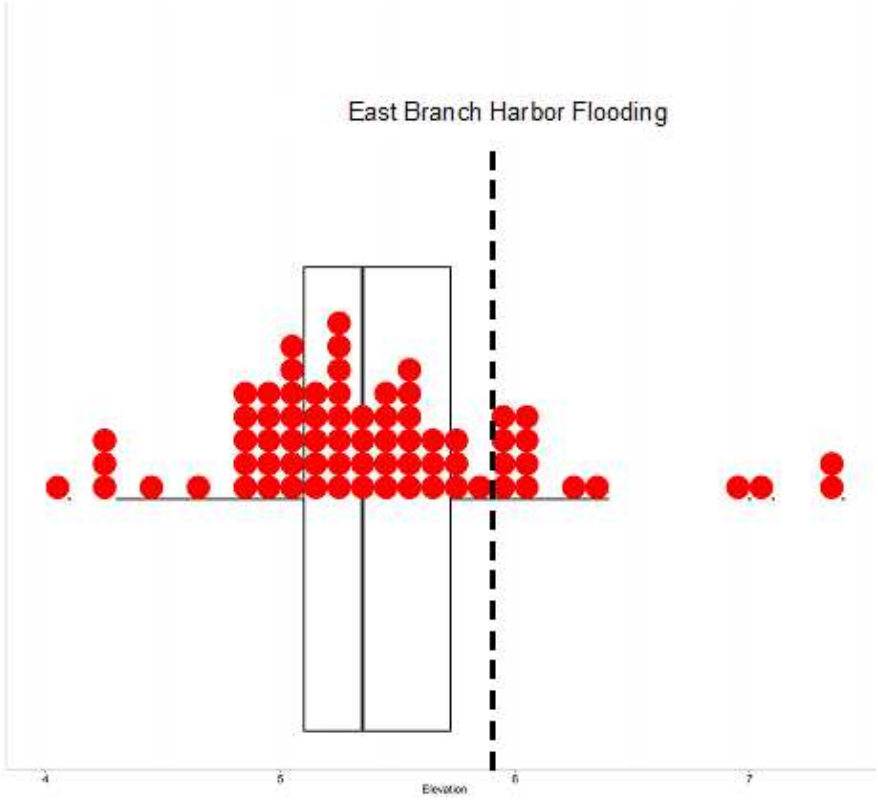

Figure 60 - Distribution of NGC in month of March 1970-2014 versus Stamford Harbor Elevation. Red circles represent individual NGC in the month of March

Figure 60 shows NGC for the month of March over the period of operation (1970-2014). As plot shows, most NGC occur to the left of the East Branch Harbor flood threshold of 5.9 feet NAVD88. The historical operational record shows that for a total of 518 navigation gate closures, 116 closures out of the 518 (29 %) prevented flood damages by not allowing the East Branch Harbor water level to exceed 5.9 feet NAVD88 due to a recorded Stamford Harbor water level at or above 5.9 feet NAVD88. In 402 of the closures, Stamford Harbor levels did not reach the flood threshold of 5.9 feet NAVD88 and no exceedances of the East Branch Harbor flood threshold would have occurred. The relatively low ratio of gate closures preventing exceedances of the 5.9 feet NAVD88 flood damage threshold to total closures is caused by a combination of

forecast accuracy, operational window, risk aversion, and the additional operational target to keep the East Branch Harbor water level below 4.7 feet NAVD88 to accommodate stormwater runoff volume during closure periods.

NGC sometimes occurred more than once in each 24-hour day, and were counted as such in the operational record and in USACE damages prevented reporting. To develop a simulation model with an hourly time step capable of multiple closures in a 24-hour cycle, would require a significantly more complex model and a 1-hour time step. Since accurate, continuous hourly data at the project was not available before 2001, a model which used a daily time step or one navigation gate closure per day was created. The model incorporates the historical navigation gate closure performance to produce a forecast of gate operations which reflected the current and past decisional pattern at SHB.

The simulation model runs in a one-day time step from 1992 to 2115, which includes a 100-year period of analysis. The period 1996 to 2013 is the model verification portion of the simulation, and the period 2015 to 2115 is the actual operational forecast. The operational curve in Figure 59 is used in the model to trigger a NGC at water levels below 5.9 feet NAVD88 at the same frequency as the historical operational record.

The model adds the one-day increment of RSLR based on each SLC scenario to the monthly location parameters representing the average peak daily Stamford Harbor water level for the respective month are shown in Table 18. The RSLR increments are computed in equations 5.6 through 5.8 respectively. A snapshot of the projected Stamford Harbor annual water level statistics which will trigger NGC in the simulation model for each respective scenario in the year 2045 is shown in the box and whisker plot comparison in Figure 60. The East Branch Harbor flood threshold is annotated on Figure 60 for reference.

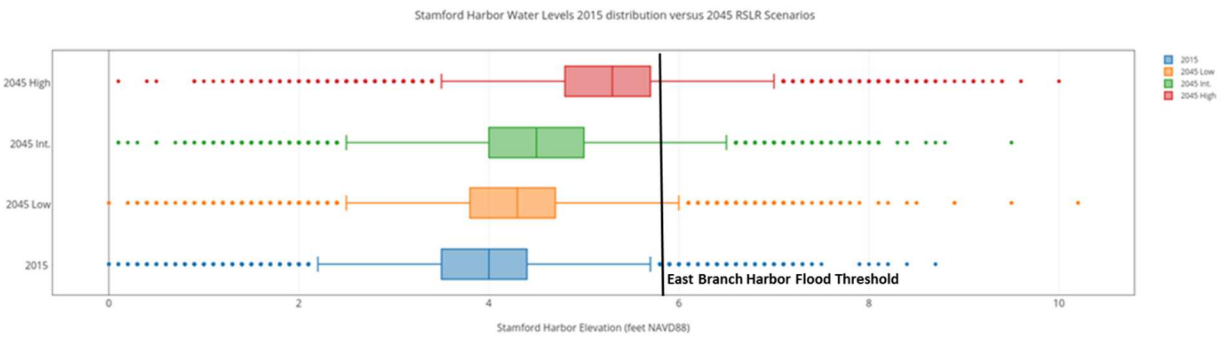

Figure 61 - Box and Whiskers comparison of projected Stamford Harbor Water Levels to the year 2045, statistics for annual series compiled from individual monthly projections

The navigation gate operation for SHB in modeled as a Bernoulli sequence (Ang 2007) with the following assumptions:

1. For a daily, one-day time step, there are only two possible occurrences, the navigation gate is open or closed.
2. P (Stamford Harbor water level Gate Closed) is constant.
3. Each trial is statistically independent. For each one-day time step, 100 trials are simulated using the R command *rbinom* (Kachitvichyanukul 1988), creating 100 elevations corresponding to each month's logistic distribution (location, scale) representing water levels in Stamford Harbor which is a trigger for the navigation gate operation. The probability of the gate closed condition is informed by the operational curve representing the probability the navigation gate being closed.

Simulation results in the 5, 50, and 95% percentiles were generated by computing the number of NGC in 100 draws for each one-day time step or 36500 (100 x 365) trials for each water year for each scenario.

5.5.3 Methodology, Computational Model Validation, Stamford Hurricane Barrier Navigation Gate Closures

The NGC simulation model was validated against NGC by water year over the period of 1993-2013. This twenty-year period had 255 one-day NGC, an average of 12.14 per year. The simulation model produced 250 one-day NGC for an average of 11.92 per year. When the simulation model results are rounded to an integer result, agreement is slightly improved with 251 NGC over the twenty-year period with an average of 11.95 per year. Table 19 presents the validation results by water year. The model was run using simulated water levels and not the actual time series incorporating the low or observed RSLR rate at SHB. The small difference in the results is likely from small differences in the water level simulation and rounding versus the actual time series. The simulation model reproduced cumulative NGC over a twenty-year period within a 98.4% level of accuracy. Figure 62 shows the model results in confidence intervals versus the actual NGC/Water Year totals. Longer term forecasts of 10-year blocks of NGC will be very accurate, while year to year forecasts should be provided with the 5/95 percent confidence intervals to capture year to year variability in NGC.

Table 19 - Actual versus Simulated NGC, 1993-2013 at the Stamford Hurricane Barrier

Water Year	Actual NGC	Simulated NGC	Simulated NGC (rounded)
1993	11	9.69	10
1994	3	10.40	10
1995	1	9.53	10
1996	9	10.49	10
1997	10	10.52	11
1998	19	11.07	11
1999	8	10.89	11
2000	10	11.17	11
2001	14	11.33	11
2002	7	10.86	11
2003	11	11.73	12
2004	3	12.19	12
2005	14	12.10	12
2006	14	12.53	13
2007	18	13.09	13
2008	10	12.89	13
2009	12	13.26	13
2010	22	13.68	14
2011	16	13.88	14
2012	17	14.09	14
2013	26	14.94	15

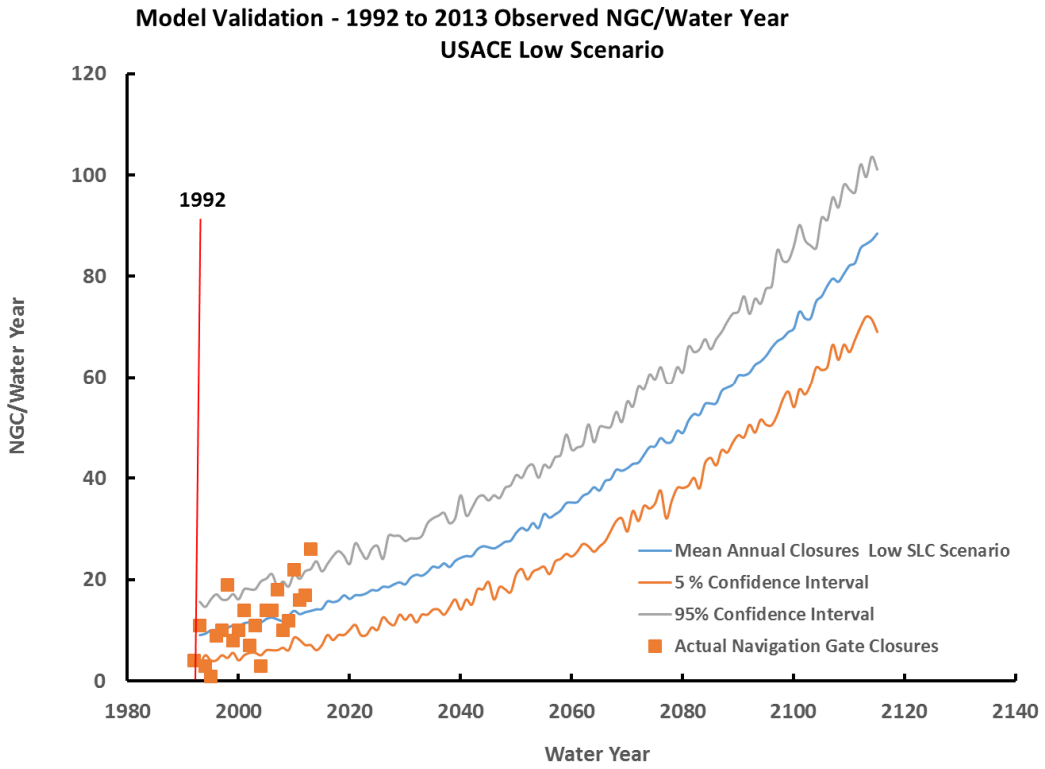

Figure 62 - Model versus actual NGC, model traces are the 5/50/95 percentile confidence intervals

5.5.4 Performance Thresholds, Reliability-Based Performance Model Results, Stamford Hurricane Barrier Navigation Gate Closures

The full results of the simulation, including those beyond the twenty-year validation period are shown in Figure 63 and Table 20. For the functional performance metric of NGC/Water Year, an ad-hoc performance threshold of 52 NGC was selected. The performance threshold represents a NGC amount which is twice the historical high NGC/Water Year, 26 in water year 2013. The performance threshold of 52 NGC/Water Year represents a potential operational cost threshold for the SHB project, since 52 NGC/Water Year represents an average of one NGC/week. The SHB is presently remotely operated, with no on-site staff. When NGC

frequency increases to an average of one NGC/week, it will likely require the SHB project to be staffed on a regular basis instead of the current on call staffing.

Table 20 - Stamford Hurricane Barrier, Functional CPRR NGC/Water Year

Infrastructure Element	Performance Metric	Performance Threshold	CI (pct.)	USACE Low (Year)	USACE Int. (Year)	USACE High (Year)
SHB Navigation Gate	NGC/Water Year	NGC > 52/Water Year	50	2082	2050	2029
SHB Navigation Gate	NGC/Water Year	NGC > 52/Water Year	5	2093	2056	2033
SHB Navigation Gate	NGC/Water Year	NGC > 52/Water Year	95	2068	2042	2026

Results of the functional CPRR show future years 2068-2093, 2042-2056, and 2026-2033 reaching the 52 NGC/Water Year threshold. The simulation model results may also be compiled in 5 to 10-year blocks of cumulative NGC/Water Years if desired.

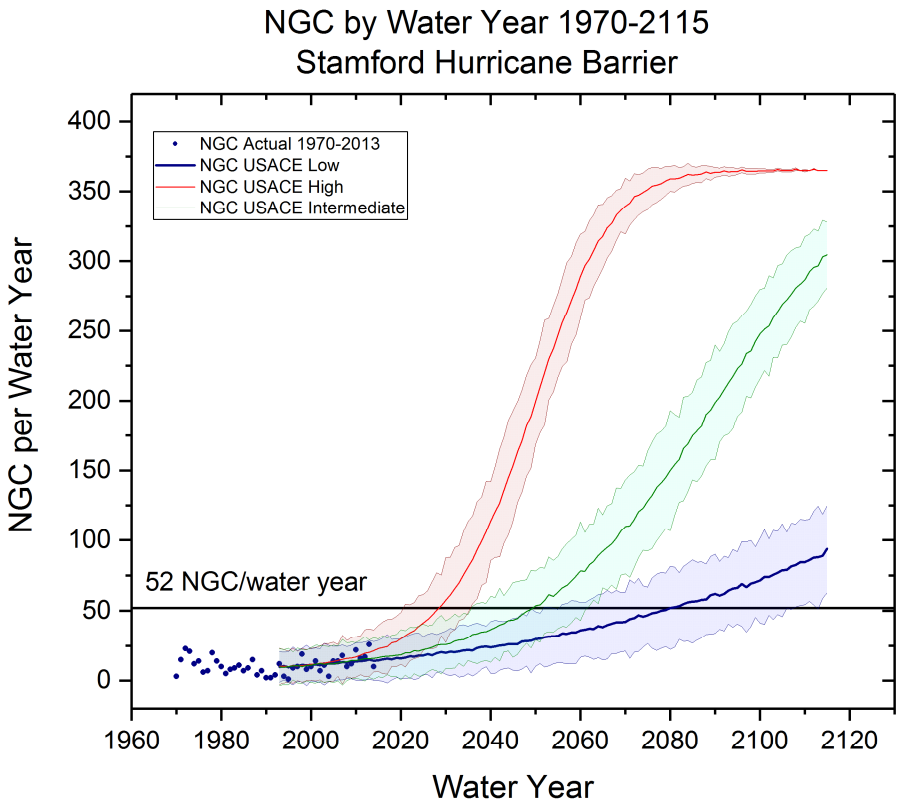

Figure 63 - Simulation of Navigation Gate Closures per Water Year, Stamford Hurricane Barrier

In the USACE high scenario, NGC/Water Year quickly climbs to 365 by 2095 and remains there as an asymptotic function to NGC/Water Year = 365, a further check on the simulation model which should stop adding NGC after 365. The medium and low scenarios also see a rapid increase in NGC/Water Year but at varying rates as RSLC accelerates at different rates in the two scenarios.

5.5.8 Methodology, A Reliability-Based Performance Model, Stamford Hurricane Barrier, Navigation Access

Results of the function-time series performance model for NGC/Water Year provide important information, and can be used to develop a reliability estimate for future navigation

traffic access into and out of East Branch Harbor. The work flow for producing the East Branch Harbor navigation access reliability-time series is shown in Figure 64 below.

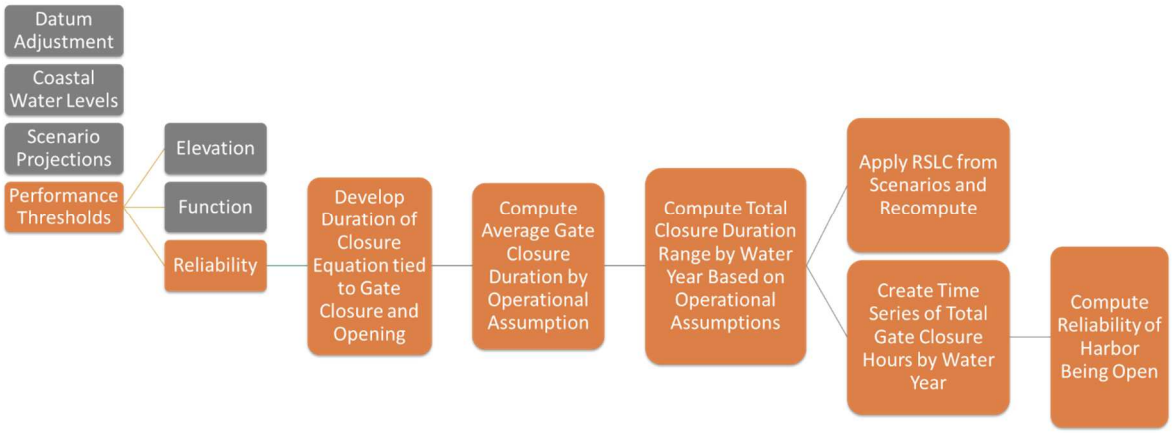

Figure 64 – Workflow for a reliability-based performance model for East Branch Harbor navigation access.

The existing gage record was examined, and a record of NGC duration was obtained. The most frequent duration of closure, was 5 hours. Figure 65 shows a plot of NGC from 2002-2014, with the corresponding peak Stamford Harbor water level shown. The longest closure was for Hurricane Sandy in October 2012, 72 hours. Of the 172 NGC's examined, the average duration of closure was 5.74 hours.

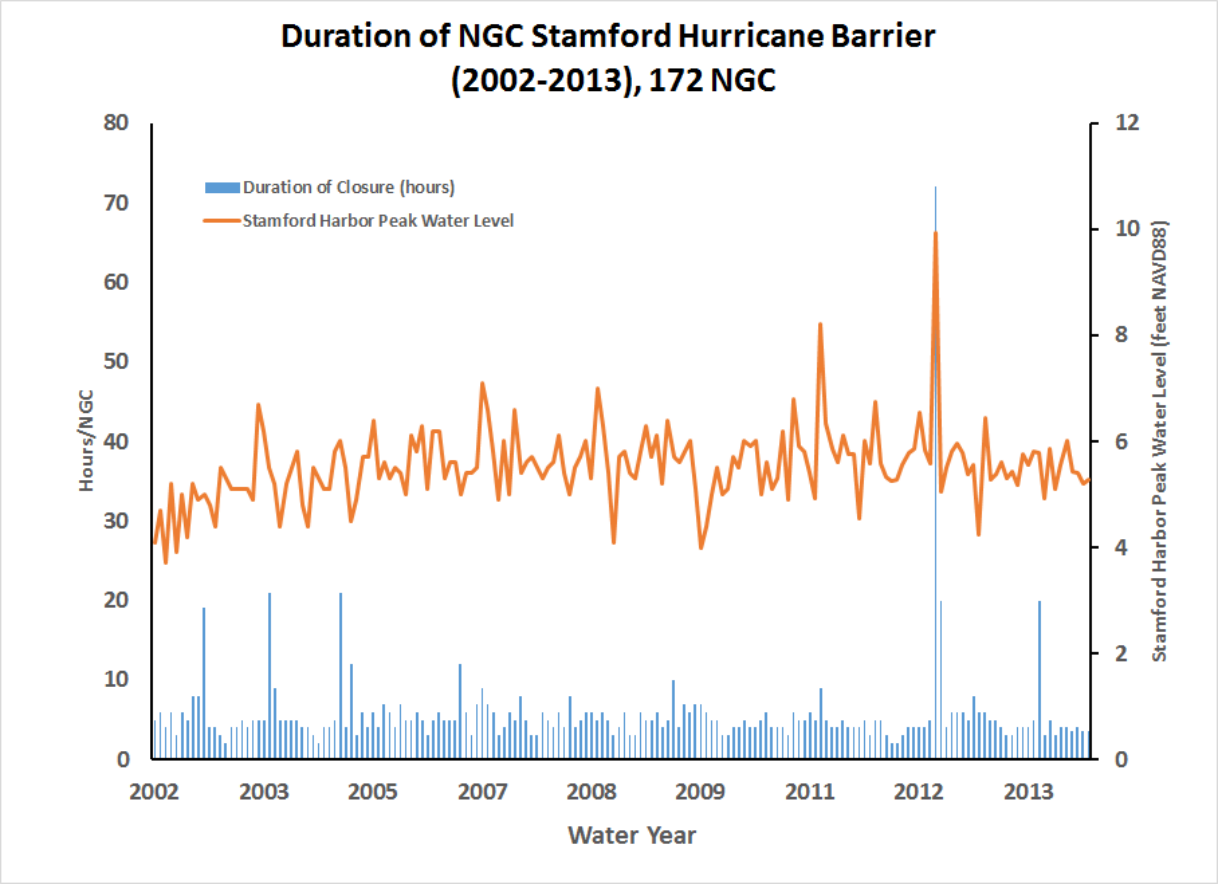

Figure 65 - Duration analysis of 172 NGC, 2002-2014 Stamford Hurricane Barrier.

One method to develop a duration of closure estimate, is to simply multiply the observed duration of closure by the NGC/Water Year metric to obtain an estimate of closure time in hours. This would be an estimate on the observed record. For example, using the ad-hoc performance threshold developed in section 5.6, the duration of closure at the 52 NGC/Water Year performance threshold would be:

$$5.74\frac{hour}{NGC}\times 52\frac{NGC}{WaterYear}=298.48\frac{hour}{WaterYear} \tag{5.9}$$

Modifying the general performance equation (4.22),

$$G = \frac{R - S}{R} \tag{5.10}$$

Where R is equal to the number of hours/Water Year (365.242 x 24), 8765.81 hours, and S is equal to NGC in hours/Water Year. An estimate of the reliability of East Branch harbor being open at the 52 NGC/Water Year threshold is developed from the performance function:

$$G = 8765.81 \frac{hour}{WaterYear} - 298.48 \frac{hour}{WaterYear} = 8467.28 \frac{hour}{WaterYear} \tag{5.11}$$

$$G = \frac{8467.28\, hour/WaterYear}{8765.81\, hour/WaterYear} = 0.9659 = 96.6\% \tag{5.12}$$

Using the historical average duration, a reliability estimate of navigation access for East Branch Harbor is 96.6% at the performance threshold for NGC/Water Year of 52. This simplified assumption could then be used to develop a range of NGC duration estimates for a reliability-based series performance model. A more robust, alternative approach was developed which considers potential NGC operational strategies to maintain interior drainage harbor storage requirements would form the basis of a bounded estimate.

5.5.9 Methodology, NGC Operational Strategies, Stamford Hurricane Barrier, Navigation Access

The operational guidance for the SHB project stipulates that the navigation gate closure operation should be made as to not allow the East Branch harbor to exceed 4.7 feet NAVD88 (USACE 2008). This leads to two possible operations, an operation in which significant rainfall is expected, requiring maximum use of the East Branch Harbor for stormwater runoff while the navigation gate is closed which will lead to a longer closure duration or an operation where little

or no rainfall is expected, leading to closure at a higher water level and shorter duration. Figure 66 displays a conceptual diagram of the NGC operation when the gate is closed.

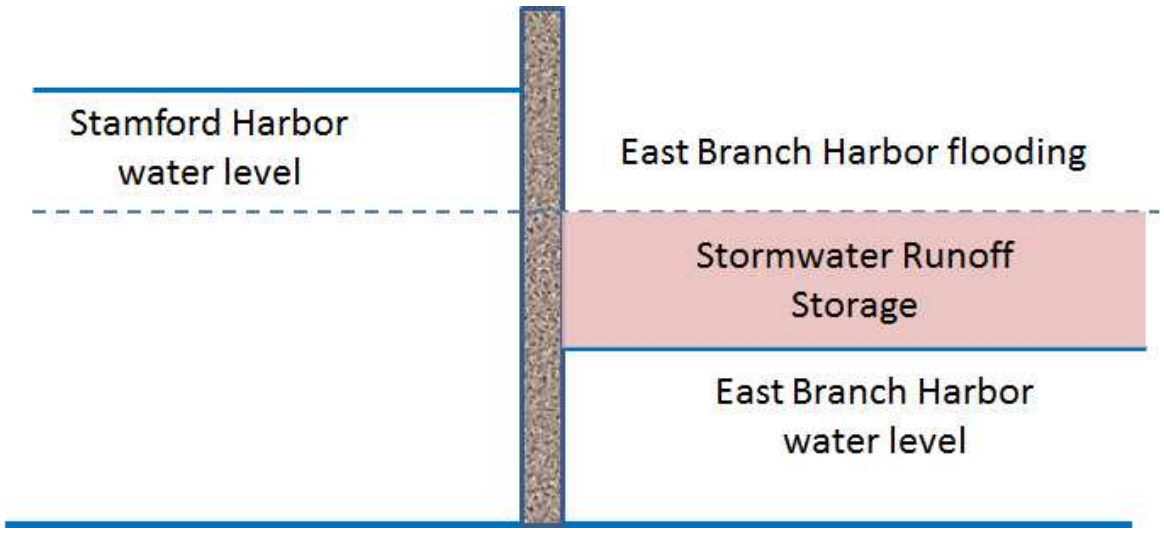

Figure 66 - Conceptual diagram of Stormwater management goal guiding NGC at the Stamford Hurricane Barrier

The duration of the NGC is thus influenced by management of the East Branch Harbor level for stormwater runoff from the 1200-acre catchment and potential local rainfall associated with an NGC. With increasing water levels caused by RSLR, risk of the East Branch Harbor flood threshold being flooded by rainfall will begin to increase over current levels once RSLR impacts low tide levels to the point where it is at or above -1.1 feet NAVD88. Conceptually this is shown in Figure 67. When MLLW reaches -1.1 feet NAVD, harbor storage to support interior drainage will be impacted and risk of flooding from local rainfall during an NGC will increase as MLLW rises above -1.1 feet NAVD88 as RSLR is added. MLLW at or above -1.1 feet NAVD88 may be defined as a performance threshold for interior drainage of the catchment during a gate closure.

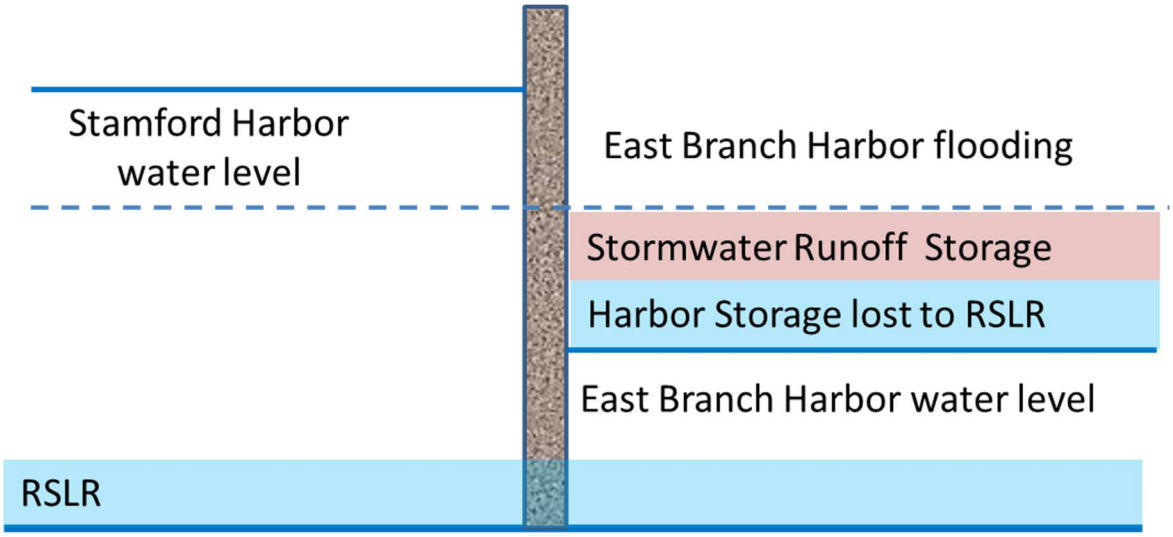

Figure 67 - Conceptual diagram of a stormwater management goal guiding NGC at the Stamford Hurricane Barrier impacted by RSLR

To estimate closure duration by NGC operation, an equation was developed which considers the rate of the rise and fall of the Stamford Harbor water level, which governs the operation decisions in a NGC. The equation which estimates NGC duration in hours is given by:

$$NGC = \frac{12.42hour}{\pi} \times \cos^{-1}\left[\frac{(2GC - SH - MLLW}{SH - MLLW}\right] + \frac{12.42hour}{\pi} \times \cos^{-1}\left[\frac{(2GO - SH - MLW}{SH - MLW}\right] \quad (5.13)$$

where *NGC* = Navigation Gate Closure duration in hours

GC = Stamford Harbor water level at which gate is closed (feet NAVD88)

SH = Peak Stamford Harbor water level (feet NAVD88)

MLLW- Mean Lower-Low Water, Stamford Harbor tidal datum (feet NAVD88)

MLW- Mean Lower Water, Stamford Harbor tidal datum (feet NAVD88)

GO - Stamford Harbor water level at which gate is opened (feet NAVD88)

To develop duration estimates for the range of possible operations, several variable assignments must be made along with assumptions. The NGC simulation model outputs an average peak Stamford Harbor elevation by water year, this number is used in the equation 5.13 computation of duration. GC elevations are determined by a with rainfall or without rainfall assumption where:

1. GC = elevation -1.10 feet NAVD88 or MLLW whichever is lower (with rainfall, maximizes harbor storage for stormwater runoff)
2. GC = elevation 4.7, the East Branch water level operational target (minimizes duration of NGC)

The GC elevations assigned to the operational strategies represent extremes of possible NGC operations, realistically the number of without rainfall NGC will increase with RSLR. The GO elevation is assigned a value of 4.7 feet NAVD88 in both cases.

5.5.10 Performance Threshold Results, Reliability-Based Performance Model, Stamford Hurricane Barrier, Navigation Access

The reliability of navigation access in and out of East Branch Harbor results show a time series of reliability in one-year time steps to 2115 (Figure 68). The error bands represent the range of possible NGC operations, with the solid line representing the average reliability between the two operations.

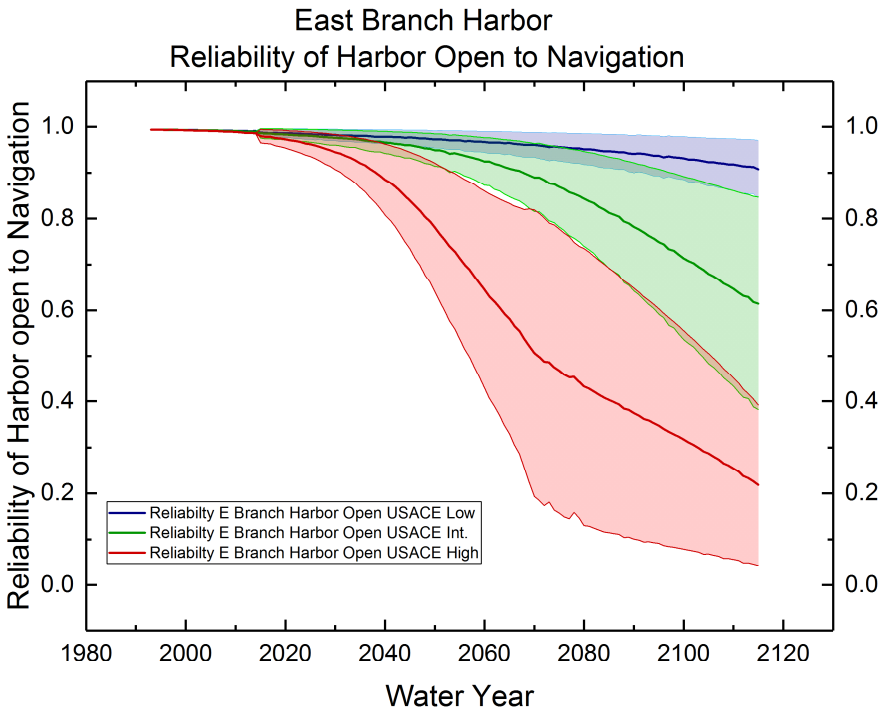

Figure 68 - Reliability projections of Navigation access to East Branch Harbor, Stamford, CT for future RSLC scenarios

While the solid line represents an average reliability between a NGC strategy with or without rainfall, the actual reliability will tend toward above the line since it is likely that there will be more no-rainfall operations in the future as NGC increases due to RSLR.

Table 21 shows selected outputs from the East Branch Harbor reliability based CPRR analysis. Under the USACE High scenario, in 2080 NGC will range from 10 to 17.5 hours, resulting in reliabilities of 58 to 28 percent for navigation access. Flood risk from stormwater runoff increases greatly with increased NGC combined with higher average Stamford Harbor water levels resulting in longer potential closure durations.

A specific performance threshold was not defined for navigation access, one can inspect the results and assign threshold values and corresponding impact time frames.

Table 21 - Selected results, Reliability-Based performance model for East Branch Harbor Navigation Access

Scenario	Water Year	Average NGC (hours/NGC)	No Navigation Access (hours/WY)	Reliability	Average Stamford Harbor Elevation (feet NAVD88)
Historical Average	2002-2014	5.74	N/A	N/A	5.58
USACE Low No-Rainfall	2030	4.97	99.44	0.989	5.58
USACE Low Rainfall	2030	10.52	210.46	0.976	5.58
USACE Int. No-Rainfall	2030	5.13	133.33	0.987	5.62
USACE Int. Rainfall	2030	10.70	278.30	0.968	5.62
USACE High No-Rainfall	2030	5.43	315.11	0.964	5.69
USACE High Rainfall	2030	11.19	648.76	0.926	5.69
USACE Low No-Rainfall	2080	5.35	278.18	0.968	5.66
USACE Low Rainfall	2080	11.09	576.44	0.934	5.66
USACE Int. No-Rainfall	2080	6.14	921.51	0.895	5.89
USACE Int. Rainfall	2080	12.16	1824.60	0.792	5.89
USACE High No-Rainfall	2080	10.15	3644.58	0.584	7.45
USACE High Rainfall	2080	17.54	6297.67	0.282	7.45

6.0: CONCLUSIONS

New coastal infrastructure plans, and designs will recognize the paradigm shift in assumptions from hydrologic stationarity to non-stationarity in coastal water levels and adjust. As we transition into the new paradigm, there is a significant knowledge gap which must address built coastal infrastructure vulnerability based on the realization that the underlying design assumptions may be invalid at present or in the near future as the impacts of global sea level rise continue. Restating the research objectives from Section 1.2, the primary conclusions of the work completed to date are:

- *Define a framework to assess vulnerability. The framework should be applicable to a wide range of coastal infrastructure types and geographic areas.*

The CPRR framework to assess vulnerability of coastal infrastructure was presented in Section 3.0, with the following major elements: (1) datum adjustment, (2) coastal water levels, (3) scenario projections, and (4) performance thresholds. The four elements are applied in order, and vulnerability is defined by the determination of performance thresholds. Performance thresholds are defined by the intersection of coastal water level time series, and performance models based on elevation, function or reliability are projected 100 years into the future.

- *Develop methodologies to execute the framework. The methodologies should account for the impact of non-stationarity in past and future water levels for the design and performance of existing coastal infrastructure.*

Methodologies and workflows were developed and are associated with each of the four framework elements. Table 22 summarizes some of the methodologies built for each major framework element.

Table 22 - Summary of methodologies developed for the CPRR by framework element

Datum Adjustment	Coastal Water Levels	Scenario Projections	Performance Thresholds
Use closest NOAA tide gauge for base RSLC rate	Use tide gauge records, daily, monthly data	USACE and NOAA global sea level rise scenarios recommended	Use reliability model for performance function $G = R - S$
Compute linear RSLC rate from observed tide gauge mean sea level data	De-trending gauge data to 1992 removes bias due to RSLR, and creates a stationary data set	Methods developed to construct a scenario, using equations 3.6 and 3.7	Select the correct critical coastal water level for performance analysis
Establishes "datum base year" (midpoint of current tidal datum)	Create composite historical record and continuous (systematic record) for AEP's	Procedures demonstrated applying RSLC to PDF developed for (logistic/monthly) and (GEV/annual)	Performance Model types (elevation, function, reliability), plot against projected coastal water level time series to find performance threshold
Key infrastructure features and water levels in local tidal datum adjusted to a common geodetic datum (NAVD88), future projections remain tied to common datum	Apply probability distributions (PDF) - GEV, logistic, log normal for data	Projections made forward in time (100 years)	Using reliability, Parametric and non-parametric uncertainty may be added to the performance model to add precision at the scenario level
Defining relationships, and nomenclature between past tidal	Apply TWL model, assume gage data is SWL		Thresholds within a time window defined by scenarios

and geodetic datums			

- *Demonstrate the applicability of the framework and conduct vulnerability assessments for two case studies with different infrastructure types in different geographic areas.*

The case study of the San Francisco Waterfront on the United States west coast utilized the elevation and reliability-based performance models. The two techniques provided an effective contrast, the elevation-based performance model was effective at showing multiple infrastructure elevations along with the associated crossings or thresholds (Figure 34). The reliability analysis demonstrated the impact of elevation uncertainty on the performance of the four selected infrastructure elements of the San Francisco Waterfront area. The reliability-based performance model may can be used to determine the vulnerability in terms of AEP, or in terms of probability of failure of the infrastructure element. The reliability-based performance analysis enabled direct comparisons of four separable elements (Figures 39 and 40, Table 16). A direct comparison of results from the elevation-based and reliability-based performance models is shown in Tables 14 and 15. The additional tier of analysis provided by applying the reliability-based performance model effectively demonstrated the impact of applying uncertainty to the infrastructure design elevation, in this case through elevation uncertainty. This methodology can be readily applied to as-built coastal levees and other flood protection structures which may have uneven profiles.

The case study of navigation gate closures (NGC) at the Stamford Hurricane Barrier on the United States east coast, proved to be a challenging and effective demonstration of a function-based performance model. A predictive model capable of reproducing the historical

NGC provided a projection of future NGC/water year using three sea level change scenarios. A reliability-based performance model was applied to address overall reliability of long term navigation access in and out of East Branch Harbor.

Both case studies were in different geographic locations, demonstrating the utility and repeatability of the framework and recommended methods. The major framework elements and associated methods were shown to be adaptable to a wide range of project types. Table 23 summarizes the critical water levels and time scales used in the CPRR application at both sites.

Table 23 - Key Water levels, performance models applied in Case Studies

Case Study	Performance Model	Critical Water Level	Performance Time Step
San Francisco Waterfront	Elevation-based	King Tide, 10%, 1%	Annual
San Francisco Waterfront	Reliability-based	GEV distribution, AEP	Annual
Stamford Hurricane Barrier – Navigation Gate Closure	Function-based	Logistic distribution, seasonal (12 months) Daily peaks	Daily/Water Year
Stamford Hurricane Barrier – Navigation Harbor Access	Reliability-based	Logistic Distribution Daily peaks/Operational Assumptions	Hourly/Water Year

REFERENCES

AECOM, (2016) *San Francisco Bay Tidal Datums and Extreme Tides Study, Final Report February 2016,* Prepared for Federal Emergency Management Agency and San Francisco Bay Conservation and Development Commission, 140p

Arns, A., Wahl, T., Haigh, I. D., Jensen, J., and Pattiaratchi, C. (2013). Estimating extreme water level probabilities: a comparison of the direct methods and recommendations for best practise. *Coastal Engineering*, *81*, 51-66.

Balica, S. F., Wright, N. G., and van der Meulen, F. (2012). A flood vulnerability index for coastal cities and its use in assessing climate change impacts. *Natural Hazards*, *64*(1), 73-105.

Bindoff, N. L., Willebrand, J., Artale, V., Cazenave, A., Gregory, J. M., Gulev, S., and Shum, C. K. (2007). Observations: oceanic climate change and sea level.

Burks-Copes, K., E. Russo, S. Bourne, M. Case, A. Davis, C. Fischenich, M. Follum, H. Li, L. Lin, S. Lofton, K. McKay, P. Mlakar, A. Morang, S. Pranger, R. Pickett, J. Ratcliff, J. Rullán-Rodríguez, M. Schultz, J. Simms, E. Smith, J. Smith, C. Talbot, and K. Winters. (2014) *Mission Capabilities: Final Technical Report*. Strategic Environmental Research and Development Program Report RC 1701.

Carter, T. R. (2007). General guidelines on the use of scenario data for climate impact and adaptation assessment (Task group on data and scenario support for impact and climate assessment-TGICA), Intergovernmental Panel on Climate Change, Version 2, Geneva.

Chadwick, B., P.F. Wang, M. Brand, R. Flick, A. Young, W. O'Reilly, P. Bromirski, W. Crampton, R. Guza, J. Helly, T. Nishikawa, S. Boyce, M. Landon, M. Martinez, I. Canner, and B. Leslie (2014) *A Methodology for Assessing the Impact of Sea Level Rise on Representative Military Installations in the Southwestern United States*. Strategic Environmental Research and Development Program Report RC 1703. Alexandria, VA: Strategic Environmental Research and Development Program.

Church, J. A., and White, N. J. (2011). "Sea-level rise from the late 19th to the early 21st century." Surv. Geophys. 32(4–5), 585–602.

Coles, S., Bawa, J., Trenner, L., and Dorazio, P. (2001). An introduction to statistical modeling of extreme values (Vol. 208). London: Springer.

Cooley, D. (2013). Return periods and return levels under climate change. In Extremes in a changing climate (pp. 97-114). Springer Netherlands.

Cullen, A.C., and H.C. Frey. 1999. *Probabilistic techniques in exposure assessment: a handbook for dealing with variability and uncertainty in models and inputs.* Springer.

Delignette-Muller M.L., and C. Dutang. 2015. *fitdistrplus: An R Package for Fitting Distributions.* Journal of Statistical Software. February 2015, Volume 64, Issue 4.

Donoghue, J.F.; J.B. Elsner, B.X. Hu, S.A. Kish, A.W. Niedoroda, Y. Wang, and M. Ye (2012) *Effects of Near-Term Sea-Level Rise on Coastal Infrastructure.* Strategic Environmental Research and Development Program Report RC 1700. Alexandria, VA: Strategic Environmental Research and Development Program.

Dwarakish, G. S., Vinay, S. A., Natesan, U., Asano, T., Kakinuma, T., Venkataramana, K., and Babita, M. K. (2009). Coastal vulnerability assessment of the future sea level rise in Udupi coastal zone of Karnataka state, west coast of India. *Ocean & Coastal Management*, *52*(9), 467-478.

El-Raey, M. (1997). Vulnerability assessment of the coastal zone of the Nile delta of Egypt, to the impacts of sea level rise. *Ocean & coastal management*, *37*(1), 29-40.

Flick, R. E., Knuuti, K., and Gill, S. K. (2012). Matching Mean Sea Level Rise Projections to Local Elevation Datums. *Journal of Waterway, Port, Coastal, and Ocean Engineering*, *139*(2), 142-146.

Ford, J. D., and Smit, B. (2004). A framework for assessing the vulnerability of communities in the Canadian Arctic to risks associated with climate change. *Arctic*, 389-400.

Füssel, H. M. (2007). Vulnerability: a generally applicable conceptual framework for climate change research. *Global environmental change*, *17*(2), 155-167.

GAO (2015) Government Accountability Office, Report to Congressional Committees. Army Corps of Engineers Efforts to Assess the Impact of Extreme Weather Events. GAO-15-660 (Washington, D.C.: July, 2015).

Garster, J.G. M. W. Huber, and K.D. White (2015) US Army Corps of Engineers Screening-Level Assessment of Projects with Respect to Sea Level Change. Civil Works Technical Report, CWTS 2015-16, US Army Corps of Engineers: Washington, DC.

Goda, Y. (1985). *Random Seas and Design of Maritime Structures*. University of Tokyo Press: Tokyo.

Hall, J. A., and Marqusee, J. (2013). Assessing Impacts of Climate Change on Coastal Military Installations: Policy Implications. DEPUTY DIRECTOR OF DEFENSE RESEARCH AND ENGINEERING ARLINGTON VA STRATEGIC ENVIRONMENTAL RESEARCH AND DEVELOPMENT PROGRAM.

Hashimoto, T., Stedinger, J. R., and Loucks, D. P. (1982). Reliability, resiliency, and vulnerability criteria for water resource system performance evaluation. *Water resources research*, *18*(1), 14-20.

Haigh, I. D., Wijeratne, E. M. S., MacPherson, L. R., Pattiaratchi, C. B., Mason, M. S., Crompton, R. P., and George, S. (2014). Estimating present day extreme water level exceedance probabilities around the coastline of Australia: tides, extra-tropical storm surges and mean sea level. *Climate Dynamics*, *42*(1-2), 121-138.

Hinkel, J., and Klein, R. J. (2009). Integrating knowledge to assess coastal vulnerability to sea-level rise: The development of the DIVA tool. *Global Environmental Change*, *19*(3), 384-395.

Horton, R., Herweijer, C., Rosenzweig, C., Liu, J., Gornitz, V., and. Ruane, A. C. (2008). Sea level rise projections for current generation CGCMs based on the semi-empirical method. Geophysical Research Letters, 35(2).

Houston, J. R., and Dean, R. G. (2011). "Sea-level acceleration based on U.S. tide gauges and extensions of previous global-gauge analyses." J. Coastal Res., 27(3), 409–417.

Houston, J. R. (2012). Global sea level projections to 2100 using methodology of the Intergovernmental Panel on Climate Change. Journal of Waterway, Port, Coastal, and Ocean Engineering, 139(2), 82-87.

Hunter, J. R. (2013). *Derivation of Victorian Sea-Level Planning Allowances*. Tech. rep., Flexible Contracting Services, Hobart, Australia, research conducted for the Victorian Coastal Council.

Ionescu, C., Klein, R. J., Hinkel, J., Kumar, K. K., and Klein, R. (2009). Towards a formal framework of vulnerability to climate change. *Environmental modeling & assessment*, *14*(1), 1-16.

IPCC, 1991. Assessment of the vulnerability of coastal areas to sea level rise: A common methodology. Revision No. 1. Report of the Coastal Zone Management Subgroup. IPCC Response Strategies Working Group, 27pp.

IPCC 1994: IPCC Technical Guidelines for Assessing Climate Change Impacts and Adaptations. Prepared by Working Group II [Carter, T.R., M.L. Parry, H. Harasawa, and S. Nishioka (eds.)] and WMO/UNEP. CGER-IO15-'94. University College -London, UK and Center for Global Environmental Research, National Institute for Environmental Studies, Tsukuba, Japan, 59 pp.

IPCC 2001. Climate Change 2001: The Scientific Basis, edited by J.T. Houghton et al., Cambridge University Press, Cambridge, U.K.

IPCC 2007. Climate Change 2007: The Physical Science basis. Contribution of Working Group I to the Fourth Assessment Report of the Intergovernmental Panel on Climate Change, edited by S. Solomon et al., Cambridge University press, Cambridge U.K.

Jevrejeva, S., Moore, J. C., and Grinsted, A. (2010). How will sea level respond to changes in natural and anthropogenic forcings by 2100?. Geophysical research letters, 37(7).

Johnson JE and Marshall PA (editors) (2007) Climate Change and the Great Barrier Reef. Great Barrier Marine Park Authority and Australian Greenhouse Office, Australia

Kachitvichyanukul, V. and Schmeiser, B. W. (1988) Binomial random variate generation. *Communications of the ACM*, **31**, 216–222.

Kamphuis, J. (2010). Introduction to Coastal Engineering and Management, World Scientific.

Kelly, P. M., and Adger, W. N. (2000). Theory and practice in assessing vulnerability to climate change andFacilitating adaptation. *Climatic change*, *47*(4), 325-352.

Klein, R. J., and Nicholls, R. J. (1999). Assessment of coastal vulnerability to climate change. *Ambio*, 182-187.

Kriebel, David L., and Joseph D. Geiman. (2014). "A coastal flood stage to define existing and future sea-level hazards." Journal of Coastal Research 30.5 (2013): 1017-1024.

Kumar, T. S., Mahendra, R. S., Nayak, S., Radhakrishnan, K., & Sahu, K. C. (2010). Coastal vulnerability assessment for Orissa State, east coast of India. *Journal of Coastal Research*, 523-534.

Lewsey, C., Cid, G., and Kruse, E. (2004). Assessing climate change impacts on coastal infrastructure in the Eastern Caribbean. *Marine Policy*, *28*(5), 393-409.

Liang, X., D.P. Lettenmaier, E.F. Wood, and S.J. Burges (1994). "A simple hydrologically based model of land surface water and energy fluxes for GSMs." *Journal of Geophysical Research* 99(D7), 14, 415–428.

Lowe, J. A., and Gregory, J. M. (2010). A sea of uncertainty. *Nature Reports Climate Change*, 42-43.

Milly, P. C. D., Julio, B., Malin, F., Robert, M., Zbigniew, W., Dennis, P., and Ronald, J. (2007). Stationarity is dead. *Ground Water News & Views*, *4*(1), 6-8.

Morang, A (2007). Hurricane barriers in New England and New Jersey-History and status after four decades. No. ERDC/CHL-TR-07-11. ENGINEER RESEARCH AND DEVELOPMENT CENTER VICKSBURG MS COASTAL AND HYDRAULICS LAB, 2007.

Moritz, R., P.S. O'Brien and K.D. White (2017). "Using reliability metrics to evaluate vulnerability of a coastal dike subjected to climate change." Paper 101a, ICE Breakwaters Conference, Wallingford, U.K.

Moritz, H., K. White, P. Ruggiero, W. Sweet, P. O'Brien, H. Moritz, M. Gravens, N. Nadal-Caraballo, B. Gouldby, T. Wahl, J. Podoski, and W. Veatch (2017). "An approach to evaluating coastal total water levels over varied temporal and spatial scales for future design and vulnerability assessment." Paper BW17_132, ICE Breakwaters Conference, Wallingford, U.K

NOAA (2012) Parris, A., P. Bromirski, V. Burkett, D. Cayan, M. Culver, J. Hall, R. Horton, K. Knuuti, R. Moss, J. Obeysekera, A. Sallenger, and J. Weiss. 2012. Global Sea Level Rise Scenarios for the US National Climate Assessment. NOAA Tech Memo OAR CPO-1. 37 pp.

National Geodetic Survey (2001) *Geodetic Glossary*. Revision of "Definitions of Terms Used in Geodetic and Other Surveys" (Hugh C. Mitchell (1948) U.S. Coast and Geodetic Survey *Special Publication* 242). Published on-line at http://www.ngs.noaa.gov/CORS-Proxy/Glossary/xml/NGS_Glossary.xml

National Ocean Service (2012). VDatum Manual for Development and Support of NOAA's Vertical Datum Transformation Tool, VDatum. Version 1. 01, June 2012. National Oceanic and Atmospheric Administration: Washington, DC. Available at http://vdatum.noaa.gov/

Nicholls, R. J. (2002). Analysis of global impacts of sea-level rise: a case study of flooding. *Physics and Chemistry of the Earth, Parts A/B/C, 27*(32), 1455-1466.

Nicholls, R. J., and Hoozemans, F. M. J. (1996). The Mediterranean: vulnerability to coastal implications of climate change. *Ocean & Coastal Management, 31*(2), 105-132.

Nicholls, R. J., and Misdorp, R. (1993). Synthesis of vulnerability analysis studies (pp. 181-216). Ministry of Transport, Public Works and Water Management.

NRC 1987. Responding to Changes in Sea Level, Engineering Implications, Committee on Engineering Implications of Changes in Relative Mean Sea Level, Marine Board, Commission on Engineering and Technical Systems, National Research Council. National Academy Press, Washington DC 1987, 148pp.

Obeysekera, J., & Park, J. (2013). Scenario-based projection of extreme sea levels. Journal of Coastal Research, 29(1), 1-7.

Obeysekera, J. (2013) Presentation, AGU Fall Meeting – December 2013.

Olsen, J. R., Lambert, J. H., and Haimes, Y. Y. (1998). Risk of extreme events under nonstationary conditions. Risk Analysis, 18(4), 497-510.

Order, Executive. "13653 (2013) Preparing the United States for the impacts of climate change." White House, Washington, DC (2013).

Parey, S., Malek, F., Laurent, C., and Dacunha-Castelle, D. (2007). Trends and climate evolution: Statistical approach for very high temperatures in France. Climatic Change, 81(3), 331-352.

Parey, S., Hoang, T. T. H., and Dacunha-Castelle, D. (2010). Different ways to compute temperature return levels in the climate change context. Environmetrics, 21(7 - 8), 698-718.

Patt, A., Klein, R. J., and de la Vega-Leinert, A. (2005). Taking the uncertainty in climate-change vulnerability assessment seriously. *Comptes Rendus Geoscience*, *337*(4), 411-424.

Patt, A., and Dessai, S. (2005). Communicating uncertainty: lessons learned and suggestions for climate change assessment. *Comptes Rendus Geoscience*, *337*(4), 425-441.

Pfeffer, W. T., Harper, J. T., and O'Neel, S. (2008). Kinematic constraints on glacier contributions to 21st-century sea-level rise. Science, 321(5894), 1340-1343.

Pietrowsky, R., et al., 2011. Quick Review of Using Scenarios in Support of Climate Change Analyses With Emphasis on Sea-Level Change. USACE briefing, ASA-CW Conference Room, GAO Building, March 2011, Washington,. DC.

Preston, B. L., Yuen, E. J., and Westaway, R. M. (2011). Putting vulnerability to climate change on the map: a review of approaches, benefits, and risks. *Sustainability Science*, *6*(2), 177-202.

R Core Team (2016). R: A language and environment for statistical computing. R Foundation for Statistical Computing, Vienna, Austria. URL https://www.R-project.org/.

Rahmstorf, S. 2007. A semi-empirical approach to projecting future sea level rise, Science, 315, no. 5810, pp 368-370.

Rahmstorf, S. (2010). A new view on sea level rise. *Nature reports climate change*, 44-45.

Ray, P.A. and Brown, C.M. (2015), *Confronting Climate Uncertainty in Water Resources Planning and Project Design, The Decision Tree Framework*. Washington, DC : World Bank. doi:10.1596/978-1-4648-0477-9. License: Creative Commons.

Read, L. K., and R. M. Vogel (2015), Reliability, return periods, and risk under non-stationarity, Water Resour. Res., 51, 6381–6398, doi:10.1002/2015WR017089.

Reclamation (2013) *Downscaled CMIP3 and CMIP5 Climate and Hydrology Projections: Release of Downscaled CMIP5 Climate Projections, Comparison with Preceding Information, and Summary of User Needs*. Denver, CO: U.S. Department of the Interior, Bureau of Reclamation, Technical Services Center. 47pp.

Reclamation (2014) *Downscaled CMIP3 and CMIP5 Climate and Hydrology Projections: Release of Hydrology Projections, Comparison with Preceding Information, and Summary of User Needs.* Denver, CO: U.S. Department of the Interior, Bureau of Reclamation, Technical Services Center. 110 pp.

Reeve, Dominic, Andrew Chadwick, and Christopher Fleming (2004). Coastal engineering: processes, theory and design practice. CRC Press, 2004. 514 pp.

Reeve, Dominic (2009). Risk and reliability: coastal and hydraulic engineering. CRC Press, 2009.

Rootzén, H., & Katz, R. W. (2013). Design life level: quantifying risk in a changing climate. Water Resources Research, 49(9), 5964-5972.

Rosati, J. D., and Kraus, N. C. (2009). *Sea level rise and consequences for navigable coastal inlets*. ENGINEER RESEARCH AND DEVELOPMENT CENTER VICKSBURG MS COASTAL AND HYDRAULICS LAB.

Ruggiero, P., Komar, P. D., McDougal, W. G., Marra, J. J., and Beach, R. A. (2001). Wave runup, extreme water levels and the erosion of properties backing beaches. Journal of Coastal Research, 407-419.

Salas, J. D., and Obeysekera, J. (2013). Revisiting the concepts of return period and risk for nonstationary hydrologic extreme events. *Journal of Hydrologic Engineering*, *19*(3), 554-568.

Salas, J. D., and Obeysekera, J. (2014). Revisiting the Concepts of Return Period and Risk for Nonstationary Hydrologic Extreme Events. *JOURNAL OF HYDROLOGIC ENGINEERING*, *19*(3).

Smit, B., and Wandel, J. (2006). Adaptation, adaptive capacity and vulnerability. *Global environmental change*, *16*(3), 282-292.

Smit, B., Burton, I., Klein, R. J., and Street, R. (1999). The science of adaptation: a framework for assessment. *Mitigation and adaptation strategies for global change*, *4*(3-4), 199-213.

Smith, J.B. and M. Hulme, 1998: Climate change scenarios. In: UNEP Handbook on Methods for Climate Change Impact Assessment and Adaptation Studies [Feenstra, J.F., I. Burton, J.B. Smith, and R.S.J. Tol (eds.)], United Nations Environment Programme, Nairobi, Kenya, and Institute for Environmental Studies, Amsterdam, pp. 3-1 - 3-40.

Snoussi, M., Ouchani, T., and Niazi, S. (2008). Vulnerability assessment of the impact of sea-level rise and flooding on the Moroccan coast: The case of the Mediterranean eastern zone. *Estuarine, Coastal and Shelf Science*, *77*(2), 206-213.

Sterr, H. (2008). Assessment of vulnerability and adaptation to sea-level rise for the coastal zone of Germany. *Journal of Coastal Research*, 380-393.

Strategic Environmental Research and Development Program (2013) Assessing Impacts of Climate Change on Coastal Military Installations: Policy Implications. US Department of Defense. *Level Rise and Nuisance Flood Frequency Changes around the United States.* NOAA.

Tribbia, J., and Moser, S. C. (2008). More than information: what coastal managers need to plan for climate change. *Environmental Science & Policy*, *11*(4), 315-328.

Tsimplis, M. N., Woolf, D. K., Osborn, T. J., Wakelin, S., Wolf, J., Flather, R., and Pert, F. (2005). Towards a vulnerability assessment of the UK and northern European coasts: the

role of regional climate variability. *Philosophical Transactions of the Royal Society of London A: Mathematical, Physical and Engineering Sciences*, *363*(1831), 1329-1358.

USACE (1962) Stamford Hurricane Barrier, Stamford Harbor and Westcott Cove, Connecticut. Design Memos 1-10. US Army Engineer Division-New England, Waltham, MA, USA.

USACE (1984) Shore protection manual. *US Army Corps of Engineers, Coastal Engineering Research Center, Vicksburg, MS, 2v*.

USACE (1989) Engineer Manual 1110-2-1414, Water Levels and Wave Heights for Coastal Engineering Design. US Army Corps of Engineers: Washington, DC.

USACE (2009b). Engineer Regulation 1110-2-8160 *Policies for Referencing Project Evaluation Grades to Nationwide Vertical Datums*. US Army Corps of Engineers: Washington, DC.

USACE (2010) Engineer Manual 1110-2-6056 *Standards and Procedures for Referencing Project Evaluation Grades to Nationwide Vertical Datums.* US Army Corps of Engineers: Washington, DC.

USACE (2011a) US Army Corps of Engineers. Incorporating Sea-Level Change Considerations in Civil Works Programs, EC 1165-2-212. Incorporating Sea-Level Change Considerations in Civil Works Programs, EC 1165-2-212.

USACE (2011b) *USACE Climate Change Adaptation Plan and Report*. US Army Corps of Engineers: Washington, DC.

USACE (2012a) *USACE 2012 Climate Change Adaptation Plan and Report*. US Army Corps of Engineers: Washington, DC.

USACE (2012b) Planning Bulletin 2012-02, Reissue#2 *Planning SMART Guide*. US Army Corps of Engineers: Washington, DC.

USACE (2013) Engineer Regulation 1100-2-8162 *Incorporating Sea Level Changes in Civil Works Programs*. [Supersedes EC 1165-2-211 (2009) and EC 1165-2-212 (2011)] US Army Corps of Engineers: Washington, DC.

USACE (2013c) *Hurricane Sandy Coastal Projects Performance Evaluation Study*. US Army Corps of Engineers North Atlantic Division: New York, NY. Available at http://www.nan.usace.army.mil/About/Hurricane_Sandy/CoastalProjectsPerformanceEvaluationStudy.aspx

USACE (2013d) *Coastal Risk Reduction and Resilience*. CWTS 2013-3. Washington, DC: Directorate of Civil Works, US Army Corps of Engineers: Washington, DC. Available at

USACE (2014a) *USACE 2014 Climate Change Adaptation Plan*. US Army Corps of Engineers: Washington, DC.

USACE (2014b) *Engineer Technical Letter 1100-2-1, Procedures to Evaluate Sea Level Change: Impacts, Responses, and Adaptation*. US Army Corps of Engineers: Washington, DC. Available at http://www.publications.usace.army.mil/Portals/76/Publications/EngineerTechnicalLetters/ETL_1100-2-1.pdf

USACE (2014c) *Engineering and Construction Bulletin 2014-10, Guidance for Incorporating Climate Change Impacts to Inland Hydrology in Civil Works Studies, Designs, and Projects*. US Army Corps of Engineers: Washington, DC. Available at https://www.wbdg.org/ccb/ARMYCOE/COEECB/ecb_2014_10.pdf

USACE (2014d) *Planning Bulletin 2012-02: Planning SMART Guide, Reissue #2*. Washington, DC: US Army Corps of Engineers.

USACE (2015) Garster, J.G., M. W. Huber, and K.D. White (2015) US Army Corps of Engineers Screening-Level Assessment of Projects with Respect to Sea Level Change. Civil Works Technical Report, CWTS 2015-16, US Army Corps of Engineers: Washington, DC.

USACE (2016). "Continuing Authorities Program. Draft Federal interest determination report." San Francisco Waterfront, Continuing Authorities Program, Section 103. U.S. Army Corps of Engineers, San Francisco District, 48p.

Vermeer, M., and S. Rahmstorf 2009. Global sea level linked to global temperature, Proceedings of the National Academy of Sciences, Early Edition, October 2009, 6pp.

Villarini, G., F. Serinaldi, J.A. Smith, and W.F. Krajewski (2009). "On the stationarity of annual flood peaks in the continental United States during the 20th century." Water Resour. Res., 45, W08417, doi:10.1029/2008WR007645.

Vogel, R. M., C. Yaindl, and M. Walter (2011). "Nonstationarity: Flood magnification and recurrence reduction factors in the United States." J. Amer. Water Resour. Assoc., 47, 464–474

Volpi, E., A. Fiori, S. Grimaldi, F. Lombardo, and D. Koutsoyiannis (2015), One hundred years of return period: Strengths and limitations, Water Resour. Res., 51, 8570–8585, doi: 10.1002/2015WR017820.

Vose, R. S., Applequist, S., Bourassa, M. A., Pryor, S. C., Barthelmie, R. J., Blanton, B., and Easterling, D. R. (2014). Monitoring and understanding changes in extremes: Extratropical storms, winds, and waves. *Bulletin of the American Meteorological Society*, *95*(3), 377-386.

Watson, R. T., Zinyowera, M. C., and Moss, R. H. (1998). *The regional impacts of climate change: an assessment of vulnerability*. Cambridge University Press.

Watson, P. J. (2011). "Is there evidence yet of acceleration in mean sea level rise around mainland Australia?" J. Coastal Res., 27(2), 368–377.

White, K.D. (2016) Personal Communication.

Wu, S. Y., Yarnal, B., and Fisher, A. (2002). Vulnerability of coastal communities to sea level rise: a case study of Cape May County, New Jersey, USA. *Climate Research*, *22*(3), 255-270.

Zhang, X. and Church, J.A., 2012. Sea level trends, interannual and decadal variability in the Pacific Ocean. *Geophys. Res. Lett.*, 39(21). DOI: 10.1029/2012GL053240